

Experimental investigations of utilizing cellulosic biomass for biofuel productions
on multi-platforms

by

Yang Yang

B.S., Kansas State University, 2015

AN ABSTRACT OF A DISSERTATION

Submitted in partial fulfillment of the requirements for the degree

DOCTOR OF PHILOSOPHY

Department of Industrial and Manufacturing Systems Engineering
Carl R. Ice College of Engineering

KANSAS STATE UNIVERSITY
Manhattan, Kansas

2023

Abstract

Biofuels derived from cellulosic biomass offer one of the best near- to mid-term alternatives to fossil fuels. Consuming bioenergy instead of fossil fuels can reduce greenhouse gas emission and benefit to the nation's energy security. The conversion can be done either on biochemical platform or thermochemical platform. Cellulosic bioethanol is developed as an alternative to petroleum-based liquid fuel on the biochemical platform. It can be used on its own as a sustainable liquid transportation fuel or blended with conventional transportation fuel. On thermochemical platform, combustion is proven to efficiently utilize biomass for heat and power generation by co-firing with coal. To efficiently convert cellulosic biomass into biofuels, biomass need to go through size reduction for bioethanol conversion. Particle size is critically important to energy consumption in its preprocessing and the efficiency in bioconversion. In the application of co-firing, the resulting fuel quality after biomass densification is also crucial to make biomass a cost effective solid fuel. This research provide fundamental knowledges and insights in biofuel manufacturing on biochemical and thermochemical platforms. A guidance on the effect of particle size through the whole bioethanol conversion process is provided. An investigation on solid fuel upgrading effects from synchronized torrefaction and pelleting (STP) system is also performed. At last, a preliminary study of a pathway on integrating these two platforms of cellulosic biomass utilization is performed. This half thesis consists of 8 chapters. Firstly, an introduction of this research is given in Chapter 1. Secondly, Chapter 2 provides a literature review on cellulosic bioethanol conversion process. Chapter 3 and 4 present a comprehensive study on effect of particle size in both biomass pre-processing and bio-conversion. Chapter 5 reviews application of biomass on thermochemical platform. Chapter 6 studies the fuel upgrading effect from using STP system. A preliminary study on integrating two

platforms of cellulosic biomass utilizations is presented in Chapter 7. Finally, conclusions are presented in Chapter 8.

Experimental investigations of utilizing cellulosic biomass for biofuel productions
on multi-platforms

by

Yang Yang

B.S., Kansas State University, 2015

A DISSERTATION

Submitted in partial fulfillment of the requirements for the degree

DOCTOR OF PHILOSOPHY

Department of Industrial and Manufacturing Systems Engineering
Carl R. Ice College of Engineering

KANSAS STATE UNIVERSITY
Manhattan, Kansas

2023

Approved by:

Major Professor:
Dr. Meng Zhang

Copyright

© Yang Yang
2023

Abstract

Biofuels derived from cellulosic biomass offer one of the best near- to mid-term alternatives to fossil fuels. Consuming bioenergy instead of fossil fuels can reduce greenhouse gas emission and benefit to the nation's energy security. The conversion can be done either on biochemical platform or thermochemical platform. Cellulosic bioethanol is developed as an alternative to petroleum-based liquid fuel on the biochemical platform. It can be used on its own as a sustainable liquid transportation fuel or blended with conventional transportation fuel. On thermochemical platform, combustion is proven to efficiently utilize biomass for heat and power generation by co-firing with coal. To efficiently convert cellulosic biomass into biofuels, biomass need to go through size reduction for bioethanol conversion. Particle size is critically important to energy consumption in its preprocessing and the efficiency in bioconversion. In the application of co-firing, the resulting fuel quality after biomass densification is also crucial to make biomass a cost effective solid fuel. This research provide fundamental knowledges and insights in biofuel manufacturing on biochemical and thermochemical platforms. A guidance on the effect of particle size through the whole bioethanol conversion process is provided. An investigation on solid fuel upgrading effects from synchronized torrefaction and pelleting (STP) system is also performed. At last, a preliminary study of a pathway on integrating these two platforms of cellulosic biomass utilization is performed. This PHD dissertation consists of 8 chapters. Firstly, an introduction of this research is given in Chapter 1. Secondly, Chapter 2 provides a literature review on cellulosic bioethanol conversion process. Chapter 3 and 4 present a comprehensive study on effect of particle size in both biomass pre-processing and bio-conversion. Chapter 5 reviews application of biomass on thermochemical platform. Chapter 6 studies the fuel upgrading effect from using STP system. A preliminary study on integrating two

platforms of cellulosic biomass utilizations is presented in Chapter 7. Finally, conclusions are presented in Chapter 8.

Table of Contents

List of Figures	xii
List of Tables	xiv
Acknowledgements.....	xv
Chapter 1 - Introduction of cellulosic biofuel.....	1
1.1 Significance of cellulosic biofuel	1
1.2 A challenge in cellulosic ethanol manufacturing.....	2
1.3 A challenge in solid fuel manufacturing.....	3
1.4 Integrating two platforms of cellulosic biomass applications	4
1.5 Objectives and scope of this research.....	5
References.....	6
Chapter 2 - Literature review of key features in cellulosic bioethanol conversion process	10
Abstract.....	10
2.1 Introduction.....	10
2.2 Size reduction	11
2.3 Pretreatment	13
2.4 Physical and chemical features	14
2.5 Effect of particle size on sugar yield	16
References.....	17
Chapter 3 - Investigation on effect of particle size in biomass preprocessing.....	26
Abstract.....	26
3.1 Introduction.....	26
3.2 Experimental Procedures and Parameter Measurements.....	28
3.2.1 Size reduction.....	28
3.2.2 Pelleting	29
3.2.3 Energy consumption measurement	30
3.2.4 Pellet density and durability measurement	31
3.3 Experimental Results and Discussions	32
3.3.1 Effect of particle size on size reduction energy consumption	32
3.3.2 Effect of particle size on pelleting energy consumption.....	33

3.3.3 Effect of particle size on pellet density	34
3.3.4 Effect of particle size on pellet durability	36
3.4 Conclusions.....	37
Acknowledgement	38
References.....	38
Chapter 4 - Investigation on effect of particle size in biomass bioconversion process	45
Abstract.....	45
4.1 Introduction.....	46
4.2 Experimental procedures and parameter measurements.....	49
4.2.1 Material preparation.....	49
4.2.2 Pretreatment	50
4.2.3 Drying	51
4.2.4 Enzymatic hydrolysis.....	51
4.2.5 Accessible surface area	53
4.2.6 Crystallinity.....	54
4.2.7 Surface morphology.....	55
4.3 Experimental results and discussions	55
4.3.1 Effect of particle size on material composition	55
4.3.2 Effect of particle size on pretreatment	57
4.3.3 Effect of particle size on hydrolysis efficiency and total sugar yield	58
4.3.4 Effect of particle size on enzyme accessible surface area	62
4.3.5 Effect of particle size on crystallinity	64
4.3.6 Effect of particle size on surface morphology	66
4.4 Conclusions.....	68
Acknowledgement	69
References.....	70
Chapter 5 - Literature review of utilizing biomass as solid fuel.....	79
Abstract.....	79
5.1 Introduction.....	79
5.2 Torrefaction	81
5.3 Densification.....	81

References.....	82
Chapter 6 - Synchronized torrefaction and pelleting of biomass for bioenergy production.....	84
Abstract.....	84
6.1 Introduction.....	85
6.2 Experimental procedures and parameter measurements.....	89
6.2.1 Materials and preparation.....	89
6.2.2 Synchronized torrefaction and pelleting (STP).....	89
6.2.3 Measurement of pellet physical properties	91
6.2.4 Measurement of pellet thermochemical properties	92
6.2.5 Measurement of pellet hygroscopic properties	93
6.3 Experimental results and discussions	93
6.3.1 Process feasibility	93
6.3.2 Pellet physical properties	95
6.3.2.1 Density	95
6.3.2.2 Durability	95
6.3.2.3 Morphology.....	96
6.3.3 Pellet thermochemical properties.....	97
6.3.3.1 Thermal properties	97
6.3.3.2 Mass yield and energy yield	100
6.3.3.3 Compositional, elemental, and FTIR analyses	101
6.3.4 Pellet hygroscopic properties	103
6.3.4.1 Water immersion.....	103
6.3.4.2 Water vapor absorption.....	103
6.4 Conclusion	105
Acknowledgement	105
Reference	106
Chapter 7 - Integrating two platforms of cellulosic biomass utilizations	112
Abstract.....	112
7.1 Introduction.....	113
7.2 Experimental procedures and parameter measurements.....	117
7.2.1 Materials and preparation.....	117

7.2.2 Pretreatment and enzymatic hydrolysis	117
7.2.3 Pelleting	118
7.2.4 Measurement of material composition and higher heating value	118
7.2.5 Measurement of pellet physical properties	118
7.2.6 Measurement of pellet mechanical strengths	119
7.2.6 Measurement of pellet thermochemical properties	120
7.2.6 FTIT and NMR spectra	120
7.2.7 Measurement of pellet hygroscopic properties	121
7.3 Experimental results and discussions	122
7.3.1 Material compositions and higher heating value (HHV)	122
7.3.2 Pellet physical properties	123
7.3.3 Pellet mechanical strengths	124
7.3.4 Pellet thermochemical properties	126
7.3.5 FTIR and NMR results	128
7.3.6 Pellet hygroscopic properties	130
7.4 Conclusions	133
References	134
Chapter 8 - Conclusion and Contributions	141
8.1 Conclusions	141
8.2 Contributions	143
Appendix A- Publications during Ph.D. study	145
Publications	145

List of Figures

Figure 1.1. Major steps to produce cellulosic ethanol	3
Figure 1.2. Operations to produce torrefied biomass pellets	4
Figure 2.1. A scheme of the pretreatment function	13
Figure 3.1. Schematic of the ultrasonic assisted pelleting process	30
Figure 3.2. Durability tester	32
Figure 3.3. Effects of biomass particle size on size reduction energy consumption.	33
Figure 3.4. Effects of biomass particle size on pelleting energy consumption.....	34
Figure 3.5. Effects of biomass particle size on pellet density. (Upper error bars represent the initial density and lower error bars represent the 24-h density).....	35
Figure 3.6. Effects of biomass particle size on pellet durability.....	37
Figure 4.1. Pretreatment results: (A) total sugar recovery, (B) sugar degradation (B), and (C) hydroxymethylfurfural (HMF) and furfural formation.....	59
Figure 4.2. 72-hour hydrolysis sugar yield results: (A) never-dried, (B) oven-dried, and (C) freeze-dried biomass	60
Figure 4.3. (A) 72-hour total sugar yield and (B) enzymatic hydrolysis efficiency	62
Figure 4.4. FTIR spectra of pretreated oven dried (A) (B) and freeze dried (C) (D) particles.....	66
Figure 4.5. SEM images of unpretreated particles.....	67
Figure 4.6. SEM images of oven-dried pretreated particles	68
Figure 4.7. SEM images of freeze-dried pretreated particles	68
Figure 6.1. Operations to produce torrefied biomass pellets	87
Figure 6.2. Schematic illustration of synchronized torrefaction and pelleting (STP)	91
Figure 6.3. Pelleting temperature of corn stover (A) and big bluestem (B) under different ultrasonic power (%).....	95
Figure 6.4. Microscopic images of (A) non-torrefied corn stover particles, (B) torrefied corn stover.....	97
Figure 6.5. Thermogravimetric analysis results (A) corn stover TG profile, (B) big bluestem TG profile, (C) corn stover DTG profile, and (D) big bluestem DTG profile	98
Figure 6.6. FTIR spectra of non-torrefied and torrefied corn stover (A) and big bluestem (B).	103

Figure 6.7. Water intake images of corn stover (A, B, E and F) and big bluestem pellets (C, D, G and H).....	103
Figure 6.8. Water absorption results of corn stover (A) and big bluestem (B).....	105
Figure 7.1. Mechanical test configurations.....	119
Figure 7.2. An illustration of contact angle measurement.....	122
Figure 7.3. Thermal analyses results of raw and hydrolyzed biomass: (A) TG, (B) DTG and (C) DSC.....	128
Figure 7.4. FTIR spectra of raw, pretreated and hydrolyzed biomass.....	130
Figure 7.5. NMR spectra of hydrolyzed biomass.....	130
Figure 7.6. Contact angle (A) and Surface morphology (B-E).....	131
Figure 7.7 Water immersion images of pellets made from different percentage of hydrolyzed residues mixtures.....	132

List of Tables

Table 2.1. Summary of different size reduction equipments in literatures	12
Table 2.2. Effects of pretreatment methods on biomass compositional and structural features..	14
Table 2.3. Reported correlation between biomass physical, chemical features and enzymatic digestibility	15
Table 2.4. Reported correlations between particle size and sugar yield when different definitions are used	16
Table 3.1. Statistical analysis results on the effects of biomass particle size on the multistep bioethanol conversion (significant level is 0.05)	37
Table 4.1 Reported correlations between particle size and sugar yield when different definitions are used	48
Table 4.2 Biomass composition before pretreatment	56
Table 4.3 Pretreatment solid recovery and biomass composition after pretreatment	58
Table 4.4 Dye absorption results of Simon's stain	62
Table 4.5 XRD and FTIR crystallinity results	65
Table 6.1 A comparison among the upstream, downstream, and synchronized torrefaction and pelleting processes	89
Table 6.2 Pellet density and durability	96
Table 6.3 Elemental and compositional results	100
Table 6.4. Mass yield, HHV, and energy yield of corn stover and big bluestem pellets.....	101
Table 7.1 An overview of the main integration strategies of second-generation bioethanol production	115
Table 7.2 Composition results of raw, pretreated, and hydrolyzed corn stover	123
Table 7.3 Results of pellet durability, density, and energy density	124
Table 7.4 Results of pellet mechanical properties	125

Acknowledgements

I would like to take this opportunity to express my appreciation to my advisor, Dr. Meng Zhang, for his continuous guidance, support and encouragement during my PHD study. I also would like to thank my co-major advisor, Dr. Donghai Wang, who provides many supports and advice on conducting experiments.

My appreciations also go to Dr. Shing I. Chang and Dr. Suprem Das. Thanks for serving as my supervisory committee and providing advice and help on my academic courses.

I also would like to thank my department head, Dr. Bradley A. Kramer, for his support. My thanks also go to Mr. Timothy W. Deines for his generosity in helping my experimental work. I am also thankful for the assistance from our department staff: Mrs. Vicky Geyer, Mrs. Debbie Harper and Mrs. Danielle Brooks. I would also thank Dr. Christopher Jones and Dr. Xiuzhi Sun for the help of TGA measurement. I also thank Dr. Shuting Lei, Dr. John Wu, Dr. David Ben-Arieh, Dr. Jessica Heier Stamm and all other faculty members in my department for their kindly help on my academic courses.

I would like to acknowledge my colleagues and friends: Dr. Ke Zhang, Dr. Jun Li, Dr. Jikai Zhao, Dr. Mingman Sun, Dr. Xinya Wang and Mr. Guang Yang for their generous help.

Lastly, I would like to thank my wife Shuyi Guo for everything she has been doing to support me. My gratitude also goes to my parents for their love and support

Chapter 1 - Introduction of cellulosic biofuel

1.1 Significance of cellulosic biofuel

Bioenergy derived from cellulosic biomass (forest and agricultural residues and dedicated energy crops) has been recognized as a promising alternative to fossil fuels. With its high availability and low cost, cellulosic biomass is regarded as a sustainable resource for bioenergy production in the near to distant future. Among many bioenergy conversion technologies, making cellulosic bioethanol and co-combustion are most common used methods to utilize biomass for bioenergy.

On the biochemical platform, cellulosic ethanol is produced to replace conventional transportation fuels. It can be used on its own as a sustainable liquid transportation fuel or blended with conventional transportation fuel to meet the government's mandate of 16 billion gallons of cellulosic biofuel produced annually by 2022 in the Renewable Fuel Standard (RFS) as part of the Energy Independence and Security Act [1,2]. There are over 1 billion dry tons of cellulosic biomass that can be sustainably harvested in the U.S. every year. This amount is sufficient to produce 90 billion gallons of biofuel that can displace about 30% of the nation's current liquid fuel consumption annually [3]. Additionally, over 90% of the liquid transportation fuel used in the U.S. is petroleum-based (gasoline and diesel), to replace conventional liquid fuel also contribute to the reduction of greenhouse gas emission in to the atmosphere [4-9]. Compared to the first-generation biofuels (fuels produced from feedstocks such as corns and sugar canes, which can potentially be made into food/feed), producing biofuels from the inedible cellulosic biomass creates less competition with food/feed production for the limited agricultural farmland and other resources [5].

On the thermochemical platform, co-combustion is another efficient and clean way to derive energy from cellulosic biomass. About 40% of the world's total power is supplied by coal power plants. Adding biomass as a partial substitute in existing coal power plants poses an opportunity to generate heat and electricity and reduce the consumption of fossil fuels. Cellulosic biomass co-combustion benefits from the infrastructure that is in place for large-scale coal combustion. Some individual coal-fired power units have been converted to 100% biomass combustion, and all the power plants can be converted to run on biomass [10-13].

1.2 A challenge in cellulosic ethanol manufacturing

Figure 1.1 shows major steps of cellulosic ethanol manufacturing. Biomass particle size (after size reduction) is a crucial input process parameter with impacts on both the feedstock preprocessing and bioconversion stages. Biomass particle size is closely related to the energy consumption in size reduction. More energy will be consumed when smaller biomass particle size is produced. However, smaller particles size can provide higher transportation and handling efficiency. It also has positive influences to the conversion rate of fermentable sugar in hydrolysis, but there is a drawback on the total sugar recovery. In the current literature, there are no commonly accepted guidelines on how to select biomass particle size in order to conserve energy in the feedstock preprocessing stage while still achieving good biofuel yield in the bioconversion stage.

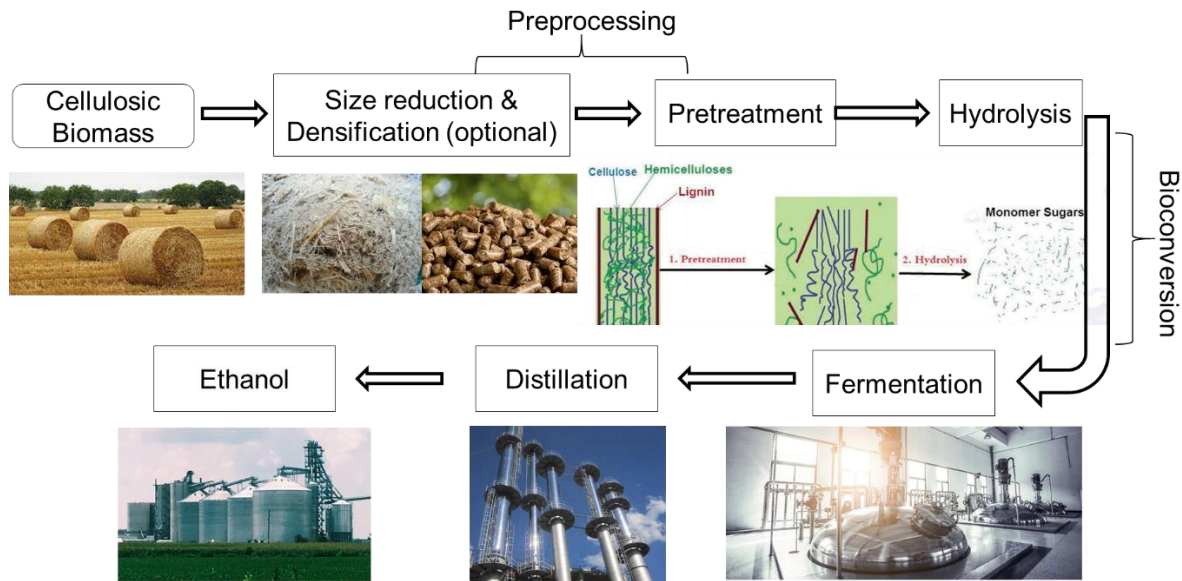


Figure 1.1. Major steps to produce cellulosic ethanol

1.3 A challenge in solid fuel manufacturing

Producing torrefied pellets is the prevailing technique to overcome the barriers caused by characteristics of raw biomass such as hydrophilic natural, low energy and volumetric density, [14, 15]. As shown in Figure 1.2, upstream and downstream operations are two current solutions to produce torrefied pellets in separated steps. As the global demand for torrefied pellets is expected to double from 24.5 million metric tons to 50 million metric tons by 2024 [16]. The integration of torrefaction and pelleting is proposed to improve production efficiency, reduce logistical costs, and make intercontinental bioenergy transport economically and energetically feasible. For this purpose, synchronized torrefaction and pelleting (STP) method is developed to achieve multiple fuel upgrading effects in a single step. With the assist of ultrasonic vibration, significant amount of heat is generated due to viscoelastic heating and initiate torrefaction from the center of pellets during the operation. The accumulation of heat results in a rapid temperature increase (up to 320°C) when biomass is being pelletized. The relative lower temperature at pellet surface only provides thermal set effect to lignin content in biomass and result in good quality to

torrefied pellets. STP method is effective at enhancing pellet physical, thermochemical and hygroscopic characteristics.

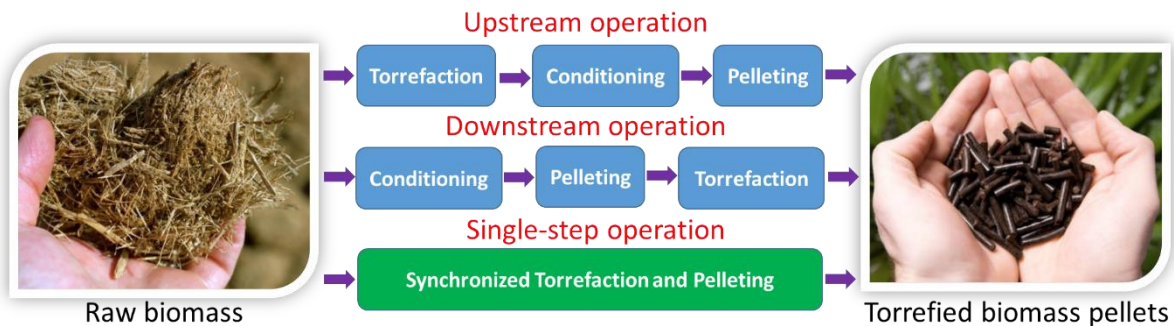


Figure 1.2. Operations to produce torrefied biomass pellets

1.4 Integrating two platforms of cellulosic biomass applications

Second-generation (2G) bioethanol production is yet to be successful commercially. Stand-alone second-generation bioethanol production is still facing significant challenges [17-19]. In order to conserve energy and cost in conversion process, several integration approaches have been proposed and investigated [19, 20]. The valorization of biomass hydrolyzed residues provides an opportunity to create an intermediate product that can serve as a renewable solid fuel or a feedstock commodity for other bio-refinery applications. Rather than directly using the raw biomass, the hydrolyzed residue should be recovered and used for heat and power generation for bioethanol production process with a combined heat and power facility. A more economical use of this residue is to utilize it as a platform chemical for high value-added products such as aromatic and phenolic compounds, cement additives, bitumen modifiers and battery materials. Making pellets with biomass hydrolyzed residues can improve the overall techno-economic performance of the process.

Condensing biomass hydrolyzed residues into pellets can increase the volumetric energy densities, improve the handling and logistic efficiency of the fuel product [21-23]. When

utilizing these pellets as platform chemical commodities, the enriched lignin content of hydrolyzed residues also offers great physical quality to the pellets due to the natural binding ability of lignin [21, 24]. Considering the strong value adding potentials of pellets made from hydrolyzed residues, an integration of combined heat and power plant (CHP) can achieve an optimized combination of biomass valorization, ethanol yield and energy output from the 2G feedstocks [25, 26].

1.5 Objectives and scope of this research

The objectives of the research on effect of biomass particle size in bioethanol conversion are as following;

To investigate the effect of particle size in biomass pre-processing and mainly focused on the effect on energy consumption, pellet density and durability.

To investigate the effect of particle size in biomass handling.

To investigate the effect of particle size in ethanol conversion on biomass physical features (surface morphology, surface area, crystallinity).

To investigate the effect of particle size in ethanol conversion on biomass chemical features (material composition, chemical compound).

To investigate the effect of particle size in ethanol conversion on total sugar recovery, hydrolysis efficiency.

The objectives of the research on synchronized torrefaction and pellet process are as following;

To investigate effects of input parameters (particle size, pressure, ultrasonic power, duration, material type) on torrefaction and pellet quality.

To investigate the impact to pellet physical properties by STP

To investigate the impact to pellet thermochemical properties by STP

To investigate the impact of pellet hygroscopic properties by STP

The objectives of the research on integrating two platforms of utilizing cellulosic biomass are as following;

To investigate the impact to pellet physical properties from adding hydrolyzed residue

To investigate the impact to pellet hygroscopic properties from adding hydrolyzed residue

To investigate the impact to pellet thermochemical properties from adding hydrolyzed residue

References

- [1] Bracmort, K., 2015, “The Renewable Fuel Standard (RFS): Cellulosic Biofuels,” R41106, Congressional Research Service, <http://nationalaglawcenter.org/wp-content/uploads/assets/crs/R41106.pdf>.
- [2] Gouli, S.S., Serdari, A.A., Stournas, S.S., and Lois, E.E., 2000, “Transportation Fuel Substitutes Derived From Biomass,” *Journal of Energy Resources Technology*, 123(1):39-43.
- [3] U.S. Department of Transportation, 2010, “Transportation’s Role in Reducing U.S. Greenhouse Gas Emissions,” http://ntl.bts.gov/lib/32000/32700/32779/DOT_Climate_Change_Report_-_April_2010_-_Volume_1_and_2.pdf.
- [4] U.S. Energy Information Administration, 2017, “Monthly Energy Review,” <http://www.eia.gov/totalenergy/data/monthly/pdf/mer.pdf>.

- [5] BP, “BP Statistical Review of World Energy,” 2016, <https://www.bp.com/content/dam/bp/pdf/energy-economics/statistical-review-2016/bp-statistical-review-of-world-energy-2016-full-report.pdf>.
- [6] Huber, G.W., 2008, “Breaking the Chemical and Engineering Barriers to Lignocellulosic Biofuels: Next Generation Hydrocarbon Biorefineries” Based on the June 25-26, 2007 Workshop, Washington, DC: National Science Foundation, Chemical, Biogengineering, Environmental and Transport Systems Division.
- [7] U.S. Energy Information Administration, 2013, “How Much Petroleum Does the United States Import and from Where?” <http://www.eia.gov/tools/faqs/faq.cfm?id=727&t=6>.
- [8] Bastani, P., Heywood, J.B., and Hope, C.,2012, “Fuel Use and CO2 Emissions Under Uncertainty From Light-Duty Vehicles in the U.S. to 2050,” *Journal of Energy Resources Technology*, 134(4):042202-042202-10.
- [9] Zhang. C., Ge, Y., Tan, J., li, L., Peng, Z., and Wang, X., 2017, “Emissions From Light-Duty Passenger Cars Fueled With Ternary Blend of Gasoline, Methanol, and Ethanol,”*Journal of Energy Resources Technology*, 139(6):062202-062202-8.
- [10] Adams, D., 2013. Sustainability of biomass for cofiring. CCC/230. London: IEA Clean Coal Centre. [www. iea-coal. org. uk/documents/83254/8869/Sustainability-of-biomass-for-cofiring, -CCC/230](http://www.iea-coal.org.uk/documents/83254/8869/Sustainability-of-biomass-for-cofiring,-CCC/230).
- [11] Chao, C.Y., Kwong, P.C., Wang, J.H., Cheung, C.W. and Kendall, G., 2008. Co-firing coal with rice husk and bamboo and the impact on particulate matters and associated polycyclic aromatic hydrocarbon emissions. *Bioresource technology*, 99(1), pp.83-93.

- [12] Kabir, M.R. and Kumar, A., 2012. Comparison of the energy and environmental performances of nine biomass/coal co-firing pathways. *Bioresource technology*, 124, pp.394-405.
- [13] Goldfarb, J.L. and Liu, C., 2013. Impact of blend ratio on the co-firing of a commercial torrefied biomass and coal via analysis of oxidation kinetics. *Bioresource technology*, 149, pp.208-215.
- [14] Zhang, M., Song, X.X., Pei, Z.J., Deines, T.W., and Treadwell, C., Ultrasonic Vibration-Assisted Pelleting of Wheat Straw: An Experimental Investigation. *International Journal of Manufacturing Research*, 2012. 7(1): p. 59-71.
- [15] Zhang, M., Song, X.X., Pei, Z.J., and Wang, D.H., Ultrasonic vibration-assisted pelleting of cellulosic biomass for biofuel production, in *Production of biofuels and chemicals: ultrasound*, Eds: Fang, Z., Smith, R.L., Jr., and Qi, X.H., Springer, 2015, New York, NY, USA.
- [16] Goh, C.S., Junginger, M., Cocchi, M., Marchal, D., Thrän, D., Hennig, C., Heinimö, J., Nikolaisen, L., Schouwenberg, P.P., Bradley, D. and Hess, R., 2013. Wood pellet market and trade: a global perspective. *Biofuels, Bioproducts and Biorefining*, 7(1), pp.24-42.
- [17] Lennartsson, P.R., P. Erlandsson, and M.J.J.B.t. Taherzadeh, Integration of the first and second generation bioethanol processes and the importance of by-products. 2014. 165: p. 3-8.
- [18] Eriksson, G. and B.J.A.E. Kjellström, Assessment of combined heat and power (CHP) integrated with wood-based ethanol production. 2010. 87(12): p. 3632-3641.

- [19] Ferreira, J.A., et al., A review of integration strategies of lignocelluloses and other wastes in 1st generation bioethanol processes. 2018. 75: p. 173-186.
- [20] Ayodele, B.V., M.A. Alsaffar, and S.I.J.J.o.C.P. Mustapa, An overview of integration opportunities for sustainable bioethanol production from first-and second-generation sugar-based feedstocks. 2020. 245: p. 118857.
- [21] Piccolo, C., F.J.B. Bezzo, and bioenergy, A techno-economic comparison between two technologies for bioethanol production from lignocellulose. 2009. 33(3): p. 478-491.
- [22] Starfelt, F., et al., Integration of torrefaction in CHP plants—A case study. 2015. 90: p. 427-435.
- [23] Song, H., et al., Techno-economic analysis of an integrated biorefinery system for poly-generation of power, heat, pellet and bioethanol. 2014. 38(5): p. 551-563.
- [24] Kaliyan, N. and R.V.J.B.t. Morey, Natural binders and solid bridge type binding mechanisms in briquettes and pellets made from corn stover and switchgrass. 2010. 101(3): p. 1082-1090.
- [25] Starfelt, F., et al., The impact of lignocellulosic ethanol yields in polygeneration with district heating—a case study. 2012. 92: p. 791-799.
- [26] Palacios-Bereche, R., A. Ensinas, and S.A.J.C.E.T. Nebra, Energy consumption in ethanol production by enzymatic hydrolysis—the integration with the conventional process using pinch analysis. 2011. 24: p. 1189-1194.

Chapter 2 - Literature review of key features in cellulosic bioethanol conversion process

Abstract

Biofuels derived from cellulosic biomass offer one of the best near- to mid-term alternatives to petroleum-based liquid transportation fuels. Biofuel conversion is mainly done through a biochemical pathway, on which size reduction, pelleting, pretreatment, enzymatic hydrolysis, and fermentation are main processes. As an input factor, biomass particle size has influences in both preprocessing and bioconversion process. Most reported studies focus on the effects of biomass particle size on a single specific process and the reported relationships between particle size and output parameters are inconsistent; as a result, in the current literature, there is no commonly accepted guidance to select the overall optimum particle size in order to minimize the energy consumption and maximize sugar yield.

2.1 Introduction

In the multistep bioethanol production process, size reduction and pretreatment are performed prior to enzymatic hydrolysis, because the bulk raw biomass cannot be processed or converted to bioethanol efficiently. Reducing biomass particle size provides biomass with higher volumetric density, improved flowability, and better handling property in logistics [1]. Pretreatment alters the recalcitrance of cellulosic biomass natural structure and separates cellulose from the hemicellulose-lignin shield by breaking the bonds and linkages in the woven cell wall. The physical and chemical modifications caused by size reduction and pretreatment make biomass more accessible to enzymes in the subsequent enzymatic hydrolysis [2]. Through extensive studies, key physical and chemical features that impact biomass enzymatic digestibility

have been identified. By classification, physical features include particle size, accessible surface area, and crystallinity. Chemical features are mainly referred to as the chemical composition fractions of cellulose, hemicellulose, and lignin so as the characteristics of the bonds and linkages amongst the three biomass structural compositions [3].

The influences of biomass physical and chemical features on its enzymatic digestibility have been broadly reported in the literature. A high enzymatic digestibility can be achieved by favorably preparing a biomass substrate, so it has large enzyme-accessible surface area [4,5], low crystallinity [2,6], and low lignin or hemicellulose contents [3,7-9].

2.2 Size reduction

Biomass size reduction is the first step for biofuel production from cellulosic biomass through biochemical pathway. Size reduction is usually performed on a mill with a sieve installed to control the size of the produced particles. During milling process, biomass materials endure impacting, compression, shearing and stretching [10]. As summarized in Table 2.1, the average particle size varies by different size reduction equipment. Hammer mills are mostly used in biomass size reduction. It has a low energy consumption with high productivity. Particles made by hammer mills are usually smaller than screen size and may cause flowability issues. Due to the cutting mechanisms, most equipment produce rod like particles. When particles with high aspect ratio are produced (attrition/dis mill), it has negative effect to flowability. Unlike other equipments, rotary by pass shear mill produce cube like particles low aspect ratio and provide good flowability. However, unable to produce fine particles is the drawback. Ball mill produce finest particles to micrometer and nanometer level but the final particle size is hard to control because no screen can be used. Knife mill can produce wider range of particles. Final

particle size is easier to control with corresponding screens. Similarly, due to flowability issue, feeding actions are usually needed when producing fine particles.

Table 2.1. Summary of different size reduction equipments in literatures

Grinding Equipment	Mean particle size range	Particle distribution	Main Particle shape	Energy consumption	Productivity	Effect of moisture	Pro/Cons
Hammer mill	Millimeter	Wide	Rod	Medium	High	Low MC<10% High MC>10%	Cost lower Grinds more fine particles (more dust) that are much smaller than screen size. It can cause flowability issue and need further sieving for target particle size
Knife mill	Centermeter/Millimeter	medium	Rod	Medium	Medium	Insignificant when particle size larger than 4mm	Produce smaller mean particle size than hammer mill Consume more energy than hammer mill, need feeding action and tool maintenance Has de-fibrate impact to material which is good for hydrolysis Can produce high aspect ratio particles which is negative to flowability
Attrition/Disk mill	Millimeter	Wide	Ribbon/Rod	High	Low	Insignificant	Can cause decrease of material crystallinity Mostly used for lab scale. It is hard to control final particle size and have flowability issue
Ball mill	Nanometer/ Micrometer	Narrow		High	Low		
Rotary bypass shear mill	Millimeter	Narrow	cubic	Low	Low	Insignificant above 1mm	Particles has low aspect ratio and give good flowability Unable to produce fine particles

2.3 Pretreatment

Raw biomass mainly consists three compositions and their contents vary by biomass types. They are cellulose (40-50%), hemicellulose (20-30%), and lignin (15-20%) on a dry weight basis [11]. Cellulose and hemicellulose are compound sugars that can be broken into fermentable sugars in enzymatic hydrolysis. Lignin contains no sugar content. The obstacle of converting compound sugars in biomass to fermentable sugars is mainly due to the presence of lignin. Lignin shields biomass as the main plant cell wall composition and interweaves with hemicellulose to surround cellulose by a network structure. This structure limits the accessibility of enzymes to compound sugars during hydrolysis. Moreover, the crystalline natural structure of cellulose chains due to extensive hydrogen bonding consequently increases the difficulty for enzymes to access compound sugars. As a result, raw biomass often requires pretreatment to liberate the sugars contained within cellulose fibers embedded in the hetero-matrix of plant cell walls to increase the yield of fermentable sugars. A scheme is shown in Figure 2.1. The sugar yield in enzyme hydrolysis can then be enhanced after pretreatment.

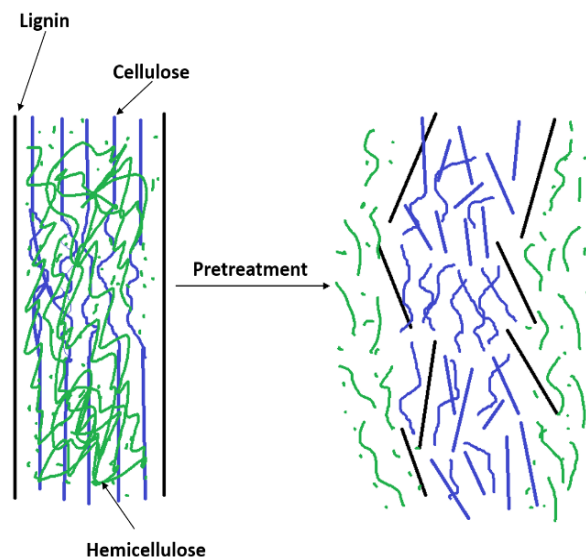


Figure 2.1. A scheme of the pretreatment function

Pretreatment methods can be classified into chemical, physical, physicochemical methods [12-14]. Dilute acid, dilute alkaline, liquid hot water, and ammonia fiber explosion (AFEX) are among the several well studied in the literature. It has been indicated that the modification on biomass compositional and structural features by pretreatment are critically important for increasing the fermentable sugar yield in enzymatic hydrolysis [15]. As shown in Table 2.2, effects of pretreatment methods on biomass compositional and structure features are different. Delignification of dilute alkaline and ammonia fiber explosion pretreatment results in biomass structural disruption and increased enzyme accessible surface area. However, not all the pretreatments aim at removing lignin, the removal of hemicellulose by dilute acid, liquid hot water, and metal oxide pretreatments substantially alters lignin structure and disrupt hetero-matrix network structure between hemicellulose and lignin. The high pressure in ammonia fiber explosion (AFEX) and supercritical CO₂ aids on reducing biomass crystallinity, rendering cellulose more amenable to enzymatic hydrolysis.

Table 2.2. Effects of pretreatment methods on biomass compositional and structural features

Pretreatment method	Decrease crystallinity	Remove hemicellulose	Remove lignin
Dilute acid	×	√	×
Dilute alkaline	×	×	√
Liquid hot water	√	√	×
Ammonia fiber explosion (AFEX)	√	×	√
Supercritical CO ₂	√	×	×
Metal oxide	×	√	×

×: not effective; √: effective

2.4 Physical and chemical features

Key physical and chemical features that impact biomass enzymatic digestibility are widely studied and identified. By classification, physical features include particle size, accessible surface area, and crystallinity. Chemical features are mainly referred to as the chemical

composition fractions of cellulose, hemicellulose, and lignin so as the characteristics of the bond and linkage between the three compositions [3].

Table 2.3. Reported correlation between biomass physical, chemical features and enzymatic digestibility

Aspects	Factors	Correlations	References	
Physical features	Particle size	Unpretreated	Negative	[20, 21]
			Positive	[22, 23]
		Pretreated	Neutral	[24, 25]
			Negative	[20, 26]
	Accessible surface area	Positive	[24, 27]	
Crystallinity	Negative	[2, 6]		
Chemical features	Lignin content	Negative	[3, 28]	
	Hemicellulose content	Negative	[7, 9]	

The correlations between physical and chemical features of biomass and enzymatic digestibility in the literature are summarized in Table 2.3, a high enzymatic digestibility can be achieved by having substrates with larger accessible surface area, lower crystallinity, lower lignin and hemicellulose contents, but the reported correlations between particle size and enzymatic digestibility are inconsistent. Positive (larger particle size has higher enzymatic digestibility), neutral (no correlation) and negative correlations (smaller particle size has higher enzymatic digestibility) have been reported. When enzymatic hydrolysis is directly performed to digest un-pretreated biomass, consistent results are reported that particle size of the biomass has negative correlation with enzymatic digestibility, but the correlation is rather weak. When pretreatment is performed, three different correlations are reported. The effects of biomass particle size on enzymatic digestibility are mostly concluded by simply comparing the sugar yield. However, modifications of biomass physical features on a microscopic level (crystallinity reduction and accessible surface area increase) and chemical features (hemicellulose and lignin

removal) in pretreatment have major impact to biomass enzymatic digestibility since the enhancement by pretreatment is much more significant (>70%) than that simply by size reduction (up to <50%) [19].

2.5 Effect of particle size on sugar yield

Sugar yield definitions used in the literature are found to be different, and this variation caused the inconsistency in the reported correlations as summarized in Table 2.4. Most studies reported the correlations by using enzymatic hydrolysis efficiency to investigate the percentage of compound sugar digested in hydrolysis; when this definition is used, it seems to be commonly agreed that compound sugar in small particles can be more efficiently digested into fermentable sugar than in large particles. When enzymatic hydrolysis sugar yield or total sugar yield definitions are used, inconsistent correlations have been reported. A higher enzymatic hydrolysis efficiency and enzymatic hydrolysis sugar yield of small particles do not necessarily mean small particles should be selected favorably in bioethanol production. The correlation in favor of small particles can be deceptive as small particles' advantage in hydrolysis can be outweighed by their drawbacks in pretreatment.

Table 2.4. Reported correlations between particle size and sugar yield when different definitions are used

Sugar yield definition	Definition explanation	Correlation	Reference
Enzymatic hydrolysis efficiency	Percentage of grams of compound sugar digested to grams of fermentable sugar added to hydrolysis	Negative	[20,29-34]
		Positive	[35]
Enzymatic hydrolysis sugar yield	Grams of fermentable sugar yield per 1g of dry biomass added to hydrolysis	Negative	[36,37-39]
		Neutral	[40]
		Positive	[41,42]
Total sugar yield	Grams of fermentable sugar yield per 1g of dry biomass added to pretreatment	Negative	[43]
		Positive	[44,45]

Particle size of biomass used in reported studies can be classified into two ranges: particle size smaller than 1 mm can be considered as micron meter level and particle size larger than 1 mm can be considered as a millimeter level. Despite the pretreatment method varied, the particle size smaller than 1 mm showed the trend that smaller particle size results in higher sugar yield. In contrast, particle size is larger than 1 mm, two different trends were reported in various literatures.

Table 2.5 Reported relationship between cellulosic biomass particle size and enzymatic hydrolysis sugar yield of two biomass particle size ranges

Particle range	Relationship	reference
≤ 1 mm	Smaller particle size results in high sugar yield	[20,46-50] [31]
≥ 1 mm	Smaller particle size results in high sugar yield	[34] [51]
	Larger particle size results in high sugar yield	[23,42,52,53] [54]

References

- [1] Hess, J.R., Wright, C.T. and Kenney, K.L., 2007. Cellulosic biomass feedstocks and logistics for ethanol production. *Biofuels, Bioproducts and Biorefining: Innovation for a sustainable economy*, 1(3), pp.181-190. doi.org/10.1002/bbb.26
- [2] Fan, L.T., Lee, Y.H. and Beardmore, D.H., 1980. Mechanism of the enzymatic hydrolysis of cellulose: effects of major structural features of cellulose on enzymatic hydrolysis. *Biotechnology and Bioengineering*, 22(1), pp.177-199. doi.org/10.1002/bit.260220113
- [3] Zhu, L., O'Dwyer, J.P., Chang, V.S., Granda, C.B. and Holtzapple, M.T., 2008. Structural features affecting biomass enzymatic digestibility. *Bioresource Technology*, 99(9), pp.3817-3828. doi.org/10.1016/j.biortech.2007.07.033

- [4] Sinitsyn, A.P., Gusakov, A.V. and Vlasenko, E.Y., 1991. Effect of structural and physico-chemical features of cellulosic substrates on the efficiency of enzymatic hydrolysis. *Applied Biochemistry and Biotechnology*, 30(1), pp.43-59. doi.org/10.1007/BF02922023
- [5] Zeng, M., Mosier, N.S., Huang, C.P., Sherman, D.M. and Ladisch, M.R., 2007. Microscopic examination of changes of plant cell structure in corn stover due to hot water pretreatment and enzymatic hydrolysis. *Biotechnology and Bioengineering*, 97(2), pp.265-278. doi.org/10.1002/bit.21298
- [6] Chang, V.S. and Holtzapple, M.T., 2000. Fundamental factors affecting biomass enzymatic reactivity. In *Twenty-first symposium on biotechnology for fuels and chemicals* (pp. 5-37). Humana Press, Totowa, NJ. DOI: 10.1007/978-1-4612-1392-5_1
- [7] Digman, M.F., Shinnars, K.J., Casler, M.D., Dien, B.S., Hatfield, R.D., Jung, H.J.G., Muck, R.E. and Weimer, P.J., 2010. Optimizing on-farm pretreatment of perennial grasses for fuel ethanol production. *Bioresource Technology*, 101(14), pp.5305-5314. doi.org/10.1016/j.biortech.2010.02.014
- [8] Zhu, J., Wan, C. and Li, Y., 2010. Enhanced solid-state anaerobic digestion of corn stover by alkaline pretreatment. *Bioresource Technology*, 101(19), pp.7523-7528. doi.org/10.1016/j.biortech.2010.04.060
- [9] Grohmann, K., Mitchell, D.J., Himmel, M.E., Dale, B.E. and Schroeder, H.A., 1989. The role of ester groups in resistance of plant cell wall polysaccharides to enzymatic hydrolysis. *Applied Biochemistry and Biotechnology*, 20(1), pp.45-61. doi.org/10.1007/BF02936472

- [10] Zhang, W., Liang, M. and Lu, C., 2007. Morphological and structural development of hardwood cellulose during mechanochemical pretreatment in solid state through pan-milling. *Cellulose*, 14(5), pp.447-456.
- [11] Singh, K., Risse, M., Das, K.C., Worley, J., 2009, "Determination of Composition of Cellulose and Lignin Mixtures Using Thermogravimetric Analysis," *Journal of Energy Resources Technology*, 131(2):022201-022201-6.
- [12] Brodeur, G., Yau, E., Badal, K., Collier, J., Ramachandran, K.B. and Ramakrishnan, S., 2011. Chemical and physicochemical pretreatment of lignocellulosic biomass: a review. *Enzyme research*, 2011.
- [13] Mood, S.H., Golfeshan, A.H., Tabatabaei, M., Jouzani, G.S., Najafi, G.H., Gholami, M. and Ardjmand, M., 2013. Lignocellulosic biomass to bioethanol, a comprehensive review with a focus on pretreatment. *Renewable and Sustainable Energy Reviews*, 27, pp.77-93.
- [14] Agbor, V.B., Cicek, N., Sparling, R., Berlin, A. and Levin, D.B., 2011. Biomass pretreatment: fundamentals toward application. *Biotechnology advances*, 29(6), pp.675-685.
- [15] 7. Agbor, V.B., Cicek, N., Sparling, R., Berlin, A. and Levin, D.B., 2011. Biomass pretreatment: fundamentals toward application. *Biotechnology advances*, 29(6), pp.675-685.
- [16] Li, J., Zhang, M. and Wang, D., 2018. Corn stover pretreatment by metal oxides for improving lignin removal and reducing sugar degradation and water usage. *Bioresource technology*, 263, pp.232-241.

- [17] N. Mosier, C. Wyman, B. Dale, R. Elander, Y.Y. Lee, M. Holtzapple, M. Ladisch, Features of Promising Technologies for Pretreatment of Lignocellulosic Biomass, *Bioresource Technology*, 96 (2005) 673-686
- [18] Brodeur, G., Yau, E., Badal, K., Collier, J., Ramachandran, K.B. and Ramakrishnan, S., 2011. Chemical and physicochemical pretreatment of lignocellulosic biomass: a review. *Enzyme research*, 2011.
- [19] Vidal, B.C., et al., Influence of feedstock particle size on lignocellulose conversion—a review. 2011. 164(8): p. 1405-1421.
- [20] Chundawat, S.P., et al., Effect of particle size based separation of milled corn stover on AFEX pretreatment and enzymatic digestibility. 2007. 96(2): p. 219-231.
- [21] Lamsal, B.P., R. Madl, and K.J.B.R. Tsakpunidis, Comparison of feedstock pretreatment performance and its effect on soluble sugar availability. 2011. 4(3): p. 193-200.
- [22] Zhang, M., et al., Biofuel manufacturing from woody biomass: effects of sieve size used in biomass size reduction. 2012. 2012.
- [23] Theerarattananoon, K., et al., Effects of the pelleting conditions on chemical composition and sugar yield of corn stover, big bluestem, wheat straw, and sorghum stalk pellets. 2012. 35(4): p. 615-623.
- [24] Sinitsyn, A., et al., Effect of structural and physico-chemical features of cellulosic substrates on the efficiency of enzymatic hydrolysis. 1991. 30(1): p. 43-59.
- [25] Zhang, P., et al. An experimental investigation on cellulosic biofuel manufacturing: effects of biomass particle size on sugar yield. in *ASME 2011 International Mechanical*

- Engineering Congress and Exposition. 2012. American Society of Mechanical Engineers Digital Collection.
- [26] Dasari, R.K. and R.E. Berson, The effect of particle size on hydrolysis reaction rates and rheological properties in cellulosic slurries, in *Applied biochemistry and biotechnology*. 2007, Springer. p. 289-299.
- [27] Zeng, M., et al., Microscopic examination of changes of plant cell structure in corn stover due to hot water pretreatment and enzymatic hydrolysis. 2007. 97(2): p. 265-278.
- [28] Zhu, J., C. Wan, and Y.J.B.t. Li, Enhanced solid-state anaerobic digestion of corn stover by alkaline pretreatment. 2010. 101(19): p. 7523-7528.
- [29] Lin, Z., Huang, H., Zhang, H., Zhang, L., Yan, L. and Chen, J., 2010. Ball milling pretreatment of corn stover for enhancing the efficiency of enzymatic hydrolysis. *Applied Biochemistry and Biotechnology*, 162(7), pp.1872-1880. doi.org/10.1007/s12010-010-8965-5
- [30] Fernandes, É.S., Bueno, D., Pagnocca, F.C. and Brienzo, M., 2020. Minor biomass particle size for an efficient cellulose accessibility and enzymatic hydrolysis. *ChemistrySelect*, 5(25), pp.7627-7631. doi.org/10.1002/slct.202001008
- [31] Pielhop, T., Amgarten, J., von Rohr, P.R. and Studer, M.H., 2016. Steam explosion pretreatment of softwood: the effect of the explosive decompression on enzymatic digestibility. *Biotechnology for Biofuels*, 9(1), pp.1-13. doi.org/10.1186/s13068-016-0567-1
- [32] De Assis, T., Huang, S., Driemeier, C.E., Donohoe, B.S., Kim, C., Kim, S.H., Gonzalez, R., Jameel, H. and Park, S., 2018. Toward an understanding of the increase

- in enzymatic hydrolysis by mechanical refining. *Biotechnology for Biofuels*, 11(1), pp.1-11. doi.org/10.1186/s13068-018-1289-3
- [33] Nguyen, T.A.D., Kim, K.R., Han, S.J., Cho, H.Y., Kim, J.W., Park, S.M., Park, J.C. and Sim, S.J., 2010. Pretreatment of rice straw with ammonia and ionic liquid for lignocellulose conversion to fermentable sugars. *Bioresource Technology*, 101(19), pp.7432-7438. doi.org/10.1016/j.biortech.2010.04.053
- [34] Ballesteros, I., Oliva, J.M., Negro, M.J., Manzanares, P. and Ballesteros, M., 2002. Enzymic hydrolysis of steam exploded herbaceous agricultural waste (*Brassica carinata*) at different particule sizes. *Process Biochemistry*, 38(2), pp.187-192. doi.org/10.1016/S0032-9592(02)00070-5
- [35] Chambon, C.L., Verdía, P., Fennell, P.S. and Hallett, J.P., 2021. Process intensification of the ionoSolv pretreatment: effects of biomass loading, particle size and scale-up from 10 mL to 1 L. *Scientific Reports*, 11(1), pp.1-15. doi.org/10.1038/s41598-021-94629-z
- [36] Dasari, R.K. and Berson, R.E., 2007. The effect of particle size on hydrolysis reaction rates and rheological properties in cellulosic slurries. In *Applied biochemistry and biotecnology* (pp. 289-299). Humana Press. doi.org/10.1007/978-1-60327-181-3_26
- [37] Dougherty, M.J., Tran, H.M., Stavila, V., Knierim, B., George, A., Auer, M., Adams, P.D. and Hadi, M.Z., 2014. Cellulosic biomass pretreatment and sugar yields as a function of biomass particle size. *Plos One*, 9(6), p.e100836. doi.org/10.1371/journal.pone.0100836
- [38] Weerachanchai, P., Leong, S.S.J., Chang, M.W., Ching, C.B. and Lee, J.M., 2012. Improvement of biomass properties by pretreatment with ionic liquids for

- bioconversion process. *Bioresource Technology*, 111, pp.453-459.
doi.org/10.1016/j.biortech.2012.02.023
- [39] Chang, V.S., Burr, B. and Holtzapple, M.T., 1997. Lime pretreatment of switchgrass. In *Biotechnology for fuels and chemicals* (pp. 3-19). Humana Press.. DOI: 10.1007/978-1-4612-2312-2_2
- [40] Zhang, P., Zhang, Q., Pei, Z.J. and Pei, L., 2011, January. An experimental investigation on cellulosic biofuel manufacturing: effects of biomass particle size on sugar yield. In *ASME International Mechanical Engineering Congress and Exposition* (Vol. 54891, pp. 321-326). doi.org/10.1115/IMECE2011-62721
- [41] Theerarattananoon, K., Xu, F., Wilson, J., Staggenborg, S., Mckinney, L., Vadlani, P., Pei, Z. and Wang, D., 2012. Effects of the pelleting conditions on chemical composition and sugar yield of corn stover, big bluestem, wheat straw, and sorghum stalk pellets. *Bioprocess and Biosystems Engineering*, 35(4), pp.615-623. doi.org/10.1007/s00449-011-0642-8
- [42] Kaar, W.E. and Holtzapple, M.T., 2000. Using lime pretreatment to facilitate the enzymic hydrolysis of corn stover. *Biomass and Bioenergy*, 18(3), pp.189-199. doi.org/10.1016/S0961-9534(99)00091-4
- [43] Karunanithy, C. and Muthukumarappan, K., 2011. Optimization of alkali, big bluestem particle size, and extruder parameters for maximum enzymatic sugar recovery using response surface methodology. *BioResources*, 6(1), pp.762-790.
- [44] Kapoor, M., Semwal, S., Satlewal, A., Christopher, J., Gupta, R.P., Kumar, R., Puri, S.K. and Ramakumar, S.S.V., 2019. The impact of particle size of cellulosic residue

- and solid loadings on enzymatic hydrolysis with a mass balance. *Fuel*, 245, pp.514-520. doi.org/10.1016/j.fuel.2019.02.094
- [45] Bahcegul, E., Apaydin, S., Haykir, N.I., Tatli, E. and Bakir, U., 2012. Different ionic liquids favor different lignocellulosic biomass particle sizes during pretreatment to function efficiently. *Green Chemistry*, 14(7), pp.1896-1903. DOI: 10.1039/C2GC35318K
- [46] M. Zeng, N.S. Mosier, C.P. Huang, D.M. Sherman, M.R. Ladisch, Microscopic Examination of Changes of Plant Cell Structure in Corn Stover due to Hot Water Pretreatment and Enzymatic Hydrolysis, *Biotechnology and Bioengineering*, 97 (2007) 265-278.
- [47] M. Yoshida, Y. Liu, S. Uchida, K. Kawarada, Y. Ukagami, H. Ichinose, S. Kaneko, K. Fukuda, Effects of Cellulose Crystallinity, Hemicellulose, and Lignin on the Enzymatic Hydrolysis of *Miscanthus Sinensis* to Monosaccharides, *Bioscience Biotechnology and Biochemistry*, 72 (2008) 805-810.
- [48] M. Zhang, X.H. Ju, X.X. Song, X. Zhang, Z.J. Pei, D.H. Wang, Effects of Cutting Orientation in Woody Biomass Size Reduction on Enzymatic Hydrolysis Sugar Yield, *Bioresource Technology*, 194 (2015) 407-410.
- [49] A.R. Esteghlalian, M. Bilodeau, S.D. Mansfield, J.N. Saddler, Do Enzymatic Hydrolyzability and Simons' Stain Reflect the Changes in the Accessibility of 606 Lignocellulosic Substrates to Cellulase Enzymes? *Biotechnology Progress*, 17 (2001) 1049-1054.

- [50] L. Segal, J.J. Creely, A.E. Martin Jr., C.M. Conrad,. An Empirical Method for Estimating the Degree of Crystallinity of Native Cellulose Using the X-ray Diffraction, *Textile Research Journal*, 29 (1959) 786-794.
- [51] S. Monavari, M. Galbe, G. Zacchi, Impact of Impregnation Time and Chip Size on Sugar Yield in Pretreatment of Softwood for Ethanol Production, *Bioresource Technology*, 100 (2009) 6312-6316.
- [52] I. Ballesteros, J.M. Oliva, A.A. Navarro, A. González, J. Carrasco, M. Ballesteros, Effect of Chip Size on Steam Explosion Pretreatment of Softwood, *Applied Biochemistry and Biotechnology*, 84-86 (2000) 97-110.
- [53] P.F. Zhang, T.W. Deines, D. Nottingham, Z.J. Pei, D. Wang, X. Wu, Ultrasonic Vibration-Assisted Pelleting of Biomass: A Designed Experimental Investigation on Pellet Quality and Sugar Yield, in: *Proceedings of the ASME 2010 International Manufacturing Science and Engineering Conference (MSEC)*, Erie, PA, 2010.
- [54] Cullis, I. F., Saddler, J. N., & Mansfield, S. D. (2004). Effect of initial moisture content and chip size on the bioconversion efficiency of softwood lignocellulosics. *Biotechnology and Bioengineering*, 85, 413–421.

Chapter 3 - Investigation on effect of particle size in biomass preprocessing

This work is published in the paper “A Comprehensive Investigation on the Effects of Biomass Particle Size in Cellulosic Biofuel Production” Yang Yang, Meng Zhang, and Donghai Wang, ASME Journal of Energy Resources Technology 140, no. 4 (2018).

Abstract

Biofuels derived from cellulosic biomass offer one of the best near- to mid-term alternatives to petroleum-based liquid transportation fuels. Biofuel conversion is mainly done through a biochemical pathway, on which size reduction, pelleting, pretreatment, enzymatic hydrolysis, and fermentation are main processes. The literature has studied the energy consumption in a step individually. However, none have included all conversion steps. There is no commonly accepted guidance to select the overall optimum particle size in order to minimize the energy consumption in preprocessing and maximize sugar yield in biochemical conversion. This study presents a comprehensive experimental investigation converting three types of biomass (big bluestem, wheat straw, and corn stover) into fermentable sugars and studies the effects of biomass particle size in size reduction and pelleting.

Key words:

Particle size, pre-processing, size reduction, energy consumption, densification

3.1 Introduction

Today’s economy and society are overwhelmingly reliant upon liquid transportation fuels. This reality will not change dramatically in the near future. However, over 90% of the liquid transportation fuel used in the U.S. is petroleum-based (gasoline and diesel) and more than half of the petroleum is imported. [1-4]. Meanwhile, consuming petroleum-based transportation

fuels contributes to the accumulation of greenhouse gases (CO₂, SO₂, and NO_x) in the atmosphere [5,6]. Therefore, it is imperative to develop alternative liquid transportation fuels that are domestically produced and environmentally friendly.

The second-generation biofuels produced from cellulosic biomass (forest and agricultural residues and dedicated energy crops) are alternatives to conventional transportation fuels. Compared to the first-generation biofuels (fuels produced from feedstocks such as corns and sugar canes, which can potentially be made into food/feed), producing biofuels from the inedible cellulosic biomass creates less competition with food/feed production for the limited agricultural farmland and other resources [3]. Producing and using cellulosic biofuels can turn residues and wastes into energy, enhance the nation's energy security, create new employment opportunities, and improve rural economies [6]. Cellulosic biofuel can be used on its own as a sustainable liquid transportation fuel or blended with conventional transportation fuel to meet the government's mandate of 16 billion gallons of cellulosic biofuel produced annually by 2022 in the Renewable Fuel Standard (RFS) as part of the Energy Independence and Security Act [7,8]. There are over 1 billion dry tons of cellulosic biomass that can be sustainably harvested in the U.S. every year. This amount is sufficient to produce 90 billion gallons of biofuel that can displace about 30% of the nation's current liquid fuel consumption annually [9]. Furthermore, cellulosic biofuel has the potential to reduce greenhouse gas emissions. Among all the other renewable energy sources, biomass is the only sustainable carbon carrier. Biomass grows by absorbing carbon dioxide, water, and nutrients and converts them into hydrocarbons through photosynthesis. When biomass is consumed as a fuel, carbon is cycled in the atmosphere [10].

The major steps of converting cellulosic biomass feedstocks into biofuels can be divided into the feedstock preprocessing stage conducted in a field or at a depot and the bioconversion

stage performed at a biorefinery. Size reduction is a necessary process with current conversion technologies, as raw cellulosic biomass feedstocks (such as the stems of herbaceous biomass or chunks of woody biomass) cannot be directly converted into biofuels efficiently [11,12]. This process decreases cellulosic biomass particle size by mechanical methods such as milling, cutting, and chipping. The large physical size and strong structure of cellulosic biomass make size reduction a highly energy-intensive process [13]. Pelleting applies mechanical forces to compress biomass particles produced by size reduction into uniformly sized pellets or briquettes. Pelleting can increase the volumetric density of biomass from 40-200 kg/m³ to 600-1400 kg/m³, which will significantly lower the cost and improve the feedstock flowability in biomass logistics [14,15].

This study investigated the effect of particle size on energy consumption of biomass size reduction and pelting. The impact from particle size to physical characteristics of the pellets were also studied. Three particle sizes (4, 2 and 1 mm) of big bluestem, wheat straw, and corn stover were produced by knife milling and were pelletized with an ultrasonic pelleting system.

3.2 Experimental Procedures and Parameter Measurements

3.2.1 Size reduction

All materials (whole stems) were processed through a knife mill (SM 2000, Retsch, Inc., Haan, Germany) powered by a 1.5 kW three-phase electric motor. The milling chamber of the knife mill is shown in Fig. 3. Three sieves with sizes of 4, 2, and 1 mm were used to control the particle size received. In each size reduction experiment, 100 g of biomass was gradually fed into the milling chamber. The knife mill was stopped after 10 seconds when all the biomass was loaded into the milling chamber. The weight of the particles collected was measured, and the size reduction time was recorded.

3.2.2 Pelleting

As illustrated in Fig. 3.1, cellulosic biomass particles were compressed into pellets using an ultrasonic machine. This process combines an ultrasonic generation system and a pneumatic loading system. The ultrasonic generation system (Stationary USM, Sonic-Mill, Albuquerque, NM, USA) converts the 60 Hz of power line frequency to 20 kHz of electrical power.

Afterwards, the 20 kHz electrical power is converted into mechanical vibration by a piezoelectric converter. The high frequency mechanical vibration is then amplified and transmitted to the end surface of the pelleting tool. Biomass particles were compressed into a pellet inside a mold with a cylindrical cavity of 20 mm diameter. The pelleting action is driven by a pneumatic cylinder. In this study, the compress air pressure for pelleting was set at 345 kPa (50 psi). The vibration amplitude of the pelleting tool is controlled by the power supply unit. In this study, the ultrasonic power was set at 50% (of the maximum ultrasonic power the power supply unit can generate), and the pelleting duration was kept at 90 seconds. Each pellet was made of 2 g of biomass. The moisture content of the biomass particles for pelleting was approximately 7% and pelleting experiments were conducted in ambient temperature (20-22°C).

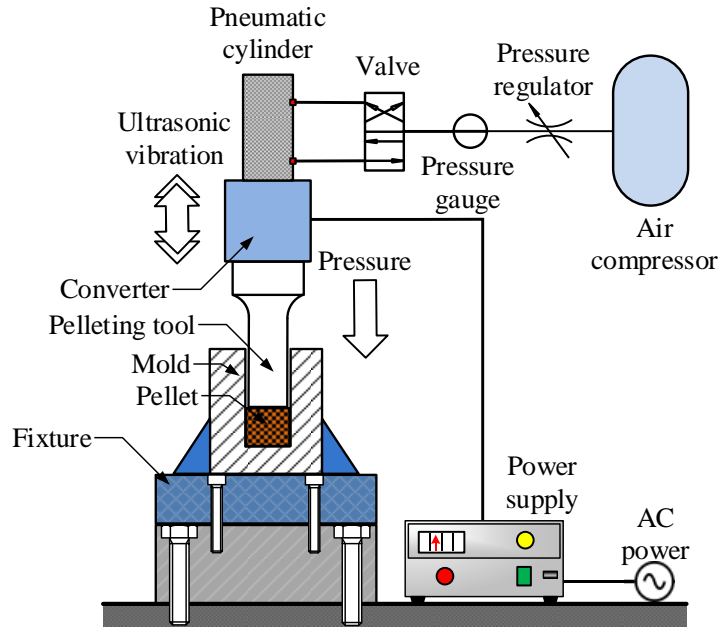


Figure 3.1. Schematic of the ultrasonic assisted pelleting process

3.2.3 Energy consumption measurement

Energy consumption in this investigation was the electrical energy consumed in size reduction and pelleting. A Fluke 189 multimeter and a Fluke 200 AC current clamp (Fluke Corp., Everett, WA, USA) were used to conduct the measurement. Current data was collected by the Fluke software. The sampling rate was two readings per second. The software recorded the average current (IAVG) in each test. The line-to-neutral voltage (V) did not fluctuate much during tests, so it was regarded as a constant of 120 V. The electrical energy consumed during each test (Et) was calculated using the following equations: size reduction (three-phase power) $E_t = \sqrt{3}I_{AVG} \cdot V \cdot t$ (J) and pelleting (single-phase power) $E_t = I_{AVG} \cdot V \cdot t$ (J). Dividing Et by the weight (w) of the biomass materials received after the tests gives energy consumption (E) per unit weight as $E = E_t(\text{kJ})/w(\text{g})$. For each experimental condition in size reduction and pelleting, eight independent energy consumption measurements were performed.

3.2.4 Pellet density and durability measurement

Pellet density and durability were employed to evaluate the pellet quality in this study. Density of a pellet was calculated by the ratio of its weight to its volume. Eight pellets were randomly chosen for density measurements. Three density values (initial density, out-of-mold density, and 24-h density) were measured for each pellet. The initial density was the pellet density at the end of each test while it was still in the mold. The inner diameter of the mold cavity was taken as the pellet diameter, and the pellet height was obtained from a digital readout attached on the pelleting tool. Out-of-mold density was the pellet density right after being unloaded from the mold, and 24-h density was the pellet density measured 24 hours after being unloaded. The latter two densities were measured to reflect the amount of spring-back (volume expansion) and the stability of a pellet during storage; these pellet dimensions were measured by a digital caliper. Durability tests were performed on an ASABE standard pellet durability tester (Seedburo Equipment Co., Des Plaines, IL, USA) (Fig. 3.2). First, test pellets (stored in ambient conditions for 24 hours) were loaded into the tester chamber. Then, the chamber was rotated at 50 rpm for 10 minutes. After each test, pellets were transferred and shaken through a U.S. No. 6 standard sieve to separate whole pellets from crumbs and loose particles. Durability is defined as the ability of densified pellets to remain intact when handled. The durability index was calculated as percentage between the mass pellets after and the mass of pellets before durability testing.



Figure 3.2. Durability tester

3.3 Experimental Results and Discussions

3.3.1 Effect of particle size on size reduction energy consumption

As shown in Figure 3.3, for all the biomass materials used in this study, size reduction energy consumption increased as biomass particle size decreased. This observed trend has been consistently reported in many studies with both the same size reduction equipment [16, 17-20] and other machines [21-25, 26-30]. In addition, to produce a specific amount of biomass particles of the same size, a size reduction machine with a higher power rating usually consumes less energy due to its higher material handling efficiency [17-20,26,31]. It was also noticed that when producing smaller biomass particles, the average current only increased slightly compared to that when producing larger biomass particles. The significant increase in energy consumption was mainly caused by the elongated time required to produce the same weight of biomass particles. In this study, for wheat straw and corn stover, the energy consumed to produce 1 mm biomass particles doubled the energy consumption to produce 2 mm particles. This significant increase in energy consumption when biomass particle size decreased from 2 mm to 1 mm was also reported when conducting size reduction of other biomass materials such as switchgrass [17-18], Miscanthus [17,18], and barley straw [24]. Comparatively, for every particle size produced,

big bluestem consumed the least amount of energy; producing 1 mm big bluestem only consumed 30% more energy than producing 2 mm big bluestem. It was observed that big bluestem particles had the best flowability amongst the three biomass materials. Particles smaller than the openings on the sieves could be discharged efficiently out of the milling chamber, which shortened the time required to produce the same amount of particles as required by the other two types. Contrarily, there is one report that found the opposite trend that producing larger particles consumed more energy [31]. This observation was mainly caused by the biomass flowability issue of larger particles (45 and 85 mm) in that they did not move through the grinder (HG-200, Vermeer Corp., Pella, IA, USA) as easily as the smaller particles (20 and 30 mm) [31].

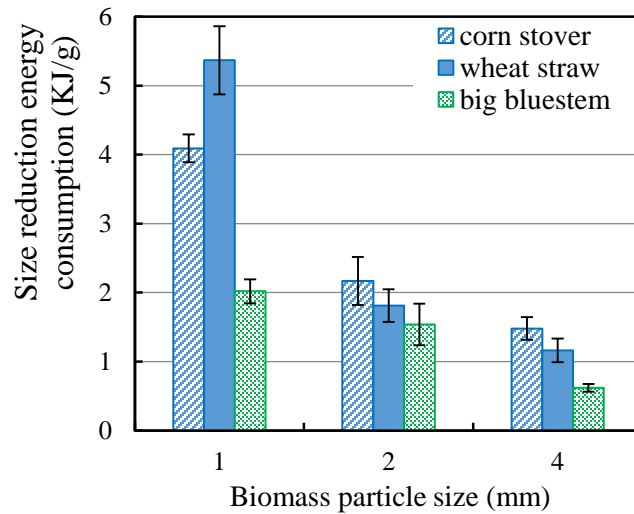


Figure 3.3. Effects of biomass particle size on size reduction energy consumption.

3.3.2 Effect of particle size on pelleting energy consumption

The effects of biomass particle size on pelleting energy consumption are shown in Figure 3.4. It was noticed that pelleting wheat straw particles consumed more energy than the other two materials. Pelleting 4 and 2 mm particles consumed more energy than pelleting 1 mm particles under the same conditions for wheat straw. This observation agreed with the predicted trend of

an empirical-model developed for this process [32]. Since larger biomass particles initially yield a lower bulk density of the particles in the mold and require more energy to be condensed into a pellet than do smaller particles [32]. For corn stover and big bluestem, biomass particle size did not significantly affect the pelleting energy consumption ($P>0.05$). Song et al. also found that the energy consumption did not change significantly when pelleting 0.45, 1, 2, and 4 mm particles; however, pelleting 8 mm particles consumed a larger amount of energy [33]. Svihus et al. [34] studied the effects of biomass particle size on pelleting energy consumption with a high capacity pelleting machine (RPM350, Münch-Edelstahl GmbH, Germany). The results indicated that there were no significant differences in energy consumption when pelleting 3 and 6.1 mm particles. Zhang et al. [35] also reported that the energy consumptions were approximately the same when pelleting 3.2 and 9.5 mm corn stover and sorghum stalk particles on a ring-die pelleting machine (CPM 2000, California Pellet Mill Co., Crawfordsville, IN, USA).

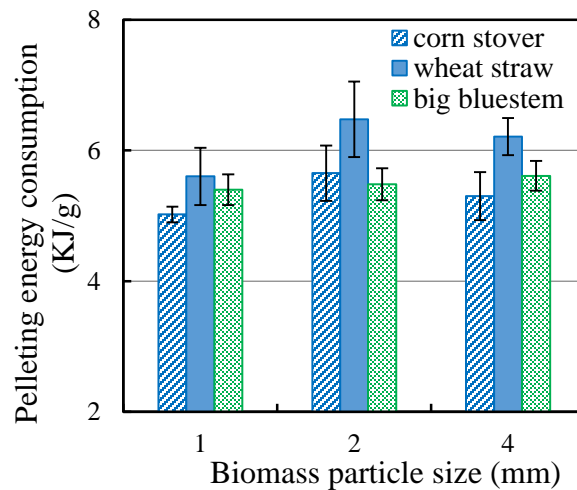


Figure 3.4. Effects of biomass particle size on pelleting energy consumption.

3.3.3 Effect of particle size on pellet density

The pellet density data is shown in Figure 3.5. Columns in the diagram show the out-of-mold density values. The upper bounds of the error bars are the initial density values and the lower bounds are the 24-h density values. It can be seen that pellets experienced a 15-25%

spring-back in their volumes when taken out of the mold. They became more stable over the next 24 hours with less than 5% spring-back occurring. Only for wheat straw pellets, the amount of spring-back increased as the particle size became larger. Wheat straw pellets had a much higher density than the other two materials, yet the density of corn stover pellets was the lowest. In general, pellets made from 2 mm particles had a slightly higher average density than that of pellets made from 1 mm particles; while pellets made from 4 mm particles had the lowest density amongst the three particle sizes. Mani et al. [36] examined the effects of compressive force, particle size, and moisture content on the density of pellets made from corn stover, wheat straw, barley straw, and switchgrass. It was found that all these variables significantly affected the pellet density, the only exception being that no significant effect was observed regarding particle size on wheat straw pellet density. Three particle sizes, 0.8, 1.6, and 3.2, were produced on a hammer mill, and smaller particles (except wheat straw) produced denser pellets. Mani et al. explained that different viscous and elastic characteristics of biomass materials contributed to the different densification behaviors since cellulosic biomass is often regarded as a viscoelastic material [37-39].

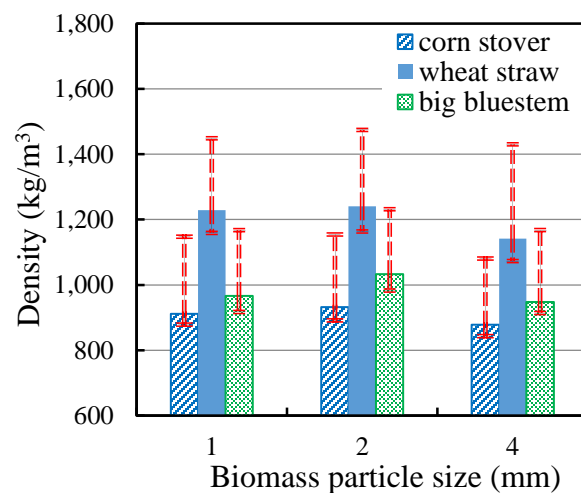


Figure 3.5. Effects of biomass particle size on pellet density. (Upper error bars represent the initial density and lower error bars represent the 24-h density)

3.3.4 Effect of particle size on pellet durability

Pellet durability results are shown in Figure 3.6. Pellets made from 1 and 2 mm biomass particles had similar durability, which was higher than that of pellets made from 4 mm biomass particles. Wheat straw pellets had the highest durability amongst the three biomass materials. Pellets made from 1 and 2 mm wheat straw particles had a nearly identical durability of 94%. The durability of pellets made from 4 mm wheat straw slightly decreased to 93%. Pellets made from 1 and 2 mm corn stover particles had a durability of 90%, and the durability decreased to 87% with 4 mm corn stover particles. Big bluestem pellets were less durable compared to the other two materials. Their durability results dropped from 86% to 80% as particle size increased from 1 to 4 mm. It has been broadly reported that finer particles generally correspond with greater durability as larger particles may serve as fissure points to initiate cracking or splitting in pellets [40]. With the same pelleting mechanism as used in this study, Zhang et al. by doing a full factorial design of experiments found that 2 mm wheat straw particles produced more durable pellets than 1 mm particles [41]. With conventional pelleting methods (without ultrasonic vibration), Singh and Kashyap reported that decreasing rice husk particle size from 5 to 4 mm increased pellet durability from 84% to 95% [42]. Franke and Rey found that the smallest particles in their study, ranging from 0.5 to 0.7 mm, were the most feasible in generating high quality pellets [43]. Hoover et al. reported that 4 mm corn stover particles produced pellets with a higher durability than the 6 mm particles [44]. In a study of alfalfa pellet durability, Hill and Pulkinen [45] noted that a decrease in particle size from 6.4 to 2.8 mm increased the durability by more than 15%. Several other researchers observed a mixture of particle sizes is more beneficial produce durable pellets. When being condensed, the mixture can increase the

inter-particle bonding and remove of inter-particle spaces more efficiently than uniformed particles [46].

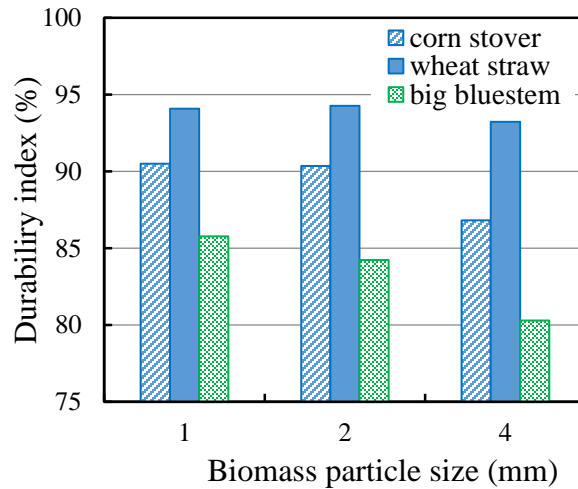


Figure 3.6. Effects of biomass particle size on pellet durability.

3.4 Conclusions

This study presented an experimental investigation on the effect of particle size in the biomass feedstock preprocessing stage with corn stover, wheat straw, and big bluestem.

Table 3.1 summarizes the effects of biomass particle size on various evaluation parameters in biomass preprocessing stage. The effects of particle size on biomass preprocessing critically depended on the biomass type. The following conclusions were drawn:

Table 3.1. Statistical analysis results on the effects of biomass particle size on the multistep bioethanol conversion (significant level is 0.05)

Biomass types	Size reduction energy consumption	Pelleting energy consumption	Pellet density
Big Bluestem	Significant	No significant	Not significant
Corn Stover	Significant	No Significant	Not significant
Wheat Straw	Significant	Significant	Not significant

(1) Generally, smaller particle tended to have better durability for all three type of materials.

(2) For big bluestem, particle size did not significantly affect pellet density and the energy consumption of pelleting.

(3) For corn stover, particle size negatively affected the energy consumption of size reduction significantly. Nevertheless, particle size did not have a significant impact on pellet density.

(4) For wheat straw, smaller particle size significantly increased the energy consumptions in size reduction and pelleting. However, particle size had no significant effects on pellet density.

Acknowledgement

This work is supported by the U.S. National Science Foundation (NSF) Award 1562671. The authors would like to acknowledge undergraduate research assistants Nick Eisenbarth, Lane Sorell, and Catharine Lei, for their help in conducting experiments and measurements for this work.

References

- [1] U.S. Energy Information Administration, 2017, “Monthly Energy Review,” <http://www.eia.gov/totalenergy/data/monthly/pdf/mer.pdf>.
- [2] BP, “BP Statistical Review of World Energy,” 2016, <https://www.bp.com/content/dam/bp/pdf/energy-economics/statistical-review-2016/bp-statistical-review-of-world-energy-2016-full-report.pdf>.
- [3] Huber, G.W., 2008, “Breaking the Chemical and Engineering Barriers to Lignocellulosic Biofuels: Next Generation Hydrocarbon Biorefineries” Based on the June 25-26, 2007 Workshop, Washington, DC: National Science Foundation, Chemical, Biengineering, Environmental and Transport Systems Division.

- [4] U.S. Energy Information Administration, 2013, “How Much Petroleum Does the United States Import and from Where?” <http://www.eia.gov/tools/faqs/faq.cfm?id=727&t=6>.
- [5] Bastani, P., Heywood, J.B., and Hope, C., 2012, “Fuel Use and CO2 Emissions Under Uncertainty From Light-Duty Vehicles in the U.S. to 2050,” *Journal of Energy Resources Technology*, 134(4):042202-042202-10.
- [6] Zhang, C., Ge, Y., Tan, J., Li, L., Peng, Z., and Wang, X., 2017, “Emissions From Light-Duty Passenger Cars Fueled With Ternary Blend of Gasoline, Methanol, and Ethanol,” *Journal of Energy Resources Technology*, 139(6):062202-062202-8.
- [7] Bracmort, K., 2015, “The Renewable Fuel Standard (RFS): Cellulosic Biofuels,” R41106, Congressional Research Service, <http://nationalaglawcenter.org/wp-content/uploads/assets/crs/R41106.pdf>.
- [8] Gouli, S.S., Serdari, A.A., Stournas, S.S., and Lois, E.E., 2000, “Transportation Fuel Substitutes Derived From Biomass,” *Journal of Energy Resources Technology*, 123(1):39-43.
- [9] U.S. Department of Transportation, 2010, “Transportation’s Role in Reducing U.S. Greenhouse Gas Emissions,” http://ntl.bts.gov/lib/32000/32700/32779/DOT_Climate_Change_Report_-_April_2010_-_Volume_1_and_2.pdf.
- [10] Brenes, M.D., 2006. “Biomass and Bioenergy: New Research,” Nova Science Publishers, Inc., ISBN: 1-59454-865-X.

- [11] Wei, L., Pordesimo, L.O., Igathinathane, C. and Batchelor, W.D., 2009. "Process Engineering Evaluation of Ethanol Production from Wood through Bioprocessing and Chemical Catalysis," *Biomass and Bioenergy*, 33(2), pp.255-266.
- [12] Kumar, P., Barrett, D.M., Delwiche, M.J. and Stroeve, P., 2009. "Methods for pretreatment of lignocellulosic biomass for efficient hydrolysis and biofuel production," *Industrial & engineering chemistry research*, 48(8), pp.3713-3729.
- [13] Zhu, W., Zhu, J.Y., Gleisner, R. and Pan, X.J., 2010. "On Energy Consumption for Size-reduction and Yields from Subsequent Enzymatic Saccharification of Pretreated Lodgepole Pine," *Bioresource Technology*, 101(8), pp.2782-2792.
- [14] Bergman, P.C.A., 2005. "Combined Torrefaction and Pelletisation. the TOP Process," Energy Centre of Netherlands, Report No. ECN-C-05-073.
- [15] Bergman, P.C., Boersma, A.R., Zwart, R.W.R. and Kiel, J.H.A., 2005. "Torrefaction for Biomass Co-Firing in Existing Coal-fired Power Stations," Energy Centre of Netherlands, Report No. ECN-C-05-013.
- [16] Zhang, M., Song, X., Deines, T.W., Pei, Z.J. and Wang, D., 2012, "Biofuel Manufacturing from Woody Biomass: Effects of Sieve Size Used in Biomass Size Reduction." *BioMed Research International*, 2012 (2012), pp. 581039.
- [17] Miao, Z., Grift, T.E., Hansen, A.C., and Ting, K.C., 2010, "Specific Energy Consumption of Biomass Particle Production and Particle Physical Property," The ASABE Annual International Meeting, Pittsburgh, PA; 20-23 June 2010, Paper Number: 1008497.

- [18] Miao, Z., Grift, T.E., Hansen, A.C., and Ting, K.C., 2011 “Energy Requirement for Comminution of Biomass in Relation to Particle Physical Properties,” *Industrial Crops and Products*, 33, pp. 504-513.
- [19] Deines, T.W., and Pei, Z.J., 2010, “Power Consumption Study in Knife Milling of Wheat Straw,” *Transactions of the North American Manufacturing Research Institution of SME*, 38, pp. 191-196.
- [20] Deines, T.W., Nottingham, D., Pei, Z.J., 2010, “Effects of Biomass Type and Sieve Size on Power Consumption in Knife Milling,” *Proceedings of the IIE Annual Conference and Expo 2010, Cancun, Mexico, June 5-9, 2010.*
- [21] Vidal, B.C., Dien, B.S., Ting, K.C. and Singh, V., 2011. “Influence of Feedstock Particle Size on Lignocellulose Conversion-A Review.” *Applied Biochemistry and Biotechnology*, 164(8), pp.1405-1421.
- [22] Cadoche, L. and López, G.D., 1989, “Assessment of Size Reduction as a Preliminary Step in the Production of Ethanol from Lignocellulosic Wastes,” *Biological Wastes*, 30(2), pp.153-157.
- [23] Schell, D.J. and Harwood, C., 1994, “Milling of Lignocellulosic Biomass,” *Applied Biochemistry and Biotechnology*, 45(1), pp.159-168.
- [24] Mani, S., Tabil, L.G. and Sokhansanj, S., 2004, “Grinding Performance and Physical Properties of Wheat and Barley Straws, Corn Stover and Switchgrass,” *Biomass and Bioenergy*, 27(4), pp.339-352.
- [25] Bitra, V.S., Womac, A.R., Chevanan, N., Miu, P.I., Igathinathane, C., Sokhansanj, S. and Smith, D.R., 2009, “Direct Mechanical Energy Measures of Hammer Mill

- Comminution of Switchgrass, Wheat straw, and Corn Stover and Analysis of their Particle Size Distributions,” Powder Technology, 193(1), pp.32-45.
- [26] Wright, C.T., Pryfogle, P.A., Stevens, N.A., Hess, J.R., and Radtke, C.W., 2006, “Value of Distributed Preprocessing of Biomass Feedstocks to a Bioenergy Industry,” Proceedings of the 2006 ASABE Annual International Meeting, Portland, OR, July 9-12, Paper number 066151
- [27] Arthur, J.F., Kepner, R.A., Dobie, J.B., Miller, G.E., and Parsons, P.S., 1982, “Tub Grinder Performance with Crop and Forest Residues,” Transactions of the ASABE. 25(6), pp. 1488-1494.
- [28] Himmel, M., Tucker, M., Baker, J., Rivard, C., Oh, K., and Grohmann, K., 1985, “Comminution of Biomass: Hammer and Knife Mills,” Biotechnology and Bioengineering Symposium, 15, pp. 39-58.
- [29] Ghorbani, Z., Masoumi, A.A., and Hemmat, A., 2010, “Specific Energy Consumption for Reduction the Size of Alfalfa Chops Using a Hammer Mill,” Biosystems Engineering, 105, pp. 34-40.
- [30] Womac, A.R., Igathinathane, C., Bitra, P., Miu, P., Sokhansanj, S., and Narayan, S., 2007, “Biomass Pre-processing Size Reduction with Instrumental Mills,” Proceedings of
- [31] Yancey, N.A., Wright, C.T., Conner, C.C., and Hess, J. R., 2009, “Preprocessing Moist Lignocellulosic Biomass for Biorefinery Feedstocks,” Proceedings of the 2009 ASABE Annual International Meeting, Reno, NV, June 21-24, No.08-14983

- [32] Song, X.X., Zhang, M., Pei, Z.J., and Wang, D.H., 2014, "Ultrasonic Vibration-assisted Pelleting of Wheat Straw: A Predictive Model for Energy Consumption Using Response Surface Methodology," *Ultrasonics*, 54(1), pp. 305-311.
- [33] Song, X.X., Zhang, M., Deines, T.W., Zhang, P.F., and Pei, Z.J., 2013, "Energy Consumption Study in Ultrasonic Vibration-assisted Pelleting Of Wheat Straw for Cellulosic Biofuel Manufacturing," *International Journal of Manufacturing Research*, 8(2), pp. 135-149.
- [34] Svihus, B., Kløvstad, K.H., Perez, V., Zimonja, O., Sahlström, S., Schüller, R.B., Jeksrud, W.K. and Prestløkken, E., 2004. "Physical and Nutritional Effects of Pelleting of Broiler Chicken Diets Made from Wheat Ground to Different Coarsenesses by the Use of Roller Mill and Hammer Mill," *Animal Feed Science and Technology*, 117(3), pp.281-293.
- [35] Zhang, Q., Zhang, P., Pei, Z.J., Wilson, J., McKinney, L. and Pritchett, G., 2011, "Ultrasonic-vibration assisted Pelleting for Cellulosic Ethanol Manufacturing: An Experimental Investigation of Power Consumption," ASME 2011 International Mechanical Engineering Congress and Exposition, Denver, Colorado, November 11-17, 2011, IMECE 2011-64307.
- [36] Mani, S., Tabil, L.G., Sokhansanj, S., 2006. "Effects of Compressive Force, Particle Size and Moisture Content on Mechanical Properties of Biomass Pellets from Grasses," *Biomass Bioenergy* 30 (7), 648–654.
- [37] Mani, S., Tabil, L.G. and Sokhansanj, S., 2003. "Compaction of Biomass Grinds-an Overview of Compaction of Biomass Grinds," *Powder Handling and Processing*, 15(3), pp.160-168.

- [38] Song, X.X., Zhang, M., Pei, Z.J., and Wang, D.H., 2015, "Ultrasonic Vibration-assisted (UV-A) Pelleting of Wheat Straw: a Constitutive Model for Pellet Density," *Ultrasonics*, 60, pp. 117-125.
- [39] Song, X.X., Yu, X.M., Zhang, M., Pei, Z.J., and Wang, D.H., 2014, "A Physics-based Temperature Model for Ultrasonic Vibration-assisted Pelleting of Cellulosic Biomass," *Ultrasonics*, 54(7), pp. 2042-2049.
- [40] McBain, R., 1966, "Pelleting Animal Feed," American Feed Manufacturers Association. Arlington, VA, USA.
- [41] Chundawat, S.P., Venkatesh, B. and Dale, B.E., 2007. "Effect of Particle Size Based Separation of Milled Corn Stover on AFEX Pretreatment and Enzymatic Digestibility," *Biotechnology and bioengineering*, 96(2), pp.219-231.
- [42] Singh, D., & Kashyap, M. M. 1985. "Mechanical and Combustion Characteristics of Paddy Husk Briquettes," *Agricultural Wastes*, 13(3), 189-196.
- [43] Franke, M., & Rey, A. 2006. "Pelleting Quality," *World Grain*, 24(5), 78-79.
- [44] Hoover, A.N., Tumuluru, J.S., Teymouri, F., Moore, J. and Gresham, G., 2014. "Effect of Pelleting Process Variables on Physical Properties and Sugar Yields of Ammonia Fiber Expansion Pretreated Corn Stover," *Bioresource technology*, 164, pp.128-135.
- [45] HILL, B., AND D.A. PULKINEN, 1988 "A Study of the Factors Affecting Pellet Durability and Pelleting Efficiency in the Production of Dehydrated Alfalfa Pellets," A Special Report, 25; Saskatchewan Dehydrators Association, Tisdale, SK, Canada.
- [46] PAYNE, J.D. 1978 "Improving Quality of Pelleted Feeds;" *Milling Feed and Fertilizer*, 161(5), pp.34-41.

Chapter 4 - Investigation on effect of particle size in biomass bioconversion process

This work is published in the paper “Effects of particle size on biomass pretreatment and hydrolysis performances in bioethanol conversion” Yang Yang, Jikai Zhao, Meng Zhang, and Donghai Wang, Journal of Biomass Conversion and Bio-refinery. 2022:PP 1-14

Abstract

Many studies have investigated how particle size as a biomass physical feature influences sugar yield exclusively in enzymatic hydrolysis. However, without considering the effects of particle size on biomass preprocessing and pretreatment, it is difficult to select an optimal particle size range for bioethanol production considering the multistep nature of this process. Comprehensive effects of particle size on biomass preprocessing, pretreatment, and enzymatic hydrolysis were evaluated in this study by assessing biomass compositional and morphological features, characterizing biomass crystallinity and enzyme-accessible surface area, and studying hydrolysis sugar yield and its efficiency. Results indicated that submillimeter small particles (0.5, 0.25, and <0.25 mm) experienced greater pretreatment severity and 5-10% more structural composition removal than their millimeter level counterparts (1-4 mm). Although small particles had about 10% higher enzymatic hydrolysis efficiency, the low pretreatment solid and sugar recoveries neutralized their enzymatic hydrolysis efficiency advantage over large particles. This trade-off suggested that there may exist little value in reducing particle size further under millimeter level, comparable total sugar yield can be achieved by biomass of millimeter particle sizes; in the meanwhile, employing millimeter particle sizes can conserve energy in biomass preprocessing since comminution is highly energy-intensive and costly.

Keywords

Bioethanol, biomass, enzymatic hydrolysis, particle size, pretreatment, sugar yield

4.1 Introduction

As the world gradually transitioning to the renewable sector for low-carbon energy resources, cellulosic biomass provides good sustainability for fuel production as an alternative to petroleum-based liquid transportation fuels. Effectively breaking down the polysaccharides in cellulosic feedstocks to fermentable monosaccharides is the key to economically producing bioethanol. Cellulosic biomass is the most abundant bioresource produced on earth, and it has three main components (by dry weight percentage): cellulose (40–50%), hemicellulose (25–30%), and lignin (15–20%). Cellulose is stabilized by hydrogen bonds and stacks as crystalline chains. Hemicellulose and lignin crosslink with cellulose chains to form micro-fibrils. This shielded network structure and the packed crystalline cellulose lead to the natural recalcitrance of raw biomass, which limits the efficiencies of processing and converting cellulosic biomass at all stages in bioethanol production [1].

In the multistep bioethanol production process, size reduction and pretreatment are performed prior to enzymatic hydrolysis, because the bulk raw biomass cannot be processed or converted to bioethanol efficiently. Reducing biomass particle size provides biomass with higher volumetric density, improved flowability, and better handling property in logistics [2]. Pretreatment alters the recalcitrance of cellulosic biomass natural structure and separates cellulose from the hemicellulose-lignin shield by breaking the bonds and linkages in the woven cell wall. The physical and chemical modifications caused by size reduction and pretreatment make biomass more accessible to enzymes in the subsequent enzymatic hydrolysis [3]. Through extensive studies, key physical and chemical features that impact biomass enzymatic digestibility have been identified. By classification, physical features include particle size, accessible surface area, and crystallinity. Chemical features are mainly referred to as the chemical composition

fractions of cellulose, hemicellulose, and lignin so as the characteristics of the bonds and linkages amongst the three biomass structural compositions [4].

The influences of biomass physical and chemical features on its enzymatic digestibility have been broadly reported in the literature. A high enzymatic digestibility can be achieved by favorably preparing a biomass substrate, so it has large enzyme-accessible surface area [5,6], low crystallinity [3,7], and low lignin or hemicellulose contents[4,8-10]. However, the reported correlations between biomass particle size and enzymatic digestibility are inconsistent. Positive (larger particle size has higher enzymatic digestibility), neutral (no significant correlation), and negative correlations (smaller particle size has higher enzymatic digestibility) have all been reported. When enzymatic hydrolysis is directly performed to digest untreated biomass, consistent results have been reported that biomass particle size has a negative correlation with enzymatic digestibility [11,12], but the correlation is rather weak. When biomass pretreatment is performed before hydrolysis, all three correlations positive, neutral [5,13], and negative [11,14] have been observed. Moreover, the effects of biomass particle size on enzymatic digestibility are mostly concluded by solely comparing enzymatic hydrolysis sugar yield. However, in pretreatment, the modifications of biomass physical features on a microscopic level (e.g., crystallinity reduction and accessible surface area increase) and chemical features (e.g., hemicellulose and lignin removal) are believed to have more direct and substantial impacts on biomass enzymatic digestibility, since the enzyme-accessibility enhancement by pretreatment is much more significant than that achieved by mechanical comminution (size reduction) [15].

Table 4.1 Reported correlations between particle size and sugar yield when different definitions are used

Sugar yield definition	Definition explanation	Correlation	Reference
Enzymatic hydrolysis efficiency	Percentage of grams of compound sugar digested to grams of fermentable sugar added to hydrolysis	Negative	[11,16-21]
		Positive	[22]
Enzymatic hydrolysis sugar yield	Grams of fermentable sugar yield per 1g of dry biomass added to hydrolysis	Negative	[14,23-25]
		Neutral	[13]
		Positive	[26,27]
Total sugar yield	Grams of fermentable sugar yield per 1g of dry biomass added to pretreatment	Negative	[28]
		Positive	[29,30]

In addition, sugar yield definitions used in the literature are found to be different, and this variation also caused the inconsistency in the reported correlations as summarized in Table 1.

Most studies reported the correlations by using enzymatic hydrolysis efficiency to investigate the percentage of compound sugar digested in hydrolysis; when this definition is used, it seems to be commonly agreed that compound sugar in small particles can be more efficiently digested into fermentable sugar than in large particles. When enzymatic hydrolysis sugar yield or total sugar yield definitions are used, inconsistent correlations have been reported. A higher enzymatic hydrolysis efficiency and enzymatic hydrolysis sugar yield of small particles do not necessarily mean small particles should be selected favorably in bioethanol production. The correlation in favor of small particles can be deceptive as small particles' advantage in hydrolysis can be outweighed by their drawbacks in pretreatment. For example, after dilute acid or steam explosion pretreatment, large particles usually have higher solid and sugar recoveries than small particles. So, if total sugar yield definition is used to consider the overall effects of particle size on pretreatment and hydrolysis, positive relationships are largely reported [29,30]. Moreover, size reduction is an energy-intensive process, more energy will be consumed to produce smaller particles [31,32]. Also, particle size ranges appeared to affect the comprehension of particle size

effects because particle size showed inconsistent effects when different particle size ranges (e.g., submillimeter vs. millimeter ranges) were used [11,32].

Wheat straw biomass was used in this study. Wheat is the world most widely grown crop [34]. About 400 million tons of wheat straw are globally available, which can be used in production of biofuels. About 100 billion liters of bioethanol are produced using wheat straw on an annual basis [35]. Dilute sulfuric acid pretreatment was selected in this study as it is the most widely used commercial pretreatment method because of its low cost and high efficiency in lignin removal [8]. The objective of this research is to comprehensively connect biomass particle size with its enzymatic digestibility by studying the effects of particle size on the modifications of biomass physical and chemical features. The effects of particle size on pretreatment sugar recovery, enzyme-accessible surface area, crystallinity, and biomass surface morphology were investigated. Considering pretreatment sugar recovery and total sugar yield, the necessity to conduct fine size reduction (submillimeter) was evaluated. A resource-efficient guidance for particle size selection was provided.

4.2 Experimental procedures and parameter measurements

4.2.1 Material preparation

The wheat straw material used in this study was collected from the East Central Kansas Experiment Field of Kansas Agricultural Experiment Station. The initial moisture content was approximately 8%. It was measured by following the NREL analytical procedure [36]. Biomass particles were prepared on a knife mill (SM 2000, Retsch, Inc., Germany) and separated on a sieve shaker (with 4, 2, 1, 0.5, 0.25 and <0.25 mm sieve openings) (RO-TAP, W.S. Tyler, Mentor, OH) to obtain different size levels. All the six size groups of biomass particles were

stored under a humidity-controlled condition. In the rest of the work, the sizes of the sieve openings will be referred to as particle sizes.

4.2.2 Pretreatment

Dilute sulfuric acid (2%) pretreatment was employed. For each pretreatment, a 10% solid loading (w/w) slurry with 20 g biomass and 200 ml dilute sulfuric acid were well mixed in a 600 mL glass liner and pretreated in a pressure reactor (4760A, Parr Instrument Co., Moline, IL) at 120 °C for 30 minutes. This condition was selected to limit the formation of sugar degradation products such as furfural and 5-hydroxymethylfurfural (HMF), which not only reduce pretreatment sugar recovery but also act as fermentation inhibitors. After pretreatment, the solid and liquid fractions were separated on suction filtration units. The solid fraction was washed with distilled water to remove inhibitors and residual acids. The distilled water used in washing was collected and combined with the supernatant of the pretreatment slurry. The combined liquid was then transferred and diluted into a 1 L volumetric flask for further composition analysis.

Pretreatment solid recovery rate (RS) is used to evaluate the solid weight recovery and loss during pretreatment. It is calculated as Eq. (1), where WAP is the biomass dry weight after pretreatment and WBP is biomass dry weight before pretreatment.

$$R_S(\%) = \frac{W_{AP}}{W_{BP}} \times 100 \quad \text{Eq. (1)}$$

Pretreatment sugar recovery is used to study how much compound sugars (cellulose and xylose) are recovered and remain in the solid fraction of the pretreated biomass. Composition analyses before and after pretreatment were executed by following NREL analytical procedure [38]. Cellulose and xylose recoveries (RC and RX) are calculated as shown in Eqs. (2) and (3), where AC and AX are the cellulose and xylose compositions (%) in the biomass after

pretreatment. A'_C and A'_X are the cellulose and xylan compositions (%) in the biomass before pretreatment.

$$R_C(\%) = \frac{W_{AP} \times A_C}{W_{BP} \times A'_C} \times 100 \quad \text{Eq. (2)}$$

$$R_X(\%) = \frac{W_{AP} \times A_X}{W_{BP} \times A'_X} \times 100 \quad \text{Eq. (3)}$$

Structural carbohydrates in pretreated and raw materials were measured on an HPLC (1200 HPLC, Agilent Technologies Inc., Santa Clara, CA) with an RCM-Monosaccharide Ca²⁺ (7.8×300 mm, Rezex) column. The total sugar, byproducts, and degradation products in the liquid fraction were measured with an Aminex HPX-87H ion exclusion column (7.8×300 mm, Bio-Rad) by following NREL analytical procedure [39].

4.2.3 Drying

Pretreated biomass samples were dried by two methods, including oven drying (105°C for 4 hours) and freeze drying (−80°C for 72 hours) to prepare them ready for subsequent analyses and measurements.

4.2.4 Enzymatic hydrolysis

Twenty milliliter of 5% solid loading (w/w) slurry was prepared with 1 g pretreated biomass (dry weight), 1 mL enzyme complex Accellerase 1500™ (DuPont Genencor Science, Wilmington, DL), and sodium acetate buffer solution (50 mM, pH 4.8, 0.02% sodium azide) in a 125 mL hydrolysis flask. The enzyme complex contains glucanase, β-glucosidase, xylanase, and β-xylosidase with an endoglucanase activity of 2200–2800 CMC U/g, a β-glucosidase activity of 450–775 pNPG U/g, a xylanase activity of 660 U/g, and a β-xylosidase activity of 60 U/g. Hydrolysis reaction was incubated at 50 °C in a water bath shaker operated at 110 rpm for 72 hours. The supernatant of each hydrolysis slurry sample (100 μL) was extracted every 12 hours.

After collection, the supernatant was mixed with distilled water at a ratio of 1:9 in 1.5 mL microcentrifuge tubes and boiled in a water bath (100°C) for 15 mins to inactivate enzymes. After that samples were centrifuged, filtered, and transferred into HPLC vials for sugar analysis.

The HPLC system was used to measure glucose and xylose concentrations in the hydrolysis slurry. Enzymatic hydrolysis sugar yields (YHG and YHX) were then calculated, as shown in Eqs. (4) and (5), to measure the amount of fermentable sugar (glucose and xylose) yield per unit dry weight of biomass,

$$Y_{HG}(\text{g}/1\text{g of biomass}) = \frac{C_G \times V}{W_H} \quad \text{Eq. (4)}$$

$$Y_{HX}(\text{g}/1\text{g of biomass}) = \frac{C_X \times V}{W_H} \quad \text{Eq. (5)}$$

where C_G and C_X are the concentration (g/L) of glucose and xylose detected by HPLC, V is the total volume (L) of the hydrolysis slurry, W_H is the dry weight (g) of the biomass loaded into the hydrolysis flask.

Enzymatic hydrolysis efficiencies (E_C and E_X) are expressed as the percentage of cellulose converted to glucose and the percentage of xylan converted to xylose by enzymatic hydrolysis, and they are calculated as Eqs. (6) and (7):

$$E_C(\%) = \frac{C_G \times V}{1.11 \times W_H \times A_C} \times 100 \quad \text{Eq. (6)}$$

$$E_X(\%) = \frac{C_X \times V}{1.14 \times W_H \times A_X} \times 100 \quad \text{Eq. (7)}$$

where, factors 1.11 and 1.14 are the cellulose-to-glucose and xylan-to-xylose conversion factors, respectively. These two factors reflect the weight gain when hydrolyzing compound sugars to fermentable sugars. Total sugar yields (TC) and (TX) provide interpretations about how much fermentable sugar (glucose and xylose) a unit dry weight of biomass (before pretreatment)

can yield through pretreatment and enzymatic hydrolysis combined. They are calculated as shown in Eqs. (8) and (9).

$$T_C(\text{g}/1\text{g of biomass}) = Y_{HG} \times R_S \quad \text{Eq. (8)}$$

$$T_X(\text{g}/1\text{g of biomass}) = Y_{HX} \times R_S \quad \text{Eq. (9)}$$

4.2.5 Accessible surface area

A modified Simon's stain method [37] was used to measure and quantitatively demonstrate the relative enzyme accessible surface area by comparing the amounts of dye solutions absorbed by pretreated biomass. Pontamine Fast Sky Blue 6 BX (FB) and Pontamine Fast Orange 6NR dyes (FO) (Sigma-Aldrich) were used to prepare the stain mixture. The orange dye solution was filtered with a 100K Amicon Ultra 15 mL centrifugal filter apparatus (Sigma-Aldrich). The top fraction in the filter was collected and dried to prepare the stain mixture. The blue dye has small molecular size and a low affinity towards cellulose. The orange dye has large molecular size and a much stronger affinity towards cellulose. If cellulose is shielded by hemicellulose and lignin, thus, pores on fiber wall are small, the small-molecular-sized blue dye can penetrate in and access cellulose, but the large-molecular-sized orange dye cannot. Cellulose then adsorbs only the blue dye. On the other hand, when the shield on cellulose is disrupted, and the pores on fiber wall are large enough for the orange dye to penetrate, cellulose adsorbs the orange dye preferentially because of the orange dye's stronger affinity to cellulose. It is also known that cellulosic biomass with larger pore size is more amenable in hydrolysis, with more available surface area for enzymes to access. It has been indicated that cellulosic biomass sample with higher orange dye adsorption has more enzyme accessible surface area in hydrolysis [35]. The stain process was performed on oven dried, freeze dried, and suction filtered pretreated biomass samples. For oven dried and freeze-dried samples, 100 mg pretreated biomass from each

particle size group was weighed and moved into separate centrifuge tubes. 1 mL of Simon's stain mixture was added together with distilled water to make up the volume of the sample mixture in the tube as 10.0 mL. For suction-filtered samples, moisture content was measured before creating the mixture. The amount of distilled water added to each sample varied according to the samples' moisture contents. These tubes were then incubated at 70 °C for 48 hours.

The concentrations of the blue and orange dyes remained in the stain solution were measured by performing UV spectrum scan of the supernatant on a spectrophotometer (Epoch 2, BioTek, Winooski, VT). The absorbance was read at 500 nm and 620 nm. The extinction coefficients (ϵ) for the blue and orange dyes were calculated by the established linear relationships between the absorbance and concentration of dye solutions. For each dye, absorbance measurements were conducted for five dye concentrations. The coefficients generated by regression are $\epsilon_B/500 = 7.35$, $\epsilon_B/620 = 28.5$, $\epsilon_O/500 = 39.62$, and $\epsilon_O/620 = 1.95$. The blue and orange dye concentrations (C_B and C_O) remained in the supernatant of each stain solution can be calculated with Eqs. (10) and (11) according to the Lamber-Beer law, where A is the absorption of mixed dye solution at 500 or 620 nm, and L is the optical path length.

$$A_{500} = \epsilon_{O/500}LC_o + \epsilon_{B/500}LC_B \quad \text{Eq. (10)}$$

$$A_{620} = \epsilon_{O/620}LC_o + \epsilon_{B/620}LC_B \quad \text{Eq. (11)}$$

4.2.6 Crystallinity

The degree of biomass crystallinity is determined by the ratio between crystalline and amorphous regions in biomass and expressed as crystallinity index (CrI) [3]. In this study, CrI was measured by an X-ray diffractometer (MiniFlex II, Rigaku Americas Corporation, Woodland, TX). Biomass samples were scanned at 1°/min from $2\theta = 10^\circ$ to 30° with a step size

of 0.02° . As shown in Eq. (12), I_{002} is the intensity of crystalline 002 peak at $2\theta = 22.5^\circ$. And I_{am} is the intensity of the amorphous band at $2\theta = 18.7^\circ$.

$$CrI = \frac{I_{002} - I_{am}}{I_{002}} \quad \text{Eq. (12)}$$

FTIR spectroscopy was also used to investigate the crystalline level of the biomass particles. The spectrometer (Spectrum 400 FT-IR, PerkinElmer Co., MA) recorded spectra in absorbance mode with wavenumber ranging from 400 to 4000 cm^{-1} . The detection resolution was 4 cm^{-1} in the absorbance mode with 16 scans per test. The spectrum of air was scanned as the background. The absorption bands at 1430 and 898 cm^{-1} were used to calculate the cellulose crystallinity index according to Eq. (13) [40], where LOI is lateral order index and A is the absorbance value of the corresponding band. Before tests, materials were size reduced to less than 0.2 mm on a cyclone mill.

$$LOI = \frac{A_{1430}}{A_{898}} \quad \text{Eq. (13)}$$

4.2.7 Surface morphology

Morphological images of raw and pretreated biomass samples were taken on a scanning electron microscope (S-3500N Hitachi High-Tech America, Inc., IL).

4.3 Experimental results and discussions

4.3.1 Effect of particle size on material composition

Compositions of unpretreated biomass particles were different across particle size groups in terms of carbohydrate and lignin fractions (Table 4.2). Compound sugars in the compositions before and after pretreatment are cellulose and hemicellulose; they are presented as potential fermentable monosaccharide equivalencies (cellulose as glucose and hemicellulose as xylose and arabinose) for easy comparisons with hydrolysis results. The 0.25 and <0.25 mm particle groups

had significantly less potential glucose, xylose, arabinose together with a lower lignin content. They were nearly 6%, 4%, 1% and 3% less than the structural carbohydrates in biomass particles from the 0.5 to 4 mm groups. Based on the observation under an optical microscope, a significant portion of larger particles were from the stem of wheat straw. Smaller particles were mostly from the leaves and veins of wheat straw. As wheat straw stem is richer in cellulose and lignin than leaves and veins, it is more rigid. This tenacious natural of stem consequently remains as larger particles and the less rigid leaf and vein portion is more likely to be ground into smaller particles during size reduction. This difference can lead to the composition variation amongst different particle size groups [41].

Table 4.2 Biomass composition before pretreatment

Particle size	Extraction recovery %	Glucose %*	Xylose %*	Arabinose %*	Lignin %	Ash %
4 mm	88.22±1.22 ^a	38.68±0.84 ^a	26.18±0.26 ^a	2.45±0.04 ^c	16.66±0.24 ^a	1.27±0.07 ^e
2 mm	85.36±3.12 ^{ab}	38.76±0.33 ^a	26.16±0.33 ^a	2.65±0.03 ^a	16.89±0.41 ^a	1.54±0.02 ^b
1 mm	84.23±2.54 ^{ab}	38.55±0.21 ^a	26.28±0.42 ^a	2.54±0.02 ^b	16.35±0.24 ^a	1.37±0.03 ^d
0.5 mm	80.15±3.87 ^{bc}	37.61±0.37 ^a	26.32±0.11 ^a	2.56±0.08 ^b	16.58±0.14 ^a	1.44±0.02 ^d
0.25 mm	74.96±4.32 ^{cd}	32.51±0.15 ^b	22.19±0.35 ^b	1.37±0.04 ^d	13.13±0.22 ^b	2.36±0.02 ^b
<0.25 mm	70.27±3.65 ^d	31.79±0.42 ^b	22.11±0.54 ^b	1.04±0.04 ^e	13.24±0.31 ^b	3.66±0.04 ^a

*Presented as fermentable sugar equivalency

The high extractive (substances extracted by distilled water and/or ethanol) contents in the smaller particle size groups was another possible reason causing the composition difference amongst particle size groups. As shown in Table 4.2, the ash content of unpretreated biomass particles increased as particle size decreased. After Soxhlet extraction with distilled water and ethanol, the structural composition recovery rates of 0.25 and <0.25 mm particles (70–75%) were significantly lower than those of wheat straw particles ranging from 0.5 to 4 mm (80–88%). This indicates that smaller particles had more non-structural substances to be extracted. Since

extractives (organic acids, wax, protein, fats etc.) only account a small portion (4.96%) of the washed wheat straw [42], soil could be the major extractives. USDA classified sands (<50–2000 μm), silts (<2–50 μm), and clays (<2 μm) as the major contents of soil [43]. Extractives originated from soil were more likely to fall into the smaller particle size groups on the sieve shaker; containing soil extractives consequently lowered the total potential carbohydrate contents in smaller biomass particle groups.

4.3.2 Effect of particle size on pretreatment

The main mechanism of dilute sulfuric acid pretreatment is to separate cellulose from the hemicellulose and lignin shield by breaking the bonds and linkages in the woven biomass cell wall structure, leaving most of the hemicellulose hydrolyzed into the liquid fraction of the pretreatment slurry. This effect resulted in solid loss and biomass composition change. In Table 4.3, a general trend was observed that smaller particles had lower pretreatment solid recovery. Due to the removal of most hemicellulose, the percentage of cellulose and lignin in the pretreated biomass increased. There was little difference in pretreated biomass compositions amongst particle size groups except for the <0.25 mm group, which had slightly lower cellulose but higher ash content. Similar trends have been reported by Chambon et al. when pretreating miscanthus biomass using low-cost ionic liquid triethylammonium hydrogen sulfate [22]. No significant difference was seen in cellulose recovery values for coarse ($\sim 3 \times 1 \times 1$ cm) and medium ($\sim 3 \times 0.02 \times 0.01$ cm) particles, while a slightly greater degree of cellulose loss was noted for fine (0.18–0.85 mm) particles. Other researchers reported that there was a significant decrease in particle size of sub-millimeter particles when they interacted with acid pretreatment [44,45]. This effect could lead to future decrease in pretreatment solid and sugar recoveries of sub-millimeter particles. Pretreatment sugar recovery and degradation results are detailed in Figure 4.1.

Structural composition recovery rates are shown in Figure 4.1A, where 0.25 and <0.25 mm particle size groups had significantly lower cellulose and lignin recoveries as reflected in their low solid recoveries (Table 4.3). This observation also indicates that smaller particles experienced greater pretreatment severity. As shown in Figure 1B, more xylose was hydrolyzed into the liquid fraction of the pretreatment slurry for smaller particles. However, the amount of inhibitor generation during pretreatment did not display a strong correlation with particle size groups (Figure 4.1C). This can be the result of the relative mild pretreatment temperature (120 °C) used in this study since inhibitor generation is more likely to occur under high pretreatment temperature (above 180 °C) condition for wheat straw [46].

Table 4.3 Pretreatment solid recovery and biomass composition after pretreatment

Particle size	Solid recovery %	Glucose %*	Xylose %*	Arabinose %*	Lignin %	Ash %
4 mm	44.22±1.85 ^a	54.80±0.81 ^a	13.34±0.14 ^a	3.13±0.05 ^e	27.97±0.27 ^b	0.73±0.01 ^e
2 mm	45.83±1.51 ^a	53.65±0.43 ^a	13.64±0.21 ^a	3.72±0.09 ^d	27.72±0.16 ^b	0.71±0.02 ^e
1 mm	43.98±1.04 ^a	53.99±0.27 ^a	12.29±0.24 ^b	4.61±0.04 ^c	27.85±0.36 ^b	0.88±0.02 ^d
0.5 mm	40.67±0.79 ^b	51.07±0.76 ^{ab}	13.45±0.38 ^a	4.98±0.05 ^b	26.07±0.77 ^c	2.50±0.02 ^c
0.25 mm	35.64±0.50 ^c	53.55±0.44 ^a	12.61±0.41 ^b	4.53±0.06 ^c	26.33±0.63 ^c	2.96±0.01 ^b
<0.25 mm	34.95±0.99 ^c	49.13±0.48 ^c	12.06±0.59 ^b	5.39±0.08 ^a	28.22±0.11 ^a	4.03±0.02 ^a

*Presented as fermentable sugar equivalency

4.3.3 Effect of particle size on hydrolysis efficiency and total sugar yield

Pretreated biomass was processed with two drying options including oven drying and freeze drying. A third control group of pretreated biomass that was never dried was also included for comparison. The moisture content in the never-dried biomass was counted as part of the hydrolysis buffer solution. Results of 72-hour glucose yield are shown in Figure 4.2. As indicated by their higher glucose yield in Figure 4.2A, smaller biomass particles from the never-dried group were more accessible to enzymes than larger particles. Similar trend can be observed

within all three groups (never-, oven-, and freeze-dried) when comparing their 12-hour hydrolysis glucose yield results in Figures 4.2B and 4.2C. This observation indicates that enzymatic hydrolysis of cellulose occurred more rapidly with smaller particles at the initial stage because smaller particles experienced greater pretreatment severity that tended to render biomass physical and chemical features for better enzymatic accessibility. The increased enzymatic accessibility of biomass substrates boosted a higher glucose yield. However, as enzymatic hydrolysis went on, only 0.25 mm biomass particles had a significant higher glucose yield than other particle size groups after 72 hours. After the easy-to-access portion of the pretreated biomass interacted with enzymes first, biomass with high recalcitrance remained, and the hydrolysis reaction slowed down and eventually reached equilibrium. As the hydrolysable amounts of cellulose from each particle size group were quite close to each other (Table 4.2), glucose yield results were consequently similar amongst particle size groups after 72 hours.

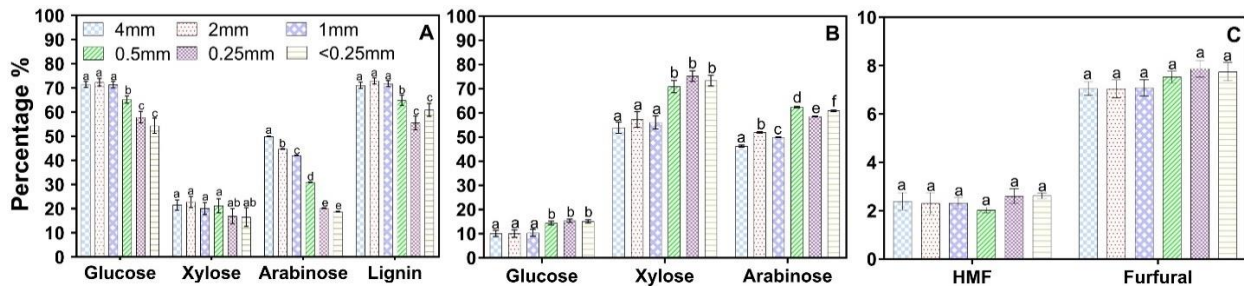


Figure 4.1. Pretreatment results: (A) total sugar recovery, (B) sugar degradation (B), and (C) hydroxymethylfurfural (HMF) and furfural formation

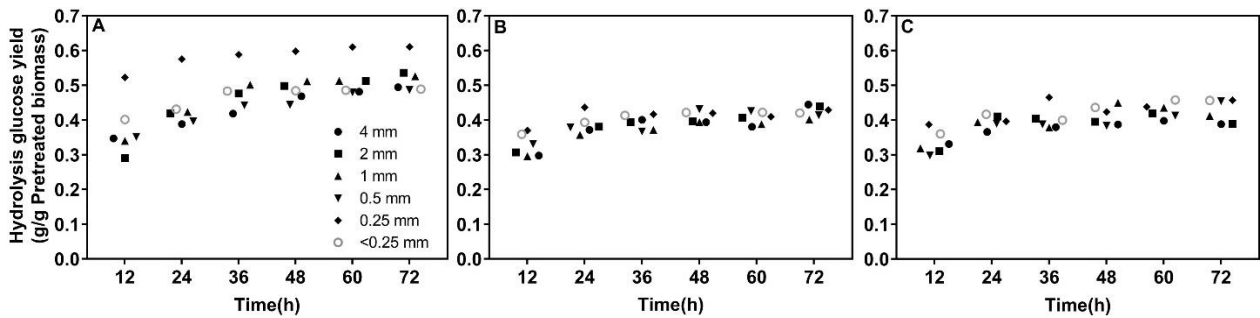


Figure 4.2. 72-hour hydrolysis sugar yield results: (A) never-dried, (B) oven-dried, and (C) freeze-dried biomass

When comparing hydrolysis sugar yield across the three groups prepared by different drying methods in Figure 4.2, it can be seen that the initial and equilibrium glucose yields were significantly impacted by drying methods. For both oven-dried and freeze-dried biomass, the initial hydrolysis sugar yields for smaller particles were still higher but the advantages over larger particles were not as significant as they were in the never-dried group. Moreover, the amount of glucose yields of both oven-dried and freeze-dried samples were much lower than those of the never-dried samples. This alternation of biomass pore structure by drying ultimately weakened or nearly neutralized the effects of particle size on pretreatment severity and the difference in enzyme accessible surface area created by different levels of pretreatment severity. It suggests that the collapse of large pores and small pore walls during drying consequently hindered the substrates' enzymatic accessibility. The drying processes that caused an irreversible physical contraction of the biomass cell wall has been mentioned as "fiber hornification" (the stiffening of the polymer structure that takes place in cellulosic materials upon drying) [47].

By comparing enzymatic hydrolysis efficiency, a trend can be seen from the unpretreated material group (raw) that smaller particles had higher enzymatic hydrolysis efficiencies and higher total sugar yields (Figure 4.3). After pretreatment, the enzymatic hydrolysis efficiencies (Figure 4.3B) of all groups were improved significantly. However, enzymatic hydrolysis efficiencies of particles in the submillimeter groups showed slight advantage. It is noted that for never-dried biomass, the highest enzymatic hydrolysis efficiency was not contributed by the smallest particles (<0.25 mm). Chambon et al. also reported that medium ($\sim 3 \times 0.02 \times 0.01$ cm) particles had a higher enzymatic hydrolysis efficiency than large ($\sim 3 \times 1 \times 1$ cm) and fine (0.18–

0.85 mm) particles. Dilute acid pretreatment removed the majority of hemicellulose and some of lignin. As shown in Table 4.3, hemicellulose removal was more effective for smaller particles, but lignin removal (delignification) showed a different trend: the smallest particles had the lowest delignification, but the 0.5 and 0.25 mm particles had the highest delignification. A similar observation was explained as the re-precipitation of lignin onto the large surface area of small particles during pretreatment led to the low delignification, and this suggests that the presence of lignin has a stronger negative effect on enzymatic hydrolysis efficiency than the positive effect of hemicellulose removal [22]. Vidal et al. discussed the concept of maximal particle size in pretreatment; that is the particle size below which no increase in pretreatment effectiveness was observed. For dilute acid pretreatment, this size is <3 mm (sieve opening) [15]. Supported by theoretical diffusion modeling done by Kim and Lee to examine the diffusivity of sulfuric acid in different biomass [48], if biomass particles are smaller than the critical particle sizes, diffusion is not an obstacle hindering pretreatment effectiveness. Critical particle sizes were calculated for four biomass feedstocks (switchgrass, straw, stover, and wood), ranging from 1.0 to 3.2 mm diameter (spherical geometry) or 0.3 to 1.1 mm thickness (plate geometry).

This discussion suggests that particle size had little effects when pretreatment was conducted as substrates of all range of particle sizes were rendered sufficiently susceptible to enzymatic hydrolysis. After taking pretreatment solid recovery into account, the low pretreatment solid recovery of small biomass particles further weakened their slight advantage in enzymatic hydrolysis efficiency. Total glucose yields amongst six biomass particle sizes of wheat straw showed no significant difference (p -value >0.05). There seemed to be little value of performing submillimeter size reduction. Particle size was a weak indicator of total sugar yield (fermentable sugar per gram of unpretreated biomass). These insights are in line with particle

size range of 2–6 mm recommended by Cadoche and López [49] and the roles of biomass particle size in pretreatment and enzymatic hydrolysis analyzed by Vidal et al [15].

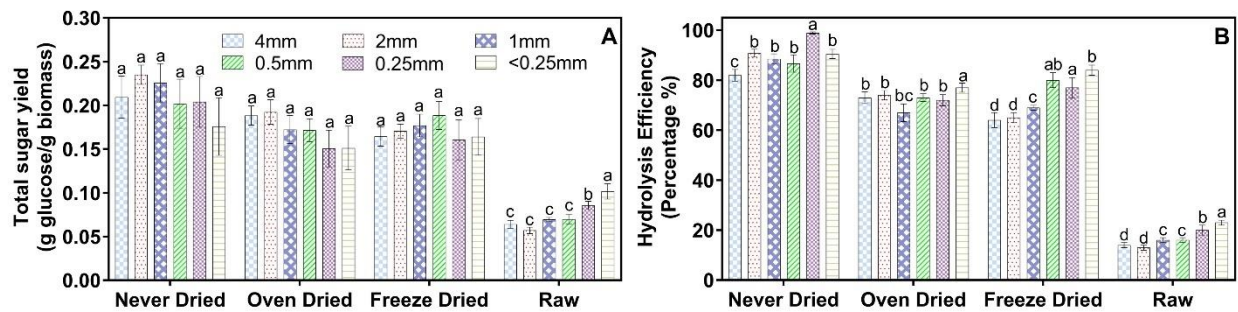


Figure 4.3. (A) 72-hour total sugar yield and (B) enzymatic hydrolysis efficiency

4.3.4 Effect of particle size on enzyme accessible surface area

Cellulase enzymes are measured to have a hydrodynamic radius bigger than 5 nm [50]. The hydrodynamic radius of the orange dye molecules (5–7 nm) is comparable to that of cellulase enzymes. Therefore, the capacity that a biomass sample absorbs the orange dye molecules can be used as a measurement of its accessibility to enzymes during hydrolysis. The blue dye consists of much smaller molecules than the orange dye. By adding the absorbing capacity of blue dye, the total dye absorption can be used to represent the total surface area of biomass substrates.

Table 4.4 Dye absorption results of Simon’s stain

Particle size	Oven-dried sample				Freeze-dried sample				Never-dried sample			
	Orange mg/g	Blue mg/g	Total mg/g	Ratio	Orange mg/g	Blue mg/g	Total mg/g	Ratio	Orange mg/g	Blue mg/g	Total mg/g	Ratio
4 mm	49.29	27.73	77.03	1.78	46.21	23.64	69.86	1.95	56.89	37.43	94.32	1.51
2 mm	47.39	25.24	72.63	1.88	47.62	25.64	73.27	1.86	53.11	32.09	85.21	1.65
1 mm	46.38	27.45	73.83	1.68	45.25	22.46	67.72	2.01	54.05	33.51	87.55	1.61
0.5 mm	48.34	26.52	74.86	1.82	47.63	25.77	73.41	1.85	56.42	36.71	93.13	1.53
0.25 mm	50.47	29.26	79.74	1.72	52.37	31.92	84.29	1.64	60.67	42.62	103.29	1.42
<0.25 mm	51.18	30.30	81.48	1.69	50.23	29.11	79.34	1.73	61.15	43.31	104.44	1.41

Absorptions of the two-color dyes in Simon's stain are compared across particle size groups in Table 4.4. A general trend can be observed that a greater amount of orange dye was absorbed by smaller particles in all the particle size groups. More specifically, orange dye absorption decreased first as particle size decreased from 4 to 1 mm and then increased as particle size kept decreasing to <0.25 mm. This change is followed by the change of lignin contents in different pretreated particle size groups shown in Figure 4.1A.

The reduction of particle size also brought changes to blue dye absorptions that higher blue dye absorptions were measured with smaller particles. This observation confirmed that reducing particle size affected both enzyme accessible surface area and total surface area of pretreated biomass. However, the impacts on these two categories of surface area were different. The ratio changes between orange dye and blue dye showed a different trend as compared to that of total absorption. The decreased ratio between orange dye and blue dye reflected that the increase of accessible surface area was rather limited by reducing particle size. Further size reduction mostly increased total surface area. This conclusion agreed with the changes of glucose yield through the 72-hour hydrolysis across all groups (Figure 2). As reducing particle size provided more total surface area, enzymes reached to accessible surface faster with smaller particles and achieved a significant higher initial glucose yield at the 12 hour. After hydrolysis reached equilibrium, only minor differences in glucose yield amongst groups could be observed due to the limited increase of enzyme accessible surface area.

Both oven-dried and freeze-dried biomass had lower dye absorption accompanied by their lower total sugar yield and enzymatic hydrolysis efficiency. Drying removes the water filled in the inherent capillaries in biomass cell walls and increases the extent of cross-linking in biomass microfibrils, which result in the collapse of pore structures and the reduction of dye

absorption. Park et al. reported that smaller pores are more resistant to pore collapse during drying than larger pores [51]. As a result, enzyme accessible surface area increased by size reduction was further weakened by drying.

4.3.5 Effect of particle size on crystallinity

Cellulose is the major crystalline portion in biomass. As the majority of amorphous hemicellulose and a portion of less rigid cellulose being broken down during dilute sulfuric acid pretreatment, crystallinity index (CrI) of pretreated biomass increased as shown in Table 5. This increase is consistent with reported trends in the literature [52]. For both oven-dried and freeze-dried samples, the crystallinity indexes of large biomass particles (4, 2, 1 mm) were lower than small particles (0.5, 0.25, <0.25 mm) due to the different pretreatment severities they experienced.

FTIR spectra are shown in Figure 4.4 The absorption band at 1430 cm^{-1} is assigned to a symmetric CH₂ bending vibration that represents crystalline Cellulose I. The band at 898 cm^{-1} is associated with the C-O-C stretching at β -(1 \rightarrow 4)-glycosidic linkage in amorphous Cellulose II [40]. After pretreatment, the amorphous fraction of cellulose was supposed to be removed. However, the signals of amorphous fraction related band of pretreated biomass still existed at 898 cm^{-1} . As shown in Figure 4.4 (A and C), the absorption band became even stronger compared to the untreated samples. The presence of amorphous Cellulose II at 898 cm^{-1} indicates that pretreatment promoted the conversion of Cellulose I to Cellulose II. With further inspection on absorption intensities of 4, 1 and 0.25 mm samples, particle size had limited effect on increasing the absorption band, but the intensity of signals was slightly weakened as particle size decreased according to the amorphous fraction related band at 898 cm^{-1} . This trend also

agreed with the results obtained by the XRD measurement in this work that particle size had a positive impact on removing amorphous fractions in pretreatment.

Table 4.5 XRD and FTIR crystallinity results

Particle size	Oven-dried sample		Freeze-dried sample		Unpretreated raw biomass	
	<i>CrI</i>	<i>LOI</i>	<i>CrI</i>	<i>LOI</i>	<i>CrI</i>	<i>LOI</i>
4 mm	59.52±2.10	1.22	55.28±2.90	1.21		
2 mm	59.95±3.20	1.30	56.34±2.60	1.28		
1 mm	56.27±3.10	1.29	55.86±2.30	1.29		
0.5 mm	60.36±2.80	1.29	59.48±1.10	1.31	49.92±1.4	1.45
0.25 mm	66.14±2.20	1.35	58.56±2.10	1.30		
<0.25 mm	62.21±1.30	1.38	57.22±2.30	1.34		

The signals of crystalline Cellulose I at 1430 cm⁻¹ were rather weak and there were not significant changes after pretreatment since the crystalline Cellulose I mostly maintained its integrity through pretreatment. There were notable signal peaks presented at around 2920 and 2850 cm⁻¹. They are related to the asymmetric and symmetric methyl and methylene stretching groups of cellulose. The appearance of these two peaks indicates that an increased amount of cellulose was exposed after pretreatment, attributing to a higher overall crystallinity. Based on the absorbance from FTIR spectra, LOI index was also calculated. It is an empirical crystallinity index used to compare the relative amounts of amorphous and crystalline cellulose in pretreated and unpretreated biomass. For both oven- and freeze-dried samples (Table 4.5.), LOI index slightly dropped comparing to unpretreated materials. The lower LOI index reflects crystallinity reduction of cellulose after pretreatment and also confirms the conversion of Cellulose I to Cellulose II. It is also observed that LOI index of larger particles are smaller. This observation, again, indicates a higher pretreatment severity was experienced by small particles. However, the degree of modifications on cellulose was rather similar despite different particle sizes were used.

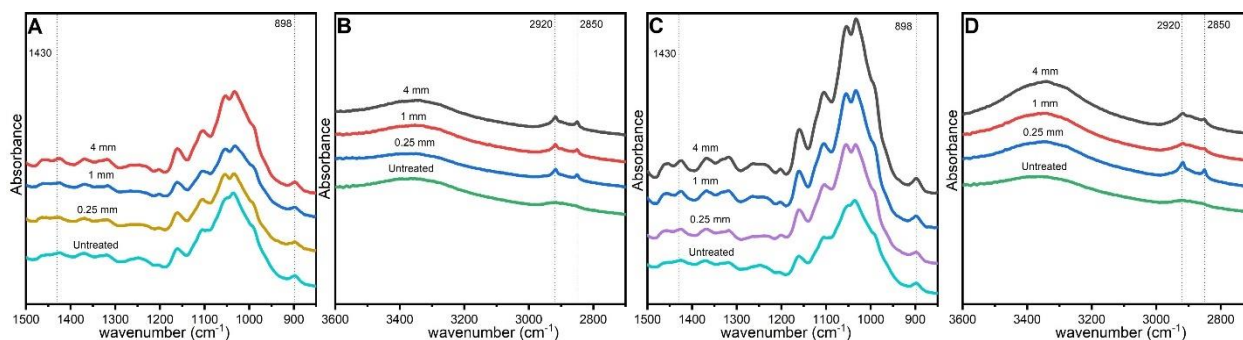


Figure 4.4. FTIR spectra of pretreated oven dried (A) (B) and freeze dried (C) (D) particles

When associating these observations with enzymatic hydrolysis results, crystallinity seems to be a secondary indicator of biomass enzymatic digestibility. After dilute acid pretreatment, biomass material became more cellulose-rich. The crystallinity of pretreated biomass may be slightly reduced, but the majority of pretreated biomass is still crystalline cellulose. The fact that hydrolysis sugar yield and enzymatic hydrolysis efficiency were still significantly increased over those of untreated biomass indicates that the crystallinity index is a weak indicator of biomass enzymatic digestibility. The bonds and crosslinks amongst cellulose, hemicellulose, and lignin in the biomass cell walls are the main recalcitrance that enzymes have to overcome to digest cellulosic biomass. With lignin, hemicellulose, and/or amorphous cellulose being removed by chemical pretreatments, biomass can be susceptible enough to enzymes, so that enzymes can interact with the substrates effectively, even it is characterized with a higher crystallinity index.

4.3.6 Effect of particle size on surface morphology

Figure 4.5 shows that both 0.25 and 1 mm untreated particles have smooth and compact surfaces. At higher magnifications (400× and 2000×), the surface morphologies are generally very similar. After pretreatment, Images A and D in Figures 6 and 7 reveal the dramatic morphological change. The surfaces of 0.25 and 1 mm pretreated particles became

rough and show cracks and fractures on the main particle body. At 400× magnification, Images B and E of Figures 4.6 and 4.7 show scale-like surface and expose some internal structure of the pretreated particles. This morphological change can be related to the biomass structural modification during pretreatment that disrupted biomass cell walls. When hemicellulose and/or lignin were removed during pretreatment, it left a significant number of voids and porosities in the cell walls (Images C and F in Figures 4.6 and 4.7) that provided more accessible area for enzymes to intact during hydrolysis. However, there was no significant difference between oven- and freeze-dried particle surfaces. The similar degree of surface-modifications of dried particles indicates that pretreatment effect on biomass morphology was determined by pretreatment condition predominately than biomass particle size.

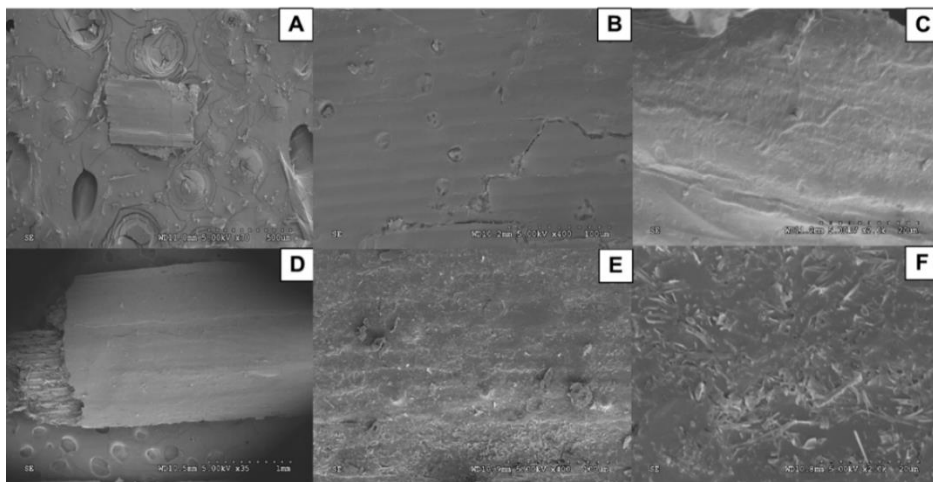


Figure 4.5. SEM images of unpretreated particles

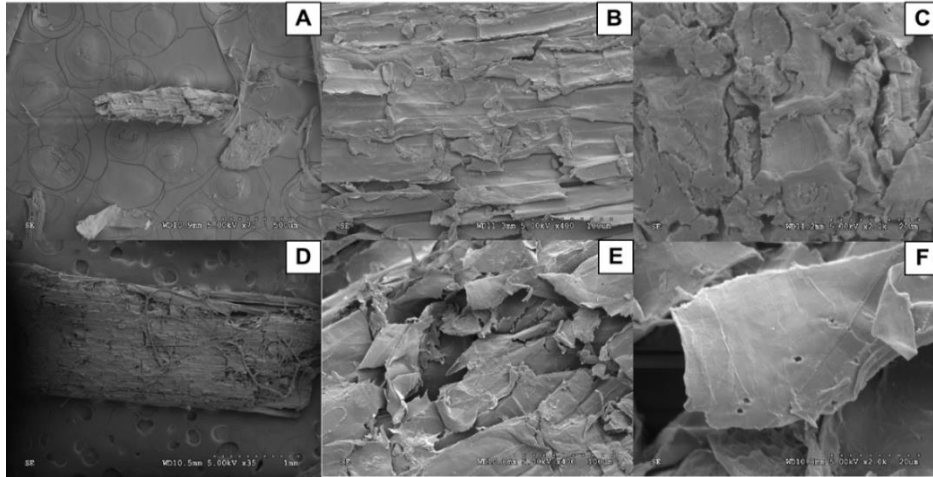


Figure 4.6. SEM images of oven-dried pretreated particles

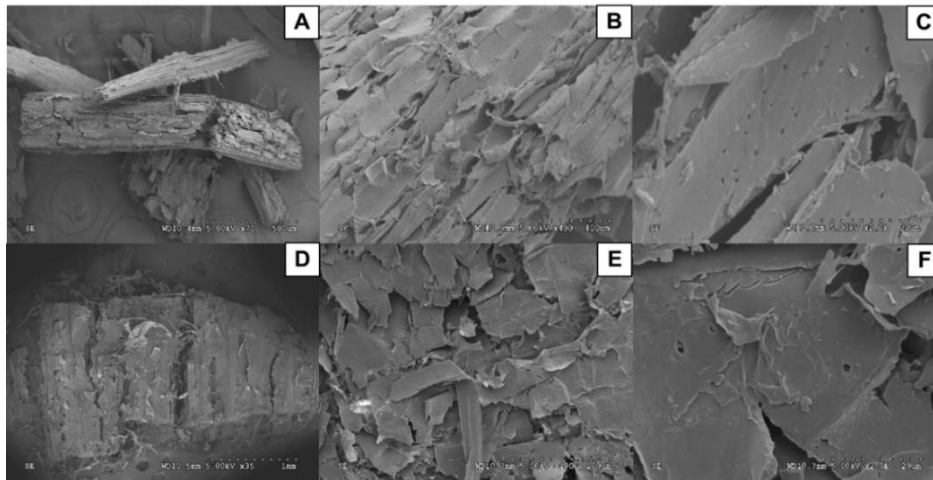


Figure 4.7. SEM images of freeze-dried pretreated particles

SEM images in Figures 5–7 are presented as 0.25 mm (A, B, C) and 1 mm (D, E, F) at 70 \times , 400 \times , and 2000 \times magnifications. Image D in each figure is at 35 \times for better illustration.

4.4 Conclusions

This study assessed how millimeter and submillimeter biomass particles performed during pretreatment and enzymatic hydrolysis. The following conclusions are drawn:

1. Size reduction (comminution) by itself was insufficient to attain economically feasible sugar yields. Unpretreated biomass has under 0.1 g total sugar per unit biomass and less than 20% of enzymatic hydrolysis efficiency.

2. Reducing particle size resulted in lower solid and cellulose recoveries but greater hemicellulose removal in pretreatment. Only 35% of the initial mass can be recovered in the pretreatment solid fraction for 0.25 and <0.25 mm particles and over 85% of the initial hemicellulose are decomposed during pretreatment.

3. Submillimeter particles showed slight advantage (<10%) over millimeter particles in enzymatic hydrolysis efficiency. The smallest particle size group (<0.25 mm) had the highest enzymatic hydrolysis efficiency for oven-dried and freeze-dried pretreated samples and unpretreated samples. For pretreated samples that were not dried, the 0.25 mm particle size group was the highest.

4. Submillimeter particles' advantage in enzymatic hydrolysis efficiency was outweighed by their low solid and sugar recoveries in pretreatment. Total sugar yields in the investigated six particle size groups showed no significant difference (p-value >0.05).

5. Enzyme-accessible surface area quantified by the orange dye absorption in Simons' stain technique could indicate the substrate's enzymatic hydrolysis efficiency and sugar yield. Whereas crystallinity index was a weak indicator of the substrate's susceptibility to enzymes.

6. Drying negatively impacted biomass enzymatic digestibility as it reduced enzyme-accessible surface area of dried biomass by collapsing its inherent pore structures.

Acknowledgement

This work was supported by the National Science Foundation of the U.S. through Award 1562671. The authors would like to acknowledge Dr. Jikai Zhao for the help in conducting experiments and measurements for this work.

References

- [1] Brodeur, G., Yau, E., Badal, K., Collier, J., Ramachandran, K.B. and Ramakrishnan, S., 2011. Chemical and physicochemical pretreatment of lignocellulosic biomass: a review. *Enzyme Research*, 2011. doi:10.4061/2011/787532
- [2] Hess, J.R., Wright, C.T. and Kenney, K.L., 2007. Cellulosic biomass feedstocks and logistics for ethanol production. *Biofuels, Bioproducts and Biorefining: Innovation for a sustainable economy*, 1(3), pp.181-190. doi.org/10.1002/bbb.26
- [3] Fan, L.T., Lee, Y.H. and Beardmore, D.H., 1980. Mechanism of the enzymatic hydrolysis of cellulose: effects of major structural features of cellulose on enzymatic hydrolysis. *Biotechnology and Bioengineering*, 22(1), pp.177-199. doi.org/10.1002/bit.260220113
- [4] Zhu, L., O'Dwyer, J.P., Chang, V.S., Granda, C.B. and Holtzaple, M.T., 2008. Structural features affecting biomass enzymatic digestibility. *Bioresource Technology*, 99(9), pp.3817-3828. doi.org/10.1016/j.biortech.2007.07.033
- [5] Sinitsyn, A.P., Gusakov, A.V. and Vlasenko, E.Y., 1991. Effect of structural and physico-chemical features of cellulosic substrates on the efficiency of enzymatic hydrolysis. *Applied Biochemistry and Biotechnology*, 30(1), pp.43-59. doi.org/10.1007/BF02922023
- [6] Zeng, M., Mosier, N.S., Huang, C.P., Sherman, D.M. and Ladisch, M.R., 2007. Microscopic examination of changes of plant cell structure in corn stover due to hot water pretreatment and enzymatic hydrolysis. *Biotechnology and Bioengineering*, 97(2), pp.265-278. doi.org/10.1002/bit.21298

- [7] Chang, V.S. and Holtzapple, M.T., 2000. Fundamental factors affecting biomass enzymatic reactivity. In Twenty-first symposium on biotechnology for fuels and chemicals (pp. 5-37). Humana Press, Totowa, NJ. DOI: 10.1007/978-1-4612-1392-5_1
- [8] Digman, M.F., Shinnars, K.J., Casler, M.D., Dien, B.S., Hatfield, R.D., Jung, H.J.G., Muck, R.E. and Weimer, P.J., 2010. Optimizing on-farm pretreatment of perennial grasses for fuel ethanol production. *Bioresource Technology*, 101(14), pp.5305-5314. doi.org/10.1016/j.biortech.2010.02.014
- [9] Zhu, J., Wan, C. and Li, Y., 2010. Enhanced solid-state anaerobic digestion of corn stover by alkaline pretreatment. *Bioresource Technology*, 101(19), pp.7523-7528. doi.org/10.1016/j.biortech.2010.04.060
- [10] Grohmann, K., Mitchell, D.J., Himmel, M.E., Dale, B.E. and Schroeder, H.A., 1989. The role of ester groups in resistance of plant cell wall polysaccharides to enzymatic hydrolysis. *Applied Biochemistry and Biotechnology*, 20(1), pp.45-61. doi.org/10.1007/BF02936472
- [11] Chundawat, S.P., Venkatesh, B. and Dale, B.E., 2007. Effect of particle size based separation of milled corn stover on AFEX pretreatment and enzymatic digestibility. *Biotechnology and Bioengineering*, 96(2), pp.219-231. doi.org/10.1002/bit.21132
- [12] Lamsal, B.P., Madl, R. and Tsakpundis, K., 2011. Comparison of feedstock pretreatment performance and its effect on soluble sugar availability. *Bioenergy Research*, 4(3), pp.193-200. doi.org/10.1007/s12155-010-9112-4
- [13] Zhang, P., Zhang, Q., Pei, Z.J. and Pei, L., 2011, January. An experimental investigation on cellulosic biofuel manufacturing: effects of biomass particle size on

- sugar yield. In ASME International Mechanical Engineering Congress and Exposition (Vol. 54891, pp. 321-326). doi.org/10.1115/IMECE2011-62721
- [14] Dasari, R.K. and Berson, R.E., 2007. The effect of particle size on hydrolysis reaction rates and rheological properties in cellulosic slurries. In *Applied biochemistry and biotechnology* (pp. 289-299). Humana Press. doi.org/10.1007/978-1-60327-181-3_26
- [15] Vidal, B.C., Dien, B.S., Ting, K.C. and Singh, V., 2011. Influence of feedstock particle size on lignocellulose conversion—a review. *Applied Biochemistry and Biotechnology*, 164(8), pp.1405-1421. doi.org/10.1007/s12010-011-9221-3
- [16] Lin, Z., Huang, H., Zhang, H., Zhang, L., Yan, L. and Chen, J., 2010. Ball milling pretreatment of corn stover for enhancing the efficiency of enzymatic hydrolysis. *Applied Biochemistry and Biotechnology*, 162(7), pp.1872-1880. doi.org/10.1007/s12010-010-8965-5
- [17] Fernandes, É.S., Bueno, D., Pagnocca, F.C. and Brienza, M., 2020. Minor biomass particle size for an efficient cellulose accessibility and enzymatic hydrolysis. *ChemistrySelect*, 5(25), pp.7627-7631. doi.org/10.1002/slct.202001008
- [18] Pielhop, T., Amgarten, J., von Rohr, P.R. and Studer, M.H., 2016. Steam explosion pretreatment of softwood: the effect of the explosive decompression on enzymatic digestibility. *Biotechnology for Biofuels*, 9(1), pp.1-13. doi.org/10.1186/s13068-016-0567-1
- [19] De Assis, T., Huang, S., Driemeier, C.E., Donohoe, B.S., Kim, C., Kim, S.H., Gonzalez, R., Jameel, H. and Park, S., 2018. Toward an understanding of the increase in enzymatic hydrolysis by mechanical refining. *Biotechnology for Biofuels*, 11(1), pp.1-11. doi.org/10.1186/s13068-018-1289-3

- [20] Nguyen, T.A.D., Kim, K.R., Han, S.J., Cho, H.Y., Kim, J.W., Park, S.M., Park, J.C. and Sim, S.J., 2010. Pretreatment of rice straw with ammonia and ionic liquid for lignocellulose conversion to fermentable sugars. *Bioresource Technology*, 101(19), pp.7432-7438. doi.org/10.1016/j.biortech.2010.04.053
- [21] Ballesteros, I., Oliva, J.M., Negro, M.J., Manzanares, P. and Ballesteros, M., 2002. Enzymic hydrolysis of steam exploded herbaceous agricultural waste (*Brassica carinata*) at different particule sizes. *Process Biochemistry*, 38(2), pp.187-192. doi.org/10.1016/S0032-9592(02)00070-5
- [22] Chambon, C.L., Verdía, P., Fennell, P.S. and Hallett, J.P., 2021. Process intensification of the ionoSolv pretreatment: effects of biomass loading, particle size and scale-up from 10 mL to 1 L. *Scientific Reports*, 11(1), pp.1-15. doi.org/10.1038/s41598-021-94629-z
- [23] Dougherty, M.J., Tran, H.M., Stavila, V., Knierim, B., George, A., Auer, M., Adams, P.D. and Hadi, M.Z., 2014. Cellulosic biomass pretreatment and sugar yields as a function of biomass particle size. *Plos One*, 9(6), p.e100836. doi.org/10.1371/journal.pone.0100836
- [24] Weerachanchai, P., Leong, S.S.J., Chang, M.W., Ching, C.B. and Lee, J.M., 2012. Improvement of biomass properties by pretreatment with ionic liquids for bioconversion process. *Bioresource Technology*, 111, pp.453-459. doi.org/10.1016/j.biortech.2012.02.023
- [25] Chang, V.S., Burr, B. and Holtzapple, M.T., 1997. Lime pretreatment of switchgrass. In *Biotechnology for fuels and chemicals* (pp. 3-19). Humana Press.. DOI: 10.1007/978-1-4612-2312-2_2

- [26] Theerarattananoon, K., Xu, F., Wilson, J., Staggenborg, S., Mckinney, L., Vadlani, P., Pei, Z. and Wang, D., 2012. Effects of the pelleting conditions on chemical composition and sugar yield of corn stover, big bluestem, wheat straw, and sorghum stalk pellets. *Bioprocess and Biosystems Engineering*, 35(4), pp.615-623.
doi.org/10.1007/s00449-011-0642-8
- [27] Kaar, W.E. and Holtzapple, M.T., 2000. Using lime pretreatment to facilitate the enzymic hydrolysis of corn stover. *Biomass and Bioenergy*, 18(3), pp.189-199.
doi.org/10.1016/S0961-9534(99)00091-4
- [28] Karunanithy, C. and Muthukumarappan, K., 2011. Optimization of alkali, big bluestem particle size, and extruder parameters for maximum enzymatic sugar recovery using response surface methodology. *BioResources*, 6(1), pp.762-790.
- [29] Kapoor, M., Semwal, S., Satlewal, A., Christopher, J., Gupta, R.P., Kumar, R., Puri, S.K. and Ramakumar, S.S.V., 2019. The impact of particle size of cellulosic residue and solid loadings on enzymatic hydrolysis with a mass balance. *Fuel*, 245, pp.514-520. doi.org/10.1016/j.fuel.2019.02.094
- [30] Bahcegul, E., Apaydin, S., Haykir, N.I., Tatli, E. and Bakir, U., 2012. Different ionic liquids favor different lignocellulosic biomass particle sizes during pretreatment to function efficiently. *Green Chemistry*, 14(7), pp.1896-1903. DOI:
10.1039/C2GC35318K
- [31] Yang, Y., Zhang, M. and Wang, D., 2018. A Comprehensive Investigation on the Effects of Biomass Particle Size in Cellulosic Biofuel Production. *Journal of Energy Resources Technology*, 140(4). doi.org/10.1115/1.4039602

- [32] Miao, Z., Grift, T.E., Hansen, A.C. and Ting, K.C., 2011. Energy requirement for comminution of biomass in relation to particle physical properties. *Industrial Crops and Products*, 33(2), pp.504-513. doi.org/10.1016/j.indcrop.2010.12.016
- [33] Hsu, T.A., Himmel, M., Schell, D., Farmer, J. and Berggren, M., 1996. Design and initial operation of a high-solids, pilot-scale reactor for dilute-acid pretreatment of lignocellulosic biomass. In *Seventeenth Symposium on Biotechnology for Fuels and Chemicals* (pp. 3-18). Humana Press, Totowa, NJ. DOI: 10.1007/978-1-4612-0223-3_1
- [34] Talebnia, F., Karakashev, D. and Angelidaki, I., 2010. Production of bioethanol from wheat straw: an overview on pretreatment, hydrolysis and fermentation. *Bioresource Technology*, 101(13), pp.4744-4753. doi.org/10.1016/j.biortech.2009.11.080
- [35] Srivastava, N., Shrivastav, A.K., Srivastava, M. and Mishra, P.K., 2020. Biofuels production using wheat straw. In *Recent Developments in Bioenergy Research* (pp. 433-441). Elsevier. doi.org/10.1016/B978-0-12-819597-0.00029-5
- [36] Sluiter, A., Hames, B., Hyman, D., Payne, C., Ruiz, R., Scarlata, C., Sluiter, J., Templeton, D. and Wolfe, J., 2008. Determination of total solids in biomass and total dissolved solids in liquid process samples. *National Renewable Energy Laboratory*, 9, pp.1-6.
- [37] Chandra, R., Ewanick, S., Hsieh, C. and Saddler, J.N., 2008. The characterization of pretreated lignocellulosic substrates prior to enzymatic hydrolysis, part 1: a modified Simons' staining technique. *Biotechnology progress*, 24(5), pp.1178-1185. doi.org/10.1002/btpr.33

- [38] Sluiter, A., Hames, B., Ruiz, R., Scarlata, C., Sluiter, J., Templeton, D. and Crocker, D.L.A.P., 2010. Determination of structural carbohydrates and lignin in biomass. Laboratory analytical procedure, (TP-510-42618).
- [39] Sluiter, A., Hames, B., Ruiz, R., Scarlata, C., Sluiter, J. and Templeton, D., 2006. Determination of sugars, byproducts, and degradation products in liquid fraction process samples. Golden: National Renewable Energy Laboratory, 11, pp.65-71.
- [40] Dumitriu, S. ed., 2004. Polysaccharides: structural diversity and functional versatility. CRC Press.
- [41] Alvo, P. and Belkacemi, K., 1997. Enzymatic saccharification of milled timothy (*Phleum pratense* L.) and alfalfa (*Medicago sativa* L.). *Bioresource Technology*, 61(3), pp.185-198.. doi.org/10.1016/S0960-8524(97)00068-0
- [42] Lu, Y.C., Lu, Y., Lu, Z.L. and Wei, X.Y., 2017. Detailed componential characterization of extractable species with organic solvents from wheat straw. *International Journal of Analytical Chemistry*, 2017. doi.org/10.1155/2017/7305682
- [43] Katz, B.S., 2014. Analysis of chemical storage and transit times to characterize water movement through a thick unsaturated zone overlying the High Plains aquifer, northwestern Kansas (Doctoral dissertation, University of Kansas).
- [44] Wang, W., Chen, X., Donohoe, B.S., Ciesielski, P.N., Katahira, R., Kuhn, E.M., Kafle, K., Lee, C.M., Park, S., Kim, S.H. and Tucker, M.P., 2014. Effect of mechanical disruption on the effectiveness of three reactors used for dilute acid pretreatment of corn stover Part 1: chemical and physical substrate analysis. *Biotechnology for Biofuels*, 7(1), pp.1-13. doi.org/10.1186/1754-6834-7-57

- [45] Zhao, J., Xu, Y., Wang, W., Griffin, J. and Wang, D., 2020. Conversion of liquid hot water, acid and alkali pretreated industrial hemp biomasses to bioethanol. *Bioresource Technology*, 309, p.123383. doi.org/10.1016/j.biortech.2020.123383
- [46] Rajan, K. and Carrier, D.J., 2014. Effect of dilute acid pretreatment conditions and washing on the production of inhibitors and on recovery of sugars during wheat straw enzymatic hydrolysis. *Biomass and Bioenergy*, 62, pp.222-227. doi.org/10.1016/j.biombioe.2014.01.013
- [47] Welf, E.S., Venditti, R.A., Hubbe, M.A. and Pawlak, J.J., 2005. The effects of heating without water removal and drying on the swelling as measured by water retention value and degradation as measured by intrinsic viscosity of cellulose papermaking fibers. *Progress in Paper Recycling*, 14(3), pp.1-9.
- [48] Kim, S.B. and Lee, Y.Y., 2002. Diffusion of sulfuric acid within lignocellulosic biomass particles and its impact on dilute-acid pretreatment. *Bioresource Technology*, 83(2), pp.165-171. doi.org/10.1016/S0960-8524(01)00197-3
- [49] Cadoche, L. and López, G.D., 1989. Assessment of size reduction as a preliminary step in the production of ethanol from lignocellulosic wastes. *Biological Wastes*, 30(2), pp.153-157. doi.org/10.1016/0269-7483(89)90069-4
- [50] Grethlein, H.E., 1985. The effect of pore size distribution on the rate of enzymatic hydrolysis of cellulosic substrates. *Bio/technology*, 3(2), pp.155-160. doi.org/10.1038/nbt0285-155
- [51] Park, S., Venditti, R.A., Jameel, H. and Pawlak, J.J., 2006. Changes in pore size distribution during the drying of cellulose fibers as measured by differential scanning

calorimetry. Carbohydrate polymers, 66(1), pp.97-103.

doi.org/10.1016/j.carbpol.2006.02.026

[52] Li, C., Knierim, B., Manisseri, C., Arora, R., Scheller, H.V., Auer, M., Vogel, K.P.,

Simmons, B.A. and Singh, S., 2010. Comparison of dilute acid and ionic liquid

pretreatment of switchgrass: biomass recalcitrance, delignification and enzymatic

saccharification. Bioresource technology, 101(13), pp.4900-4906.

doi.org/10.1016/j.biortech.2009.10.066

Chapter 5 - Literature review of utilizing biomass as solid fuel

Abstract

The U.S. is sustainably producing of over 1 billion dry tons of biomass annually. This amount of biomass is sufficient to produce bioenergy that can replace about 30 percent of the nation's current annual consumption of conventional fossil fuels. This then gives us the opportunity to turn waste into bioenergy that can assist in meeting the U.S. Renewable Fuel Standard (RFS). Besides being converted into bioethanol through the biochemical platform, biomass can also be utilized solid fuels to generate bioenergy through the thermochemical platform. Co-firing power plants use torrefied biomass pellets combined with coal for electricity generation. Upstream and downstream operations are two current solutions to produce torrefied pellets in separated steps. Torrefaction followed by pelleting or torrefaction after pelleting, are the prevailing technique that the industry is currently using to produce torrefied biomass pellets. Torrefaction converts biomass into biochar with high heating value, and pelleting densifies torrefied biochar into pellets with high durability and density.

5.1 Introduction

Bioenergy derived from cellulosic biomass (forest and agricultural residues and dedicated energy crops) has been recognized as promising alternatives to fossil fuels. Raw biomass has very low bulk density, low energy content, high moisture content, and hydrophilic nature. Such properties result in the high cost of biomass transportation, handling and storage which hinged its application either on the biochemical or thermochemical platform [1]. In order to address these problems, biomass needs to be preprocessed or pretreated before it can be used as an efficient bioenergy source. Handling, storage, and transportation cost can be lowered by increasing the density via consolidating biomass into pellets. Dense pellets require less space for storage and

transport than loose biomass [2, 3]. Density of pelleted biomass can be 600-800 kg/m³, which is much higher than the bulk density of loose biomass (40-250 kg/m³). Furthermore, cost of transportation, handling, storage pelleted biomass is also much lower than that of baled or chopped biomass [4]. Meanwhile, pellets with the uniform size and shape are easier to handle using existing grain handling and storage infrastructures, such as elevators, hoppers and conveyor belts.

Co-firing is regarded as a great opportunity for replacing solid fossil fuel used for power generation with renewable bioenergy (biomass) with lower costs and a direct decrease in greenhouse gas emissions [5]. Torrefaction has been proposed as an alternate to improve the thermochemical and hygroscopic properties of biomass [6, 7]. Co-firing power plants use torrefied biomass pellets combined with coal for electricity generation. A two-step process, torrefaction followed by pelleting, is the prevailing technique that the industry is currently using to produce torrefied biomass pellets [8]. During torrefaction process, biomass is heated in a closed atmosphere at temperature of about 200-320°C for a torrefaction time of 30 mins to a couple hours. During the torrefaction process, the water contained in the biomass as well as superfluous volatiles are released, and the biopolymers (cellulose, hemicellulose, and lignin) partly decompose, giving off various types of volatiles. The final product is the remaining solid, dry, and charred material with high heating value, which is referred to as torrefied biomass or biochar. [7]. Other advantages associated with torrefied biomass include more homogeneous composition, reduced moisture content, improved resistance to water absorption and microbial growth. After the biomass is torrefied, it is densified into pellets using conventional densification equipment (i.e. a screw extruder, a briquetting press, a rolling machine, or a ring-die pelleting

machine), to increase its mass and energy density and to improve its hydrophobic properties [9, 10].

5.2 Torrefaction

Torrefaction is a mild thermal treatment that enhances the properties of cellulosic biomass as a fuel [11]. Cellulosic biomass is heated in an inert atmosphere at temperatures ranging from 200 to 300 °C for 30 minutes to several hours. During this process, removal of the volatile substances with lower heat value leads to an increased energy density of torrefied cellulosic biomass closer to that of coal [12,13]. Meanwhile, main biomass polymers (cellulose, hemicellulose, and lignin) partially decompose giving off various types of volatiles. The final product is the remaining solid, dry, and charred material. It offers advantages including: increasing biomass energy density, reducing moisture content, enhancing the resistance to water absorption and microbial growth, offering increased friability (making torrefied biomass easier to grind) and homogeneous material properties [7,14].

5.3 Densification

Densification is a collection of biomass pre-processing methods applying mechanical forces to densify biomass particles into uniformly sized pellets or briquettes. Pelletizing can increase the volumetric density of biomass from 40-200 kg/m³ to 600-1400 kg/m³, which will significantly lower the cost of biomass logistics [12, 15]. Due to their uniform size, the flowability of pellets is similar to that of grains. This enables the use of existing grain transportation infrastructure and storage systems for pellet logistic.

References

- [1] Lindley, J. A., and L. F. Backer. "Agricultural residue harvest and collection." Prepared for Western Region Biomass Energy Program. PO# AA-PO-111671-12134 (1994).
- [2] Fasina, O. O., and S. Sokhansanj. "Storage and handling characteristics of alfalfa pellets." *Powder Handling and Processing* 8.4 (1996): 361-366.
- [3] Sokhansanj, Shahab, Janet Cushman, and Lynn Wright. "Collection and delivery of feedstock biomass for fuel and power production." (2003).
- [4] Sokhansanj, Shahab, and Lynn Wright. "Impact of future biorefineries on feedstock supply systems—equipment and infrastructure." *ASAE Annual International Meeting/CIGR XVth World Congress*, Paper. No. 024190. 2002.
- [5] Bergman, Patrick CA, et al. "Torrefaction for biomass cofiring in existing coal-fired power stations." *Energy Centre of Netherlands*, Report No. ECN-C-05-013 (2005).
- [6] Bergman, P. C. A. "Combined torrefaction and pelletization." *The TOP process* (2005).
- [7] Pimchuai, A., Dutta, A., & Basu, P. (2010). Torrefaction of agriculture residue to enhance combustible properties†. *Energy & Fuels*, 24(9), 4638-4645
- [8] Reza, M. Toufiq, et al. "Engineered pellets from dry torrefied and HTC biochar blends." *Biomass and Bioenergy* 63 (2014): 229-238.
- [9] Mani, S., L. G. Tabil, and S. Sokhansanj. "Compaction of biomass grinds—an overview of compaction of biomass grinds." *Powder Handling and Processing* 15.3 (2003): 160-168.

- [10] Sokhansanj, Shahab, et al. "Binderless pelletization of biomass." 2005 ASAE Annual Meeting. American Society of Agricultural and Biological Engineers, 2005.
- [11] Acharjee, T.C., Coronella, C.J. and Vasquez, V.R., 2011. Effect of thermal pretreatment on equilibrium moisture content of lignocellulosic biomass. *Bioresource technology*, 102(7), pp.4849-4854.
- [12] Bergman, P.C., Boersma, A.R., Zwart, R.W.R. and Kiel, J.H.A., 2005. Torrefaction for biomass co-firing in existing coal-fired power stations. Energy Centre of Netherlands, Report No. ECN-C-05-013.
- [13] Medic, D., Darr, M., Potter, B. and Shah, A., 2010. Effect of torrefaction process parameters on biomass feedstock upgrading. In 2010 Pittsburgh, Pennsylvania, June 20-June 23, 2010 (p. 1). American Society of Agricultural and Biological Engineers.
- [14] Li, H., Liu, X., Legros, R., Bi, X.T., Lim, C.J. and Sokhansanj, S., 2012. Pelletization of torrefied sawdust and properties of torrefied pellets. *Applied Energy*, 93, pp.680-685.
- [15] Bergman, P., Combined torrefaction and pelletisation. The TOP process, 2005.

Chapter 6 - Synchronized torrefaction and pelleting of biomass for bioenergy production

This work is published in the paper “A fundamental research on synchronized torrefaction and pelleting of biomass” Yang Yang, Mingman Sun, Meng Zhang, Ke Zhang, Donghai Wang and Catherine Lei, *Journal of Renewable Energy*. 2019,142, pp. 668-676

Abstract

Synchronized torrefaction and pelleting (STP) was developed as a laboratory scale process to produce torrefied pellets with a single biomass material loading. Two fuel upgrading actions (torrefaction and pelleting) happened simultaneously with the assistance of ultrasonic vibration. It was found that STP elevated biomass temperature to above 200°C in less than one minute and initiated torrefaction while biomass was pelletized in a mold. A feasibility study showed that STP consistently produced torrefied pellets with improved physical, thermochemical, and hygroscopic properties as an upgraded fuel for biomass co-combustion. STP was effective at enhancing the density and durability of torrefied pellets. Elemental analysis of torrefied biomass material showed increased carbon content, indicating higher heating values of torrefied pellets over non-torrefied biomass. Thermogravimetric analysis and Fourier-transform infrared analysis revealed loss of hydrogen and oxygen-rich matters during STP. Finally, greater hydrophobicity of torrefied pellets was exhibited by less water and vapor absorption compared with non-torrefied biomass.

Keywords

Biofuel, Biomass, Pellet, Torrefaction, Ultrasonic

6.1 Introduction

Bioenergy derived from cellulosic biomass (forest and agricultural residues and dedicated energy crops) has been recognized as a promising alternative to fossil fuels. With its high availability and low cost, cellulosic biomass is regarded as a sustainable resource for bioenergy production in the near to distant future. Among many bioenergy conversion technologies, combustion is proven to efficiently utilize biomass for heat and power generation. Consuming bioenergy instead of fossil fuels can achieve carbon neutrality because the CO₂ emitted by bioenergy consumption is equivalent to that absorbed from the environment during biomass growth [1]. About 40% of the world's total power is supplied by coal power plants, all of which can also run on biomass [2-5]. Thus, the co-combustion of biomass with solid fossil fuels in existing coal power plants is a clean way to generate heat and electricity and poses an opportunity to reduce the consumption of fossil fuels. However, several technical barriers are hindering the large-scale utilization of biomass for bioenergy production. These barriers are related to the characteristics of biomass such as low energy density, low volumetric density, high moisture content, and its hydrophilicity. These qualities of raw biomass result in high cost of biomass handling, storage and low efficiency of biomass energy conversion [6-9]. In order to address these challenges, it is necessary to preprocess biomass before it can be efficiently used as an energy resource. Biomass torrefaction and pelleting are two recognized technologies that improve the energy and volumetric densities of biomass feedstock [10-12].

Torrefaction is a mild thermal treatment (250-350°C) that upgrades raw biomass to energy-dense intermediates for co-combustion with coal [13]. During torrefaction, the moisture and superfluous matters in biomass are released and biopolymers are partially decomposed. The product of this treatment is torrefied biomass with high calorific value and energy density [14-

16]. Further advantages associated with torrefied biomass include homogeneous composition, reduced moisture content, and increased resistance to moisture absorption and microbial growth [16, 17].

It is more convenient to handle, store, and transport torrefied biomass pellets than raw biomass. Pelleting can increase the volumetric density of biomass from 40-250 kg/m³ to 600-1400 kg/m³ [14, 18]. Biomass pellets with uniform size and high flowability can be easily processed with the existing grain handling and storage infrastructure (i.e. elevators, hoppers, and conveyor belts) to significantly lower the cost of biomass logistics [14].

Producing torrefied pellets is the prevailing technique to overcome the barriers caused by characteristics of raw biomass such as low energy and volumetric density [19, 20]. The global demand for torrefied pellets is expected to double from 24.5 million metric tons to 50 million metric tons by 2024 [21]. The integration of torrefaction and pelleting is proposed to improve production efficiency, reduce logistical costs, and make intercontinental bioenergy transport economically and energetically feasible. Additionally, the product lines for integrated torrefaction and pelleting can be diversified and expanded compared to sole torrefaction or pelleting facilities [22, 23]. Figure 6.1 illustrates two current solutions to produce torrefied pellets. In the upstream operation, biomass torrefaction and conditioning are conducted first. Afterward, torrefied biomass is condensed by mechanical compression with a variety of machines (i.e. screw extruder, briquetting press for large and different shapes, rolling machine, or ring-die pelleting machine). In the downstream operation, torrefaction is carried out after pelleting.

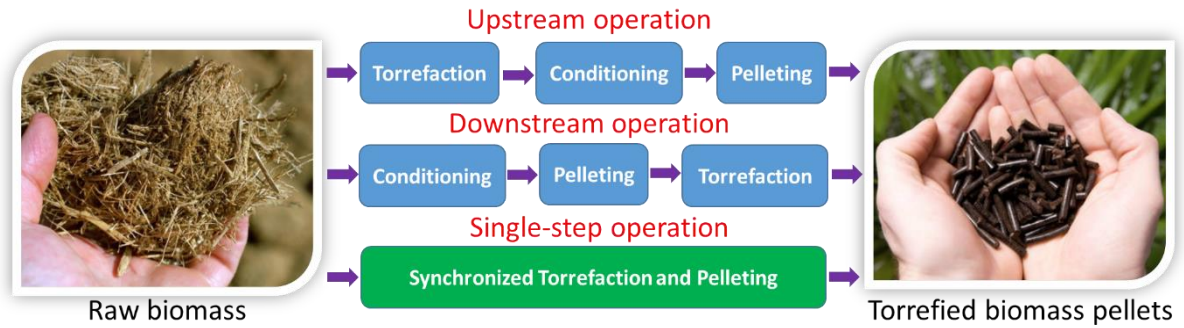


Figure 6.1. Operations to produce torrefied biomass pellets

Although some connections between biomass torrefaction and pelleting have been established, they are still two independent processes. In this study, synchronized torrefaction and pelleting (STP) was developed to produce torrefied pellets with a single biomass material loading on a laboratory scale. In this integrated solution, the two fuel upgrading actions (torrefaction and pelleting) occur simultaneously with the assistance of ultrasonic vibration within 75 seconds. As ultrasonic vibration is applied to biomass, a significant amount of heat is generated due to viscoelastic heating to initiate torrefaction. The accumulation of heat results in a rapid temperature increase (up to 320°C) when biomass is being pelletized. This characteristic of STP significantly reduces the process duration. This synchronized operation is more energy efficient as the generated heat is not only utilized to perform torrefaction but also to produce pellets of high density and durability. In current operations, torrefaction reduces pellet durability because the composition change during torrefaction leads to the loss of affinity of the added binding materials. STP, however, produces dense and durable torrefied pellets without the addition of binders due to the induced natural binding effects from the thermally softened lignin. [22, 24] Another advantage of not using binders is that the enhanced energy density and hydrophobicity of torrefied pellets will not be compromised due to the hydrophilic properties of binders such as starch and lime (Table 6.1).

Although biomass torrefaction and pelleting mechanisms have been investigated individually, no study has been conducted on the simultaneous use of these two fuel upgrading actions. The objectives of this study are to investigate the feasible conditions to produce torrefied pellets with STP and to characterize and demonstrate the fuel upgrading effects of STP on corn stover and big bluestem pellets from physical, thermochemical, and hygroscopic aspects.

Table 6.1 A comparison among the upstream, downstream, and synchronized torrefaction and pelleting processes

Property	Upstream operation		Downstream operation	Synchronized torrefaction and pelleting
	With binder	Without binder		
Density (Kg/m ³)	550-650	750-850	500-600	850-1000
Durability (%)	99%	> 90%	< 90%	~ 80%
Heating value (MJ/kg)	19-22	20-24	18-22	18-20
Heating value (MJ/m ³)	10,450-14,300	15,000-20,400	10,000-13,200	15,300-22,000
Hydrophobicity	Low	High	High	High

6.2 Experimental procedures and parameter measurements

6.2.1 Materials and preparation

The biomass materials used in this study were corn stover and big bluestem. The moisture content of both materials is approximately 8% and was determined by following the National Renewable Energy Laboratory procedure (NREL/TP-510-42621) [25]. A knife mill (Model SM 2000, Retsch, Inc., Haan, Germany) was used for biomass size reduction. Sieves with different sizes (4, 2, and 1 mm) were used to control the particle size of biomass materials prior to synchronized torrefaction and pelleting.

6.2.2 Synchronized torrefaction and pelleting (STP)

As illustrated in Figure 6.2, synchronized torrefaction and pelleting was performed on a modified ultrasonic machine (Model AP-1000, Sonic-Mill, Albuquerque, NM, USA). The STP system consists of an ultrasonic generation system and a pneumatic loading system. The ultrasonic generation system includes a power supply that converts 60 Hz conventional line electrical power into 20 kHz electrical power, a piezoelectric converter that converts high frequency electrical energy into mechanical vibrations, and a pelleting tool. The pelleting tool is a solid cylinder with a flat end. The ultrasonic vibration is amplified and transmitted to the pelleting tool, causing it to vibrate perpendicularly to the tool end surface at a high frequency.

The vibration amplitude is controlled by the power supply. A higher percentage (0 to 100%) of power produces a higher vibration amplitude and generates more heat inside the pellet. Before pelleting, 1.5 gram of biomass particles are loaded into a glass ceramic mold (Model Macor, Corning Incorporated, Corning, NY, USA), which consists of two parts: the upper part forms a cylindrical cavity with an inner diameter of 16 mm and a depth of 43 mm; the bottom part is a square plate serving as a base and it is detachable to unload the finished pellet.

Pelleting pressure is applied by a pneumatic cylinder and the pressure is controlled by a regulator. As the ultrasonic vibration is applied to the biomass, a significant amount of heat is generated to initiate torrefaction while biomass is pelletized in the glass ceramic mold. In this study, pelleting pressures of 20, 30, 40, and 50 psi were applied. Ultrasonic powers of 20%, 30%, 40%, and 50% were employed and the process duration was 50-75 seconds. After each experiment, a cylindrical torrefied pellet of 16 mm diameter and 6-8 mm height was made.

Pelleting temperature measurements were conducted to investigate the feasible conditions of STP. Temperature data were recorded using a multimeter with a thermocouple inserted into the center of a pellet. Temperature measurement started immediately after the ultrasonic power supply was turned on and stopped right after it was turned off. Data were collected at a rate of one read per second.

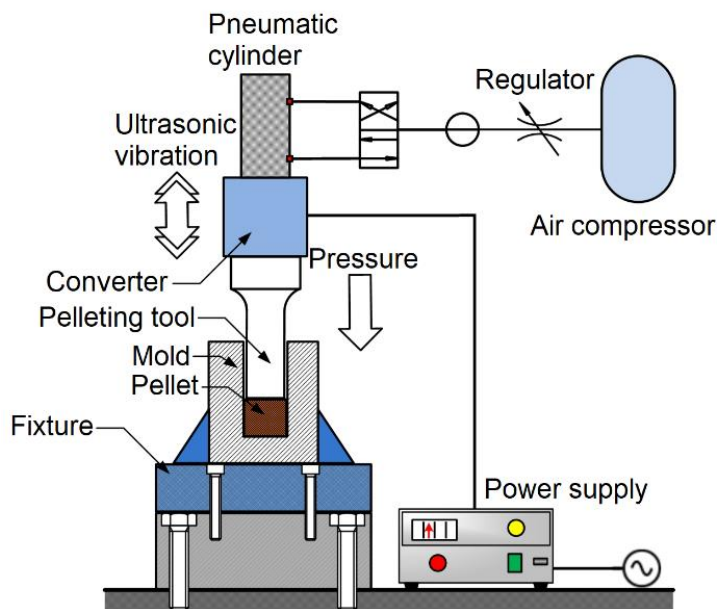


Figure 6.2. Schematic illustration of synchronized torrefaction and pelleting (STP)

6.2.3 Measurement of pellet physical properties

The volumetric density of each pellet was obtained by dividing the weight of a pellet by its volume. Measurements of pellet dimensions and weight were performed immediately after the pellet was retrieved out of the mold.

Pellet durability represents the ability to transport pellets without experiencing unacceptable breakage or generating a significant amount of fines. The durability tester (Model PDI, Seedburo Equipment Co, IL, USA) has a rotating tumbler with four compartments driven by a motor. It simulates the amount of breakage that normally occurs during pellet transportation. A set of ten pellets were loaded into each compartment. During the ten minute durability test, pellets were constantly tumbled. After the durability test, a sieve (U.S. No. 6, opening diameter = 3.15 mm) was used to separate the pellets that maintained a good cylindrical shape from the fines and debris. The remaining pellets on the sieve were then weighed and divided by their total

weight before the test. This ratio was defined as the durability index and expressed as a percentage.

An optical microscope (Model BX51, Olympus Corp. Japan) was used to observe the morphological features of biomass before and after STP.

6.2.4 Measurement of pellet thermochemical properties

Thermogravimetric analysis (TGA) is an analytical technique used to determine a material's thermal stability and its fraction of volatile components by monitoring the change in mass over time as temperature changes [26]. The temperature in the furnace of the thermogravimetric analyzer (Model TGA7, PerkinElmer Co, USA) was increased from ambient temperature to 700°C at a rate of 20°C/min in a nitrogen atmosphere and maintained at 700°C for one minute. Thermogravimetry (TG) and its differential curves (DTG) for biomass were obtained.

The torrefaction process and the effectiveness of torrefaction are characterized by three parameters: Mass Yield (MY), Energy Density ratio (ED), and Energy Yield (EY), which are defined as follows:

$$\text{MY} = \text{mass of torrefied biomass} / \text{mass of non-torrefied biomass}$$

$$\text{ED} = \text{HHV of torrefied biomass} / \text{HHV of non-torrefied biomass}$$

$$\text{EY} = \text{MY} \cdot \text{ED}$$

The higher heating value (HHV) of biomass was measured with a bomb calorimeter (Model C200, IKA Group, Germany). Approximately one gram of biomass was put into an adiabatic container and combusted for each heating value measurement.

Biomass elemental content was analyzed by with an elemental analyzer (Model Series II CHNS/O, PerkinElmer Co, USA) and biomass compositional content was determined as per the NREL laboratory analytical method (NREL/TP-510-42618) [27].

FTIR was used to investigate the structural and chemical changes of the biomass. The spectrometer (Model Spectrum 400 FT-IR, PerkinElmer Co, USA) recorded spectra in absorbance mode with the wavenumber ranging from 400 to 4000 cm^{-1} . The detection resolution was 4 cm^{-1} in the transmission mode with 16 scans per test. Before the test, torrefied and non-torrefied pellets were size reduced to less than 0.2 mm on a cyclone mill.

6.2.5 Measurement of pellet hygroscopic properties

The torrefaction process aims to improve biomass hydrophobicity. In water absorption tests, the torrefied and non-torrefied pellets were immersed in water with a solid to liquid ratio of 1:10 for 20 minutes to simulate severe water damage. Afterwards, water was filtered out using a 500 μm nylon mesh and the pellets were dried at 105°C in an oven to eliminate moisture. Afterwards, pellet integrality was compared. Vapor absorption tests were then performed to evaluate pellet hydrophobic properties. A desiccator with saturated KCl hydrate (87.5% moisture content) was used to simulate the highest average humidity reported in the US. Torrefied and non-torrefied pellets were placed in the desiccator at 25°C for 30 days. During this period, pellets were weighed every 12 hours for the first three days and every 24 hours thereafter.

6.3 Experimental results and discussions

6.3.1 Process feasibility

Pelleting temperature and time required to reach torrefaction temperature were investigated to study the feasible conditions for STP. As indicated in Figure 6.3, pelleting temperature rose at a faster rate with a higher ultrasonic power for both biomass materials. The

ultrasonic power of 20%, 30%, and 40% only elevated the pelleting temperature to a maximum of 180°C during the 60 seconds of pelleting duration, which was not sufficient to initiate torrefaction. However, an ultrasonic power of 50% substantially boosted pelleting temperature to 300°C within 50 seconds. This elevated temperature was high enough to produce a biomass pellet that was mostly torrefied. Subsequently, 50% ultrasonic power with a duration longer than 60 seconds could lead to over-torrefaction that torrefied biomass could burst out of the mold and failed to form pellets. In order to avoid over-torrefaction, the feasible duration to make torrefied pellets was investigated by performing STP from 30 to 60 seconds with a 10 second increment. By evaluating the physical quality and torrefaction completeness of torrefied pellets, a feasible duration of 50 seconds was selected. Pelleting pressure also contributed to over-torrefaction. Among pelleting pressure of 20, 30, 40 and 50 psi, pelleting temperature increased at a higher rate when a lower pelleting pressure was applied. Through extensive temperature acquisition and torrefaction completeness observation during the feasibility study, 2 mm was identified as the most feasible particle size. It was believed that there is limited inter-particle space between 1 mm biomass particles and; consequently, hindering torrefaction due to the inhabitation of ultrasonic vibration propagation. Also, 4 mm biomass particles resulted in inconsistent torrefaction completeness, which can be a result of the large variance in particle size distribution of particles processed by the 4 mm sieve. Non-torrefied pellets made with an aluminum mold were made as the control group.

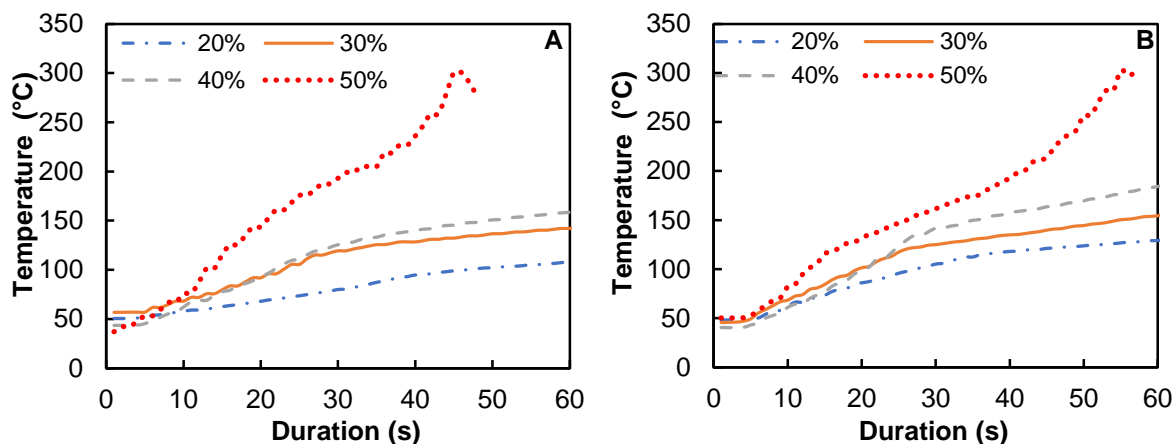


Figure 6.3. Pelleting temperature of corn stover (A) and big bluestem (B) under different ultrasonic power (%)

6.3.2 Pellet physical properties

6.3.2.1 Density

The pellet densities and durabilities of corn stover and big bluestem are listed in Table 4.2. After STP, torrefied biomass pellets showed a reduction in density compared to that of non-torrefied pellets due to the loss of volatile matter and thermal degradation of compositional content. It was found for both biomass materials that the 2 mm particles produced the highest pellet density after STP. Densities of 891 and 982 Kg/m³ were obtained for corn stover and big bluestem, respectively. The highest density of big bluestem pellets is comparable to that of torrefied pine wood pellets (925-1035 Kg/m³ at 275°C) [28].

6.3.2.2 Durability

The durability of torrefied corn stover pellets was 85.42% for 1 mm, 84.76% for 2 mm, and 76.13% for 4 mm particles. For big bluestem, torrefied pellets made of 1 mm particles had the highest durability of 79.78%. The durability of torrefied big bluestem pellets dropped to 78.33% and 71.46% for pellets made of 2 and 4 mm particles, respectively. In general, torrefied pellets had slightly lower durability than that of non-torrefied pellets. A possible reason for this

discrepancy is due to the biomass compositional change and microstructure modification during torrefaction [29]. More inter-particle gaps and voids were formed, which resulted in a more brittle and weaker fibrous structure of torrefied biomass particles because a portion of hemicellulose was removed and some cell walls were destroyed. The removal of hydroxyl groups from lignin during torrefaction resulted in increased non-polar C-C bonds. This alteration made the torrefied particles harder to bind for both types of torrefied biomass materials [30].

Table 6.2 Pellet density and durability

Property	Size (mm)	Corn stover		Big bluestem	
		Non-Torrefied	Torrefied	Non-Torrefied	Torrefied
Density (Kg/m ³)	1	1147±29.12	878±24.63	1167±25.69	967±20.62
	2	1154±26.38	891±13.37	1231±20.53	982±25.97
	4	1080±31.80	843±23.78	1157±13.84	913±23.47
Durability (%)	1	90.50	85.42	85.78	79.78
	2	90.36	84.75	84.24	78.33
	4	86.81	76.04	80.29	71.46

6.3.2.3 Morphology

Microscopic images in Figure 6.4 show a comparison of non-torrefied and torrefied corn stover. Figure 6.4A shows the smooth, glassy surface of a non-torrefied particle. The torrefied particle in Figure 6.4B also shows a smooth surface without any visible cracks at this scale (200×). This observation indicates that there could be a solid bridge on the particle surface that could enhance the binding affinity [31]. The surface of torrefied pellets (Figure 6.4D) shows obvious biomass particle melting and interlocking, which could make the particle-particle bonding strong. The reason for this is that lignin melts at a high temperature and becomes softened, acting as a natural binder between biomass particles [11]. It has been known that pelleting torrefied biomass particles is more difficult than pelleting non-torrefied biomass particles [29]. Conditioning torrefied biomass, high pelleting pressure and temperature, and binder materials are required to produce torrefied pellets of a comparable physical quality to non-

torrefied pellets. This study shows that STP can produce torrefied biomass of acceptable physical quality without applying critical pelleting conditions or binder in a single material loading fashion.

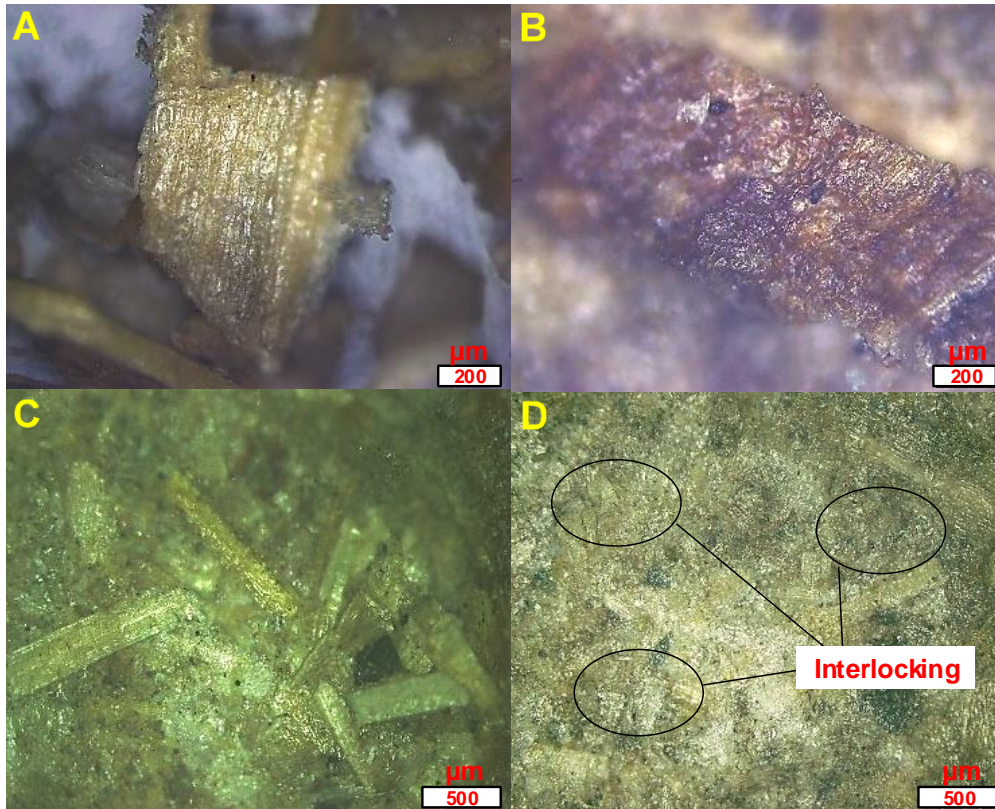


Figure 6.4. Microscopic images of (A) non-torrefied corn stover particles, (B) torrefied corn stover

6.3.3 Pellet thermochemical properties

6.3.3.1 Thermal properties

Cellulose, hemicellulose, and lignin are the three major compositions of biomass. Due to the different thermal stabilities of these compositions, their thermal decompositions occur at different temperature ranges. Generally, hemicellulose decomposes from 150 to 350°C and cellulose starts to decompose within 275 to 350°C. The decomposition of lignin occurs within a wider range at 250 to 500°C [32]. As biomass compositions change during torrefaction, the mass loss and mass loss intensity can be qualitatively identified. The TG and DTG curves in Figure

6.5 provide a comprehensive comparison of mass loss between non-torrefied and torrefied biomass. Figures 6.5A and 6.5B show a general mass loss trend of corn stover and big bluestem during thermal decomposition.

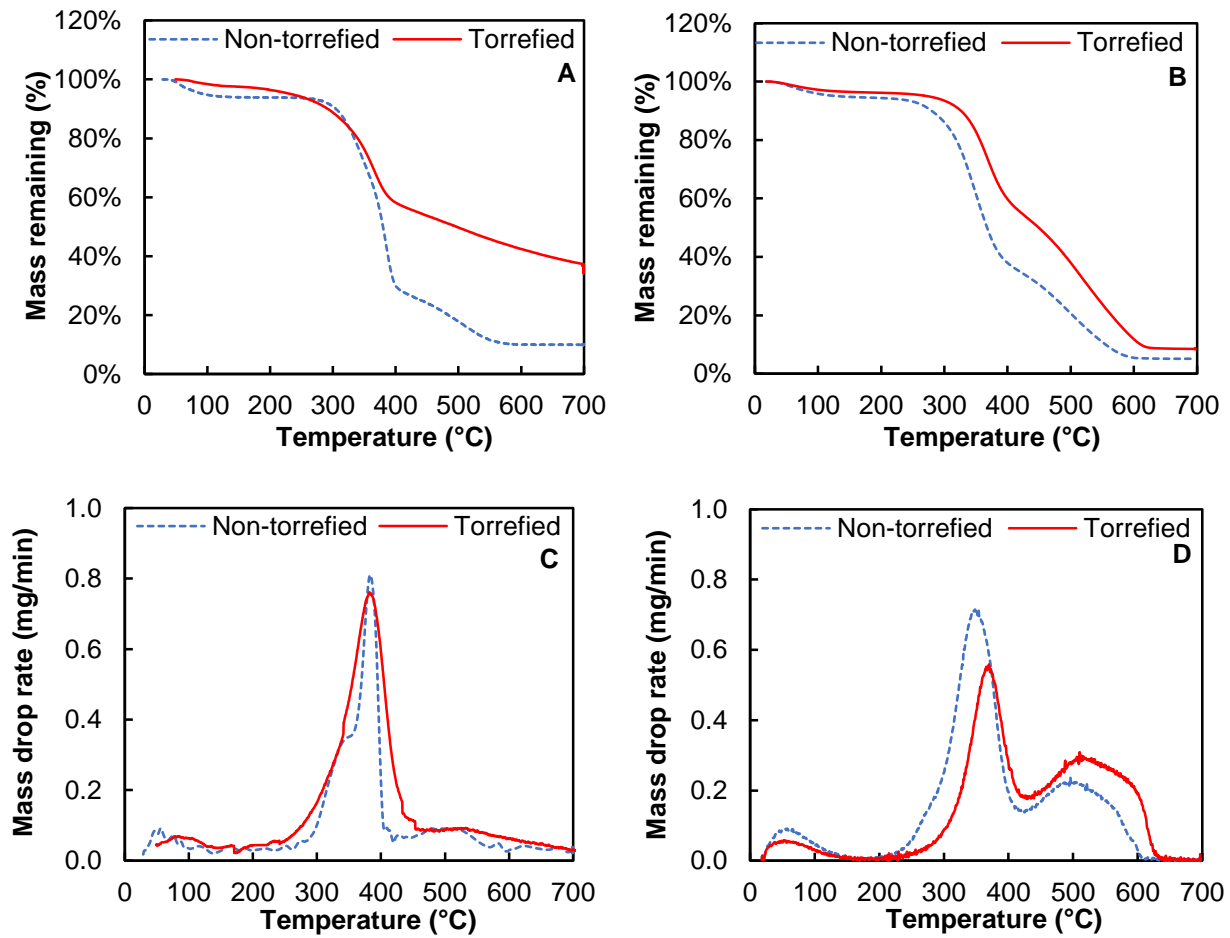


Figure 6.5. Thermogravimetric analysis results (A) corn stover TG profile, (B) big bluestem TG profile, (C) corn stover DTG profile, and (D) big bluestem DTG profile

Torrefied biomass had a higher percentage of remaining mass than did non-torrefied biomass at the same temperature. The mass loss intensity is shown in Figures 6.5C and 6.5D and reflects the thermal stability and composition change of torrefied and non-torrefied biomass. The first peak on DTG curves of both materials began around 50°C, which was associated with the liberation of moisture content. The less intensive mass loss rate of torrefied biomass at this peak

implied its better hydrophobicity than non-torrefied biomass. When the temperature reached 200°C, the mass loss related to hemicellulose and cellulose decomposition became more intense and reached a much higher peak at around 350°C for non-torrefied biomass. The main reason is that the decreased cellulose and hemicellulose contents in torrefied biomass (Table 6.3) resulted in less mass loss in further decomposition at the temperature range from 200 to 350°C.

Additionally, it was observed that the percentage of mass remaining of torrefied biomass was significantly higher than that of non-torrefied biomass when the temperature reached 500°C. This observation was attributed to the increase in lignin content by torrefaction (Table 6.3). For torrefied corn stover, there was only one peak observed around 380°C. The mass loss rate dropped dramatically and tended to be less intense after 430°C. This different behavior from big bluestem is due to lignin having a different thermal resistance during decomposition (from 200-500°C). The behaviors on DTG curves highly depends on the type of linkages between lignin polymer units [31]. The mass of torrefied corn stover decayed steadily with the increasing temperature and no peak was observed over 500°C. This indicates that most of the lignin decomposed at a lower temperature and the lignin peak overlapped with the peaks of cellulose and hemicellulose. For big bluestem, peaks were observed around 500°C for both non-torrefied and torrefied biomass. As part of linkages between lignin are more thermostable in the case, the decomposition of this portion of lignin occurred after 500°C and was reflected by the peak observed on the DTG curve [33, 34]. Since the percentage of lignin content increased after STP, a higher peak of torrefied biomass after 500°C can be observed in Figure 6.5D. The study of severely torrefied bamboo, willow, coconut shell, and woody biomass also observed the differences among materials on DTG curves over 500°C [35]. Like the corn stover in this study,

there was no peak observed for bamboo or coconut shell over 500°C, but there was a significant peak observed for woody biomass.

Table 6.3 Elemental and compositional results

		Corn stover (non-torrefied)	Corn stover (torrefied)	Big bluestem (non-torrefied)	Big bluestem (torrefied)
Composition (%)	Cellulose	41.60±0.81	31.45±0.47	48.6±1.07	28.16±0.84
	Hemicellulose	24.50±0.36	16.57±1.02	15.20±0.17	13.98±0.11
	Arabinan	1.10±0.04	1.86±0.03	0.90±0.03	1.59±0.02
	Lignin	17.20±0.22	39.31±0.96	28.0±1.43	38.50±0.04
	Ash	2.60±0.01	4.95±0.02	5.20±0.01	8.93±0.02
Element (%)	C	35.34±0.31	47.04±0.16	41.65±0.07	51.24±0.13
	H	5.76±0.07	4.74±0.09	6.74±0.09	5.11±0.02
	N	0.96±0.06	1.16±0.02	0.72±0.01	0.87±0.08
	S	1.21±0.01	1.16±0.01	1.37±0.01	1.18±0.02
	O	56.71±0.45	44.91±0.28	49.53±0.01	40.61±0.51
	O/C ratio	1.21	0.72	0.89	0.60
	H/C ratio	1.94	1.45	1.93	1.42

6.3.3.2 Mass yield and energy yield

Mass loss in torrefaction is due to the decomposition and depolymerization of cellulose, hemicellulose, and lignin [36]. The results of mass yield and energy yield of biomass pellets are listed in Table 6.4. Typically, the mass yield of biomass is 50%-90% after torrefaction. A low mass yield can result in low energy density [29]. The mass yield of torrefied corn stover and big bluestem pellets were 78.88% and 79.78%, respectively. These yields indicates that corn stover and big bluestem are suitable biomass for torrefaction to be converted into an upgraded fuel. The high heating values of torrefied corn stover (17.92 MJ/kg) and big bluestem (18.13 MJ/kg) pellets increased by 6.03% and 9.81% over non-torrefied biomass and are comparable to the high heating value of torrefied biomass pellets (18-22 MJ/kg) made by current methods [8, 9, 18]. In addition, 83.64% and 87.61% energy yield were obtained for torrefied corn stover and big bluestem pellets.

Table 6.4. Mass yield, HHV, and energy yield of corn stover and big bluestem pellets

	Corn stover			Big bluestem		
	Mass yield (%)	HHV (MJ/kg)	Energy yield (%)	Mass yield (%)	HHV (MJ/kg)	Energy yield (%)
Non-torrefied	97.68±0.99	16.90±0.21	N/A	96.82±0.62	16.51±0.14	N/A
Torrefied	78.88±2.96	17.92±0.11	83.64	79.78±2.05	18.13±0.58	87.61

6.3.3.3 Compositional, elemental, and FTIR analyses

The compositional analysis results listed in Table 6.3 indicates a biomass composition change during torrefaction. The degradation of cellulose and hemicellulose resulted in a higher mass percent of lignin in torrefied corn stover and big bluestem of 39.3% and 38.5%, respectively. After torrefaction, the carbon content increased by 11.7% for corn stover and 9.59% for big bluestem. This compositional and elemental variation consequently boosted higher heating value of torrefied biomass. Hydrogen content slightly dropped due to the loss of moisture and hydroxyl groups. The oxygen content decreased by 11.8% and 8.92% due to the release of CO₂, CO and H₂O. The H/C and O/C ratios of torrefied corn stover are 1.45 and 0.72 and 1.42 and 0.60 for big bluestem. They are close to the H/C (1.43) and O/C (0.65) ratios of bamboo that was torrefied at 250-275°C. It was also reported that the H/C and O/C ratios of torrefied bamboo decreased with elevated torrefaction temperature from 200 to 300 °C [37]. Compared to the H/C and O/C ratio of non-torrefied corn stover (1.94 and 1.21) and big bluestem (1.93 and 0.89), torrefied biomass has significantly lower H/C and O/C ratios. These results suggest that dehydrogenation and deoxygenation of biomass are the primary reactions during torrefaction.

In Figure 6.6, the FTIR spectra of corn stove and big bluestem support the results of compositional and elemental analyses. The OH-stretching vibration region at 3600-3200 cm⁻¹ indicates the amount of hydroxyl group and bonding site for water. The less intense OH-

stretching vibration of torrefied corn stover and big bluestem reveals the dehydration of cellulose and hemicellulose, which explains the reduction of hydrogen and oxygen content during torrefaction. It is reported that C=C stretching at 1400-1600 cm^{-1} represents the guaiacyl ring of lignin; the peaks on spectra of torrefied corn stover and big bluestem indicate high lignin and carbon contents after torrefaction [38, 39]. Cellulose and hemicellulose related peaks are between 1150 and 950 cm^{-1} and are higher for non-torrefied biomass. In addition, a higher peak representing cellulose can be observed from 650-550 cm^{-1} for non-torrefied big bluestem [39, 40]. The lower intensity of these signal peaks for torrefied biomass suggest that the C-O-C (1150 cm^{-1}) and C-H stretching (650 cm^{-1}) in cellulose and hemicellulose were broken down and the H/C and O/C ratios decreased during torrefaction [41, 42].

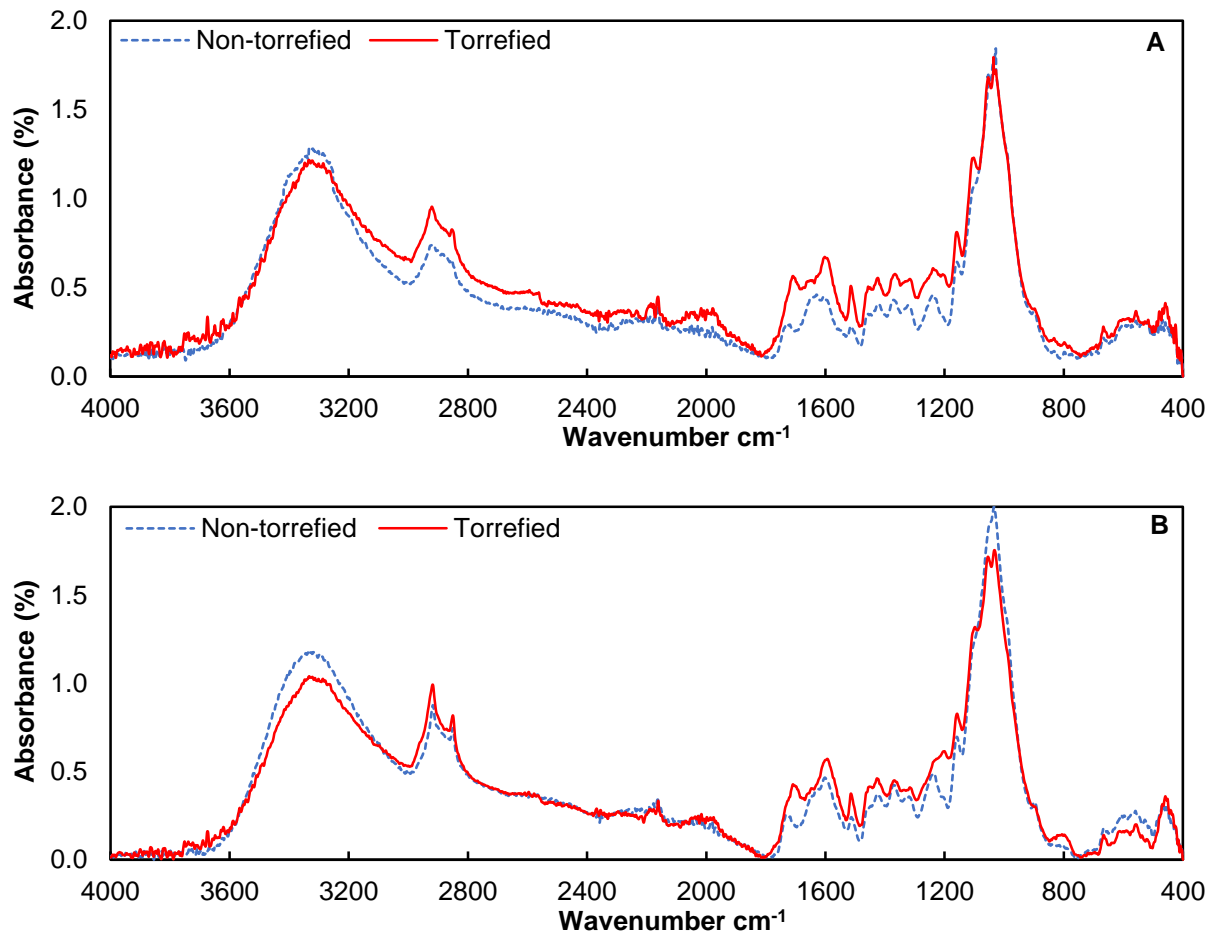


Figure 6.6. FTIR spectra of non-torrefied and torrefied corn stover (A) and big bluestem (B)

6.3.4 Pellet hygroscopic properties

6.3.4.1 Water immersion

Non-torrefied (Figures 6.7A and C) and torrefied pellets (Figures 6.7B and D) were immersed in water. The torrefied corn stover and big bluestem pellets stayed intact, while non-torrefied pellets broke into particles immediately and sank to the bottom of the beakers due to excess water absorption. After being soaked for 20 minutes and drained with nylon mesh, torrefied pellets still maintained a near cylindrical shape, but non-torrefied pellets fell apart completely. This water intake test visually demonstrated the effects of STP on improving pellet hydrophobicity.

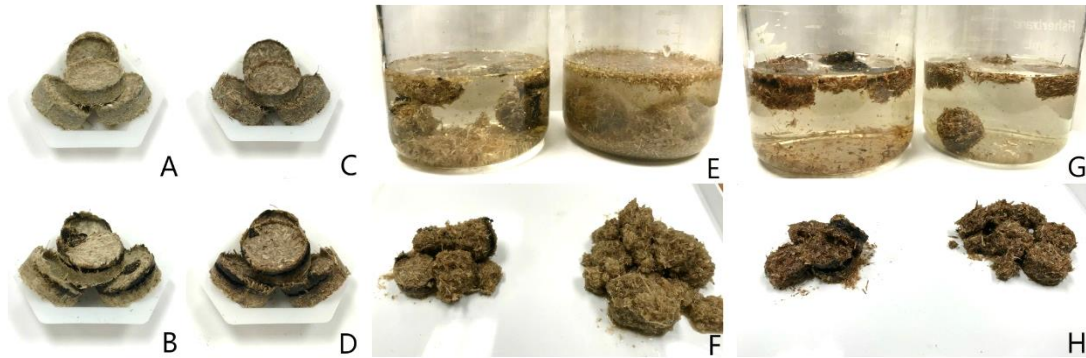


Figure 6.7. Water intake images of corn stover (A, B, E and F) and big bluestem pellets (C, D, G and H)

6.3.4.2 Water vapor absorption

Water vapor absorption experiments were conducted to evaluate pellet moisture absorption in a high humidity environment. Figure 6.8 demonstrates the 28 day moisture absorption results of non-torrefied and torrefied pellets. In general, moisture absorption trends were similar regardless of biomass type or particle sizes. The figures show that moisture content of pellets increased dramatically at the beginning of the test. The transition point of torrefied pellets and non-torrefied pellets appeared around day 3. After three days, torrefied pellets

absorbed less moisture than non-torrefied pellets. The equilibrium moisture content was reached after 22 days. According to statistical analyses, the equilibrium moisture content of non-torrefied pellets was significantly higher ($P < 0.05$) than that of torrefied pellets. This equilibrium moisture content comparison indicates that STP enhanced pellet hydrophobicity by approximately 25% and 13% for corn stover and big bluestem, respectively. This is mainly a consequence of the decrease of water absorption sites and the change of biomass material structure by removing hydroxyl groups during STP. In addition, the formation of non-polar C-C bonds also increased torrefied biomass hydrophobicity. In accordance with the FTIR results, a possible inference is that torrefaction modifies the hygroscopic nature of biomass due to the removal of hydrophilic O-H bonds during thermal decomposition. In Figure 6.6, the O-H stretching peak can be observed around 3600-3200 cm^{-1} and is associated with the rupture of the hydrogen bond. Torrefied pellets showed a less intensive O-H stretching peak, indicating that STP partially removed the O-H bond. This assumption can be further supported by the elemental and compositional changes of biomass pellets after STP. The lower hydrogen content after STP limits the moisture access into cell walls and formation of the hydroxyl groups as the cell wall component [38, 39]. A different peak pattern located at around 1705 cm^{-1} represents the C=O ester group associated with hemicellulose, indicating the partial degradation of hemicellulose during STP. As a result, the improved hydrophobicity is mainly caused by the dehydrogenation and deoxygenation during STP.

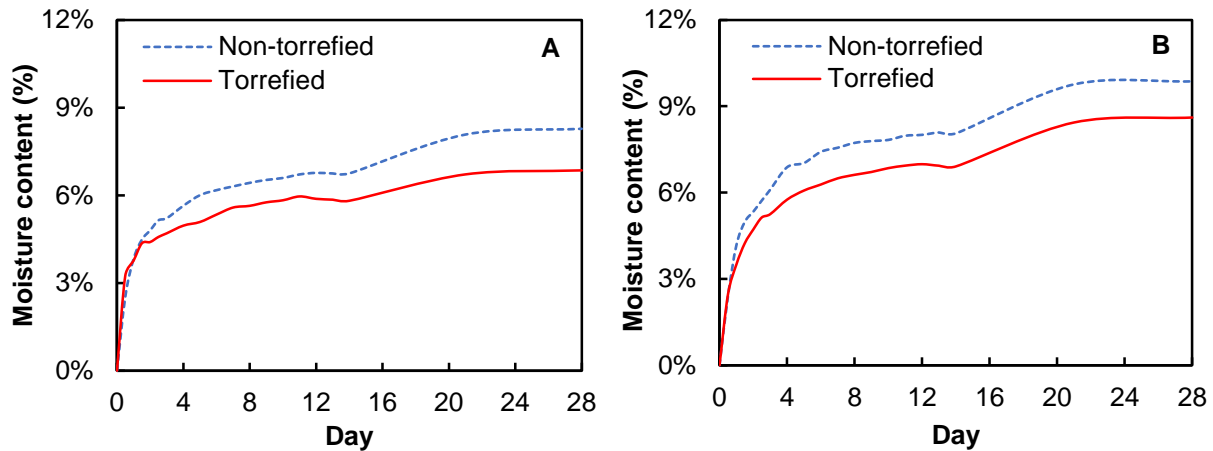


Figure 6.8. Water absorption results of corn stover (A) and big bluestem (B)

6.4 Conclusion

A laboratory scale synchronized torrefaction and pelleting (STP) was developed to produce torrefied pellets with a single material loading. Two fuel upgrading actions (torrefaction and pelleting) happened simultaneously with the assistance of ultrasonic vibration. The fuel upgrading effects were investigated from physical, thermochemical and hygroscopic aspects. STP was effective at enhancing the density and durability of torrefied biomass pellets. STP increased the higher heating value of corn stover by 6.03% and big bluestem by 9.81% over raw biomass. Pellet hydrophobicity was improved by STP as well. Torrefied pellets stayed intact in water intake test and absorbed approximately 15%-25% less moisture than non-torrefied ones.

Acknowledgement

The authors would like to acknowledge the Great Plains Biochar Initiative of USDA and Kansas Forest Service. The authors would like to thank Dr. Ke Zhang for the help in conducting experiments and measurements for this work.

Reference

- [1] Brenes, M.D., 2006. Biomass and Bioenergy: New Research. Nova Publishers.
- [2] Adams, D., 2013. Sustainability of biomass for cofiring. CCC/230. London: IEA Clean Coal Centre. www.iea-coal.org.uk/documents/83254/8869/Sustainability-of-biomass-for-cofiring,-CCC/230.
- [3] Chao, C.Y., Kwong, P.C., Wang, J.H., Cheung, C.W. and Kendall, G., 2008. Co-firing coal with rice husk and bamboo and the impact on particulate matters and associated polycyclic aromatic hydrocarbon emissions. *Bioresource technology*, 99(1), pp.83-93.
- [4] Kabir, M.R. and Kumar, A., 2012. Comparison of the energy and environmental performances of nine biomass/coal co-firing pathways. *Bioresource technology*, 124, pp.394-405.
- [5] Goldfarb, J.L. and Liu, C., 2013. Impact of blend ratio on the co-firing of a commercial torrefied biomass and coal via analysis of oxidation kinetics. *Bioresource technology*, 149, pp.208-215.
- [6] Ramamurthi, P.V., Fernandes, M.C., Nielsen, P.S. and Nunes, C.P., 2014. Logistics cost analysis of rice residues for second generation bioenergy production in Ghana. *Bioresource technology*, 173, pp.429-438.
- [7] Fasina, O. O., and S. Sokhansanj. "Storage and handling characteristics of alfalfa pellets." *Powder Handling and Processing* 8.4 (1996): 361-366.
- [8] Sokhansanj, Shahab, and Lynn Wright. "Impact of future biorefineries on feedstock supply systems—equipment and infrastructure." *ASAE Annual International Meeting/CIGR XVth World Congress*, Paper. No. 024190. 2002.

- [9] Sokhansanj, Shahab, Janet Cushman, and Lynn Wright. "Collection and delivery of feedstock biomass for fuel and power production." (2003).
- [10] Cao, L., Yuan, X., Li, H., Li, C., Xiao, Z., Jiang, L., Huang, B., Xiao, Z., Chen, X., Wang, H. and Zeng, G., 2015. Complementary effects of torrefaction and co-pelletization: Energy consumption and characteristics of pellets. *Bioresource technology*, 185, pp.254-262.
- [11] Kaliyan, N., Morey, R.V., White, M.D. and Doering, A., 2009. Roll press briquetting and pelleting of corn stover and switchgrass. *Transactions of the ASABE*, 52(2), pp.543-555.
- [12] Wang, T., Zhai, Y., Li, H., Zhu, Y., Li, S., Peng, C., Wang, B., Wang, Z., Xi, Y., Wang, S. and Li, C., 2018. Co-hydrothermal carbonization of food waste-woody biomass blend towards biofuel pellets production. *Bioresource technology*, 267, pp.371-377.
- [13] Acharjee, T.C., Coronella, C.J. and Vasquez, V.R., 2011. Effect of thermal pretreatment on equilibrium moisture content of lignocellulosic biomass. *Bioresource technology*, 102(7), pp.4849-4854.
- [14] Bergman, P., Combined torrefaction and pelletisation. *The TOP process*, 2005.
- [15] Medic, D., Darr, M., Potter, B. and Shah, A., 2010. Effect of torrefaction process parameters on biomass feedstock upgrading. In 2010 Pittsburgh, Pennsylvania, June 20-June 23, 2010 (p. 1). American Society of Agricultural and Biological Engineers.
- [16] Pimchuai, A., Dutta, A. and Basu, P., 2010. Torrefaction of agriculture residue to enhance combustible properties. *Energy & Fuels*, 24(9), pp.4638-4645.

- [17] Li, H., Liu, X., Legros, R., Bi, X.T., Lim, C.J. and Sokhansanj, S., 2012. Pelletization of torrefied sawdust and properties of torrefied pellets. *Applied Energy*, 93, pp.680-685.
- [18] Bergman, P.C., Boersma, A.R., Zwart, R.W.R. and Kiel, J.H.A., 2005. Torrefaction for biomass co-firing in existing coal-fired power stations. Energy Centre of Netherlands, Report No. ECN-C-05-013.
- [19] Zhang, M., Song, X.X., Pei, Z.J., Deines, T.W., and Treadwell, C., Ultrasonic Vibration-Assisted Pelleting of Wheat Straw: An Experimental Investigation. *International Journal of Manufacturing Research*, 2012. 7(1): p. 59-71.
- [20] Zhang, M., Song, X.X., Pei, Z.J., and Wang, D.H., Ultrasonic vibration-assisted pelleting of cellulosic biomass for biofuel production, in *Production of biofuels and chemicals: ultrasound*, Eds: Fang, Z., Smith, R.L., Jr., and Qi, X.H., Springer, 2015, New York, NY, USA.
- [21] Goh, C.S., Junginger, M., Cocchi, M., Marchal, D., Thrän, D., Hennig, C., Heinimö, J., Nikolaisen, L., Schouwenberg, P.P., Bradley, D. and Hess, R., 2013. Wood pellet market and trade: a global perspective. *Biofuels, Bioproducts and Biorefining*, 7(1), pp.24-42.
- [22] Thrän, D., Witt, J., Schaubach, K., Kiel, J., Carbo, M., Maier, J., Ndibe, C., Koppejan, J., Alakangas, E., Majer, S. and Schipfer, F., 2016. Moving torrefaction towards market introduction—Technical improvements and economic-environmental assessment along the overall torrefaction supply chain through the SECTOR project. *Biomass and bioenergy*, 89, pp.184-200.

- [23] Uslu, A., Faaij, A.P. and Bergman, P.C., 2008. Pre-treatment technologies, and their effect on international bioenergy supply chain logistics. Techno-economic evaluation of torrefaction, fast pyrolysis and pelletisation. *Energy*, 33(8), pp.1206-1223.
- [24] Kaliyan, N. and Morey, R.V., 2010. Natural binders and solid bridge type binding mechanisms in briquettes and pellets made from corn stover and switchgrass. *Bioresource technology*, 101(3), pp.1082-1090.
- [25] Sluiter, A., Hames, B., Hyman, D., Payne, C., Ruiz, R., Scarlata, C., Sluiter, J., Templeton, D. and Wolfe, J., 2008. Determination of total solids in biomass and total dissolved solids in liquid process samples. National Renewable Energy Laboratory, Golden, CO, NREL Technical Report No. NREL/TP-510-42621, pp.1-6.
- [26] Van der Stelt, M.J.C., Gerhauser, H., Kiel, J.H.A. and Ptasinski, K.J., 2011. Biomass upgrading by torrefaction for the production of biofuels: A review. *Biomass and bioenergy*, 35(9), pp.3748-3762.
- [27] Sluiter, A., Hames, B., Ruiz, R., Scarlata, C., Sluiter, J., Templeton, D. and Crocker, D., 2008. Determination of structural carbohydrates and lignin in biomass. Laboratory analytical procedure, 1617, pp.1-16
- [28] Phanphanich, M., 2010. Pelleting characteristics of torrefied forest biomass (Doctoral dissertation, University of Georgia).
- [29] Chen, W.H., Peng, J. and Bi, X.T., 2015. A state-of-the-art review of biomass torrefaction, densification and applications. *Renewable and Sustainable Energy Reviews*, 44, pp.847-866.

- [30] Nanou, P., Huijgen, W.J.J., Carbo, M.C. and Kiel, J.H.A., 2018. The role of lignin in the densification of torrefied wood in relation to the final product properties. *Biomass and Bioenergy*, 111, pp.248-262.
- [31] Reza, M.T., Lynam, J.G., Vasquez, V.R. and Coronella, C.J., 2012. Pelletization of biochar from hydrothermally carbonized wood. *Environmental Progress & Sustainable Energy*, 31(2), pp.225-234.
- [32] Antal, M.J., 1983. Biomass pyrolysis: a review of the literature part 1—carbohydrate pyrolysis. In *Advances in solar energy* (pp. 61-111). Springer, Boston, MA.
- [33] Pandey, M.P. and Kim, C.S., 2011. Lignin depolymerization and conversion: a review of thermochemical methods. *Chemical Engineering & Technology*, 34(1), pp.29-41.
- [34] Liu, Q., Wang, S., Zheng, Y., Luo, Z. and Cen, K., 2008. Mechanism study of wood lignin pyrolysis by using TG–FTIR analysis. *Journal of Analytical and Applied Pyrolysis*, 82(1), pp.170-177.
- [35] Chen, W.H. and Kuo, P.C., 2010. A study on torrefaction of various biomass materials and its impact on lignocellulosic structure simulated by a thermogravimetry. *Energy*, 35(6), pp.2580-2586.
- [36] Prins, M.J., Ptasinski, K.J. and Janssen, F.J., 2006. Torrefaction of wood: Part 1. Weight loss kinetics. *Journal of analytical and applied pyrolysis*, 77(1), pp.28-34.
- [37] Wen, J.L., Sun, S.L., Yuan, T.Q., Xu, F. and Sun, R.C., 2014. Understanding the chemical and structural transformations of lignin macromolecule during torrefaction. *Applied Energy*, 121, pp.1-9.

- [38] Pandey, K.K., 1999. A study of chemical structure of soft and hardwood and wood polymers by FTIR spectroscopy. *Journal of Applied Polymer Science*, 71(12), pp.1969-1975.
- [39] Barsberg, S., 2010. Prediction of Vibrational Spectra of Polysaccharides Simulated IR Spectrum of Cellulose Based on Density Functional Theory (DFT). *The Journal of Physical Chemistry B*, 114(36), pp.11703-11708.
- [40] Liang, C.Y. and Marchessault, R.H., 1959. Infrared spectra of crystalline polysaccharides. II. Native celluloses in the region from 640 to 1700 cm.⁻¹. *Journal of Polymer Science*, 39(135), pp.269-278.
- [41] Kristensen, J.B., Thygesen, L.G., Felby, C., Jørgensen, H. and Elder, T., 2008. Cell-wall structural changes in wheat straw pretreated for bioethanol production. *Biotechnology for biofuels*, 1(1), p.5.
- [42] Gierlinger, N., Goswami, L., Schmidt, M., Burgert, I., Coutand, C., Rogge, T. and Schwanninger, M., 2008. In situ FT-IR microscopic study on enzymatic treatment of poplar wood cross-sections. *Biomacromolecules*, 9(8), pp.2194-2201.

Chapter 7 - Integrating two platforms of cellulosic biomass utilizations

This work is submitted in the paper “utilizing biomass hydrolyzed residues as a pellet additive for solid fuels and feedstock commodities” Yang Yang, Jikai Zhao, Meng Zhang, Donghai Wang, Journal of Fuel 2023

Abstract

Biomass hydrolyzed residue is conventionally used for heat and power generation in the bioethanol production process. A more economical use of this residue is to utilize it as a platform chemical for high value-added products such as aromatic and phenolic compounds, cement additives, bitumen modifiers and battery materials. Making pellets with biomass hydrolyzed residues provides an opportunity to create an intermediate product that can serve as a renewable solid fuel or a feedstock commodity for other biorefinery applications. In this study, the quality of pellets fully or partially made from hydrolyzed corn stover residues was evaluated from physical, thermochemical, and hygroscopic perspectives. With 10% residue additive, the durability of pellets increased from 80.7% to 90.1% and reached 92.8% with further residue addition. Enhancement on pellet mechanical properties was also observed by adding 50% hydrolyzed residues. Energy density increased from 13.7 GJ/m³ to as high as 17.6 GJ/m³ with the amount of additive increased from 0% to 100%. Thermal gravimetric and differential scanning calorimetry results revealed that hydrolyzed corn stover had strengthened thermal properties (heating value, thermal stability, and exothermal performance) over raw biomass. FTIR and NMR spectra were used to explore inner-unit linkages with self-bonding effect in aromatic and side chain region of lignin structures of in hydrolyzed residues. Pellets also showed

increased hydrophobicity and better water resistance when a higher percentage of hydrolyzed residue additive was used.

Key words:

Bioethanol, Densification, Hydrolysis, Lignin, Pelleting, Valorization

7.1 Introduction

Bioethanol produced from agricultural residues, forest residues, and energy crops is one of the second-generation biofuels [1]. These non-food biomass feedstocks are mainly composed of cellulose, hemicellulose, and lignin. Extensive research has been done to develop effective pretreatment technologies and enzymes to overcome biomass recalcitrance in fuel conversion. Energy-efficient processes are also proposed to make second generation bioethanol production more economically feasible [2-4]. However, second-generation bioethanol production is yet to be successful commercially. Stand-alone second-generation bioethanol production is still facing significant challenges [5-7].

High energy demand and low ethanol yield are the most critical factors leading to the high ethanol production cost. Due to its recalcitrant characteristic, lignocellulosic biomass needs to go through pretreatment and hydrolysis before it can be converted into fermentable sugar. Pretreatment is usually performed between 120-230 °C for 15-90 minutes. This process is energy intensive and constitutes 18-33% of the total production cost [8, 9]. Enzymatic hydrolysis is also responsible for a significant amount of energy use as the process usually lasts for 48-72 hours at 50 °C. In bioethanol conversion, the low fermentable sugar concentration in hydrolysis slurry presents a constraint, because after fermentation a threshold ethanol concentration must be reached to make distillation profitable [10]. While fermentation of pentose can increase ethanol

concentration, it also adds cost due to extra microorganism consumptions for five monosaccharides fermentation [9]. In order to address these issues, several integration approaches have been proposed and investigated [7, 10].

As summarized in Table 7.1, integration strategies to conserve energy and reduce cost for second-generation bioethanol productions are divided into two streams. They are (1) integration with first-generation (1G) bioethanol process (1G2G stream) and (2) integration with existing combined heat and power plant (CHP stream). These integration concepts are mainly based on waste valorization, cogeneration, energy sharing, and recycling. In the 1G2G stream, the first and second generation bioethanol production processes usually run in parallel first and then combined at the stage of fermentation or distillation. This approach aims to obtain a liquid solution with an increased fermentable sugar or ethanol concentration. Simultaneous saccharification and fermentation (SSF) process can conserve more energy than performing enzymatic hydrolysis and fermentation separately. However, the feedstock option is rather limited to starch-based biomass if the by-product has further use, such as DDGS for animal feed. Separate hydrolysis and fermentation (SHF) needs be performed to avoid inhibitor formation and chemical contamination in the by-product. In addition, if the optimal temperatures for fermentation and hydrolysis are different, SHF should also be considered. Afterward, a high ethanol yield can still be achieved by performing distillation with a combined liquid fractions of 1G and 2G fermented slurries from separated hydrolysis and fermentation processes. Besides improving the conversion performance, this 1G2G bioethanol cogeneration path can also save initial costs by utilizing the existing infrastructure in the first-generation bioethanol plants such as CHPs, distillation columns, evaporators, and dryers [5]. Another path in the 1G2G stream is the direct use of 2G feedstocks for heat and steam generations to power bioethanol conversion

from first-generation feedstocks such as sugarcane and corn. Such configuration not only improves bioethanol techno-economic performance by saving energy and cost but also has significant environmental merit by reducing the overall greenhouse gas emissions [6].

Table 7.1 An overview of the main integration strategies of second-generation bioethanol production

Main streams	Sub-branches	Pros	Drawbacks	Refs
Integration 1G2G bioethanol	Integrate with (SSF) fermentation	Cost saving for washing and separating, enzyme and yeast	Limitation of pretreatment method and feedstock if DDGS are used as by-product	[5, 7, 10-13]
		Overall energy conservation Higher fermentable sugar concentration		
	Integrate with (SHF) distillation	Wider pretreatment and feedstock options	Extra separation of inhibitor and lignin	[7, 10, 11, 14, 15]
		Easier carry out in existing facilities		
Mass and energy integration	Overall energy conservation	Low efficiency and capacities	[6, 11, 16-19]	
	GHG emissions reduction Hot and cold utilities conservation			
Integration with CHP	Recycle heat and power from CHP for bioethanol production	Energy conservation for heating, drying and pelleting	Higher cost of facility and equipment	[20-23]
		Energy recovery Utility generation from by-product		
	Heat and power integration for pelleting, torrefaction and gas production	Energy conservation for heating, drying and pelleting	Higher cost of facility and equipment Redesign of existing facilities	[13, 19, 20, 22, 24-27]
		Product valorization		

For the same purpose of saving energy and cost, integrating a 1G2G bioethanol facility with a combined heat and power plant (CHP) is also proposed. In this stream, residual and exhaust heat from electricity generation in the CHP is used to power 1G2G ethanol conversion. Therefore, the 2G feedstock can still be used for ethanol conversion, and the hydrolyzed residues can be recovered for power generation for the CHP. These hydrolyzed biomass residues from bioethanol production are mainly composed of lignin with high HHV. Lignin-rich residues are deemed a high quality solid fuel than raw cellulosic biomass itself [28]. It is also reported that adding biomass pellet production to the CHP integrated system can further improve the overall

techno-economic performance of the system [29]. Condensing biomass hydrolyzed residues into pellets can increase the volumetric energy densities, improve handling and logistic efficiency of fuel pellets [19, 30, 31]. When utilizing these pellets as platform chemical commodities, the enriched lignin content of hydrolyzed residues also offers great physical quality to the pellets due to the natural binding ability of lignin [30, 32]. Considering the strong value adding potentials of pellets made from hydrolyzed residues, the CHP integration stream can achieve an optimized combination of biomass valorization, ethanol yield and energy output from the 2G feedstocks [13, 23]. Several studies have investigated the combustion characteristics of different fuel pellets made from hydrolyzed residues [28, 33, 34], but the impacts of adding hydrolyzed residues on pellet properties and inter particle bonding are not reported. This is a much-needed understanding, especially when pellets are used as platform chemical commodities and other energy applications such as gasification, co-firing, and lignin valorization [22, 27, 35, 36].

This study investigates how pellets' thermochemical, physical, and hygroscopic properties were strengthened by adding hydrolyzed residues to pellet production. Pellets were fully or partially (50%, 20%, and 10%) made from hydrolyzed residues. Pellet physical properties were evaluated through measuring its density, durability, and mechanical strength. Thermogravimetric (TGA) and differential scanning calorimetric (DSC) analyses were carried out to study biomass material thermal degradation behaviors. The hygroscopic properties of pellets were assessed by applying sessile drop contact angle and water immersion methods. In addition, FTIR and 2D-HSQC-NMR spectra were acquired to facilitate investigation into structural aspects of complex lignin polymers.

7.2 Experimental procedures and parameter measurements

7.2.1 Materials and preparation

The corn stover used in this study was collected from the East Central Kansas Experiment Field of Kansas Agricultural Experiment Station. Materials were air dried and had approximately 8% moisture content. Raw material and hydrolyzed residues were measured by following the NREL analytical procedure [37]. Biomass particles were prepared on a knife mill with a 2 mm opening sieve (SM 2000, Retsch, Inc., Germany).

7.2.2 Pretreatment and enzymatic hydrolysis

Dilute sulfuric acid (2%) pretreatment was employed. A 25% solid loading (w/w) slurry was prepared with 60 g biomass and 240 ml dilute sulfuric acid in a 600 ml glass liner. Pretreatment was carried out in a pressure reactor (4760A, Parr Instrument Co., Moline, IL) at 160 °C for 30 minutes. Solid-liquid separation was performed on suction filtration units after pretreatment. The solid fraction was washed with distilled water to remove inhibitors and residual acids.

Twenty milliliter of 15% solid loading (w/w) slurry was prepared with 1 g pretreated biomass (dry weight), 1 mL enzyme complex Accellerase 1500™ (DuPont Genencor Science, Wilmington, DL), and sodium acetate buffer solution (50 mM, pH 4.8, 0.02% sodium azide) in a 125 mL hydrolysis flask. The enzyme complex contains glucanase, β -glucosidase, xylanase, and β -xylosidase with an endoglucanase activity of 2200–2800 CMC U/g, a β -glucosidase activity of 450–775 pNPG U/g, a xylanase activity of 660 U/g, and a β -xylosidase activity of 60 U/g. Hydrolysis reaction was incubated at 50 °C in a water bath shaker operated at 110 rpm for 72 hours. After hydrolysis, the solid residues were washed to remove sugar contents and then dried at 80 °C for 24 hours.

7.2.3 Pelleting

Pelleting experiment was conducted on a custom made ultrasonic assisted pelleting system as described in a prior publication [38]. When ultrasonic vibration is applied to the biomass, heat is generated within very short period of time due to viscoelastic heating. Ultrasonic vibration and pelleting pressure eliminate gaps among adjacent material particles.

Simultaneously, lignin is softened by the cumulated heat and serves as a natural binder to bond particles together. For pelleting, parameters were kept unchanged. They were 20 seconds pelleting time, 50% of ultrasonic power and 20 psi of pelleting pressure. Pellets were made from corn stover and its hydrolyzed residues. The material mixtures contained by 0, 10%, 20%, 50% and 100% hydrolyzed residues by weight.

7.2.4 Measurement of material composition and higher heating value

Biomass compositions were determined as per the NREL laboratory analytical method (NREL/TP-510-42618) [39]. The higher heating value (HHV) of biomass was measured on a bomb calorimeter (Model C200, IKA Group, Germany).

7.2.5 Measurement of pellet physical properties

Pellets durability was tested on a four-compartment durability tester (Model PDI, Seedburo Equipment Co, IL,USA). A set of ten pellets were loaded into each compartment of the specially designed pellet tumbler to simulate the amount of breakage that normally occurs during pellet transportation for 10 minutes. After each test, remained pellet weight in a good cylindrical shape were separated from the fines and debris on a sieve and weighed. The ratio of remained pellets to the initial pellet weight was defined as the durability index and expressed as a percentage.

The volumetric density of each pellet was obtained by dividing the weight of a pellet by its volume. Measurements of pellet dimensions and weight were performed 48 hours after the pellet was retrieved out of the mold. A caliper and a lab analytical balance were used. Energy density (ED) is defined as:

$$ED = \text{HHV of pellet} / \text{volume of pellet} \quad \text{Eq. (1)}$$

7.2.6 Measurement of pellet mechanical strengths

Pellet mechanical properties were assessed on a universal testing machine (Shimadzu EZ-LX, Japan) with a crosshead speed of 2 mm/min. As shown in Figure 7.1, diametral and flexure compression tests were performed. There were five replicates for pellets made under each condition. Proportional stress, elastic limit, ultimate strength of the pellet were measured. Young's modulus of the pellets was calculated from the slope of proportional portion on the stress-strain curve.

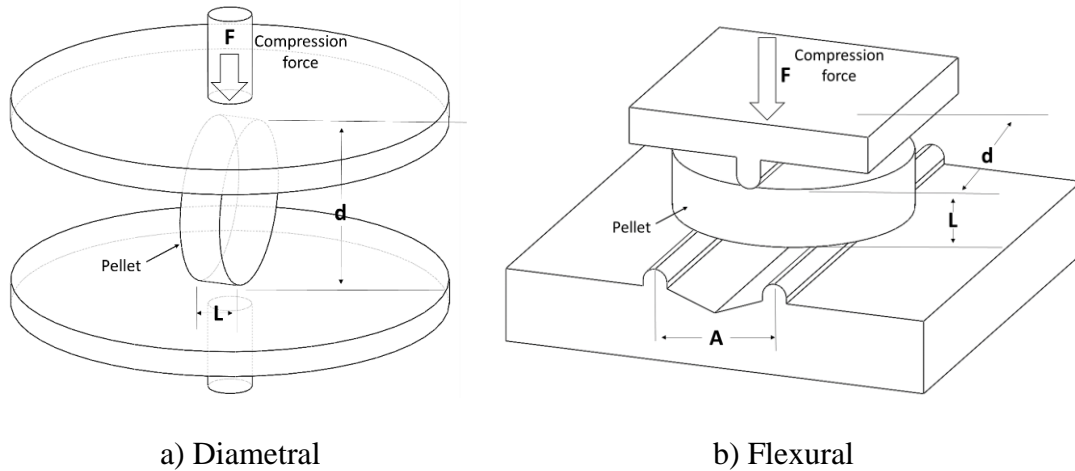


Figure 7.1. Mechanical test configurations

The compressive diametral stress σ_D was calculated as following:

$$\sigma_D = \frac{F}{rL} \quad \text{Eq. (2)}$$

Where L is the thickness of the pellet, r is the radius of pellet. The compressive diametral strain ε_D was calculated as following:

$$\varepsilon_D = \frac{d-d_i}{d} \quad \text{Eq. (3)}$$

The flexural stress σ_F was calculated as following:

$$\sigma_F = \frac{3FA}{2dL^2} \quad \text{Eq. (4)}$$

Where A is the distance between the support position, d and L are pellet diameter and thickness respectively. The flexural strain ε_F was calculated as following:

$$\varepsilon_D = \frac{6DL}{A^2} \quad \text{Eq. (5)}$$

Where D is the deflection of the pellets under compression.

7.2.6 Measurement of pellet thermochemical properties

A thermogravimetric analyzer (TGA7, PerkinElmer Co, USA) was used to obtain biomass thermogravimetric and derived thermogravimetric data. In each test, 20 mg of material was put in the crucible. Temperature increased from ambient temperature to 700 °C at a rate of 20 °C/min in a nitrogen atmosphere and was maintained at 700 °C for one minute. A differential scanning calorimeter (DSC 204 F1 Phoenix, NETZSH group, Germany) was also used and the DSC heating rate was kept the same as that used in TGA.

7.2.6 FTIR and NMR spectra

An FTIR (Model Spectrum 400 FT-IR, PerkinElmer Co, USA) recorded spectra in transmittance mode with the wavenumber ranging from 400 to 4000 cm⁻¹. The detection resolution was 4 cm⁻¹ in the transmission mode with 16 scans per test.

2D- HSQC NMR spectra were acquired on a spectrometer (500 MHz Bruker AVIII, Bruker, USA) equipped with a gradient 5–mm cryogenically-cooled carbon observe probe. About 40 mg material was dried and dissolved in 0.5 mL of DMSO-d₆ for 48 hours. ¹³C-1H

spectral were measured with a standard pulse sequence “hsqcetgpsisp.2”. All experiments were carried out at 25 °C with the following parameters: spectral width of 16 ppm in F2 (1H) dimension with 2048 data points (TD1) and 240 ppm in F1 (13C) dimension with 512 data points (TD2). Scan number was 128 and increment delay was 2 seconds. Total acquisition time was 20 hours. Data were processed by Bruker Topspin 4.3 software.

7.2.7 Measurement of pellet hygroscopic properties

The contact angle measurement was carried out based on the sessile drop method. A distilled water droplet of approximately 1 μ L was laid on the pellet surface. After that, a 30 second video was recorded from the moment when the droplet was laid. By using the Ossila contact angle software, a tangent line for each side of the droplet was fitted in each frame of the recorded video. As shown in Figure 7.2, the angle between the tangent line and the flat pellet surface was defined as the contact angle. This angle was estimated and recorded through the whole video. Measurements were carried out 5 times for pellets made under each condition. Considering the variance of pellet surface roughness, the average contact value was then presented. An optical microscope (Model BX51, Olympus Corp. Japan) was used to observe the morphological features of pellets surfaces.

To test pellet water resistance, three pellets made under each condition were immersed in a beaker filled with 300 ml water. The test lasted for 20 minutes and the solid parts were drained afterward. The integrity of pellets after water immersion was compared.

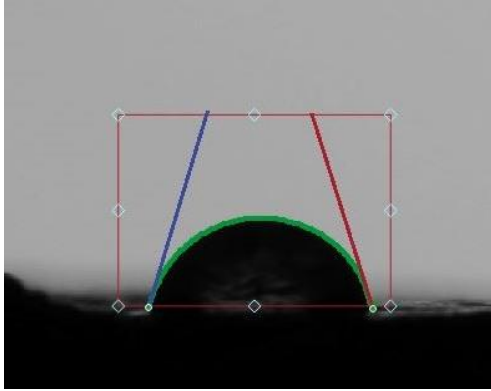


Figure 7.2. An illustration of contact angle measurement

7.3 Experimental results and discussions

7.3.1 Material compositions and higher heating value (HHV)

The compositions of corn stover changed significantly after dilute sulfuric acid pretreatment and enzymatic hydrolysis. As shown in Table 7.2, most of the hemicellulose and non-compositional components were removed due to the structure disruption of corn stovers during pretreatment. As a result, cellulose and lignin weight percentages were increased in the pretreated solids. During enzymatic hydrolysis, cellulose was largely broken down into fermentable sugar during the scarification process. The percentage of lignin substantially increased to nearly 34% in hydrolyzed residues. According to the literature, the higher heating value (HHV) of cellulose and hemicellulose is 17-17.5 MJ/kg and is 24-28 MJ/kg for lignin [40]. Because of the changes of raw corn stover compositions, the HHVs of pretreated corn stover and hydrolyzed residues increased from 16.76 MJ/kg to 17.91 MJ/kg and 18.12 MJ/kg, respectively.

Table 7.2 Composition results of raw, pretreated, and hydrolyzed corn stover

Material	Glucan %	Xylan %	Lignin %	Ash %	Non-compositional component %	HHV MJ/kg
Raw	37.85 ± 0.41	17.05 ± 0.16	14.15 ± 0.02	0.76 ± 0.06	30.04 ± 0.85	16.76
Pretreated	57.63 ± 0.02	8.12 ± 0.03	24.97 ± 0.45	2.06 ± 0.12	7.18 ± 0.08	17.91
Hydrolyzed	46.29 ± 0.11	7.62 ± 0.18	33.83 ± 0.6	3.11 ± 0.16	8.15 ± 0.04	18.12

7.3.2 Pellet physical properties

Durability evaluates the resistance of pellets to shock and abrasion conditions during handling and transportation. After mixing 10% hydrolyzed residues with raw biomass, the durability of pellets increased from 80.74% to 90.01%, compared to pellets solely made from raw biomass (Table 7.3). Further increase in pellet durability was observed after adding a higher percentage of hydrolyzed residues to the material mixtures. However, the improvement is rather limited. Durability of pellets only increased from 90.1% to 92.83% by adding 20% to 100% of hydrolyzed residues in material mixtures for pelleting. The same trend was also observed for pellet density, rising from $864.15 \pm 28.19 \text{ kg/m}^3$ to $972.46 \pm 31.43 \text{ kg/m}^3$. Furthermore, the HHV of pellets increased by adding hydrolyzed residues in pelleting, leading to a much higher energy density. Compared to pellets made from raw materials, 26.12% to 53.2% more energy is carried with the same volume of pellets by using 100% hydrolyzed residues. Such upgrading effects made pellets more durable in storage and transportation, and comparable to conventional wood and torrefied fuel pellets [41, 42].

Table 7.3 Results of pellet durability, density, and energy density

Sample	Durability (%)	Density (kg/m ³)	Energy density (GJ/m ³)
Raw	80.74%	816.98 ± 54.81	13.69 ± 0.92
10%	90.01%	864.15 ± 28.19	14.60 ± 0.47
20%	91.86%	892.03 ± 86.91	15.19 ± 0.48
50%	91.43%	917.13 ± 43.47	15.99 ± 0.76
100%	92.83%	972.46 ± 31.43	17.62 ± 0.57

7.3.3 Pellet mechanical strengths

Pellet mechanical strength results are shown in Table 7.4. The stress that a pellets can take in the axial direction was very high since pellets were made by axially compressing loose biomass particles into a cylindrical pellet in a mold. Pellets could undertake larger normal force before fracture than the maximum force the load cell could provide on the tester. As a result, only diametral and flexure compression were performed. Pellet mechanical strengths were described by proportional stress, elastic strain, and young's modulus. Ultimate strength and ductility represent the maximum resistance to fracture and the ability to be stretched to the breaking point. Diametral and flexure results show that pellets were strengthened with the additive of hydrolyzed residues. The increases of proportional stress and ultimate strength were quite limited. A very low load can be undertaken at the breaking point until the amount of hydrolyzed residue additive rose to 50%. When 100% hydrolyzed residues were used to make pellets, proportional stress, ultimate strength, and Young's modulus of pellets all increased significantly in both type of compression tests. Due to viscoelastic heating during the ultrasonic-assisted pelleting process [38], more lignin content was softened and provided a better binding effect comparing to pellets made with less hydrolyzed residues. This natural binding effect of lignin consequently improved pellet mechanical properties. Elastic strain and ductility both

increased by adding more hydrolyzed residues. It indicates that the additive of hydrolyzed residues strengthened the pellets and prevented the pellets from breaking while being deformed by a much larger load. However, there was little increase from elastic strain to ductility and from proportional stress to ultimate strength. It suggests that there was not much load undertaken by the pellets beyond the elastic limit. Additionally, the initial pelleting compressing direction and pellet shape (aspect ratio) are also essential factors to pellet mechanical strength. While using microwaved eucalyptus, and mixed wood to make pellets from axial compression, a study showed a higher strength in diametral compression with rod shape pellets [43] On the contrary, the results were higher by flexure compression in this study. The load from the axial direction created a very condensed plate shape structure. A relatively good thickness of pellets also contributed to the higher proportional stress and ultimate strength that were taken in flexure compression.

Table 7.4 Results of pellet mechanical properties

	Proportional stress Mpa		Elastic strain %		Young's Modulus Mpa		Ultimate strength Mpa		Ductility %	
	Mean	SD	Mean	SD	Mean	SD	Mean	SD	Mean	SD
Diametral										
Raw	0.38	0.04	1.20	0.01	35.06	3.71	0.49	0.12	1.43	0.01
10%	0.43	0.03	3.00	0.20	39.34	2.98	1.15	0.75	3.76	0.30
20%	0.96	0.27	1.45	0.02	88.92	20.78	1.01	0.30	2.27	0.01
50%	2.60	0.94	1.70	0.50	223.01	48.49	3.25	0.63	2.36	0.73
100%	7.89	0.47	4.35	1.20	316.26	34.95	7.92	0.96	6.78	0.88
Flexure										
raw							3.92	1.02	41.46	6.35
10%							3.98	0.21	42.30	9.93
20%	5.27	0.03	27.19	0.13	25.59	1.56	5.63	0.04	25.19	4.77
50%	10.54	1.23	24.19	3.64	79.98	6.81	10.97	0.99	26.14	3.33
100%	17.10	1.32	31.27	8.08	103.19	7.33	17.73	1.30	33.34	8.49

Notes: In some flexural tests, pellets made from raw material and 10% residue mixture yielded prematurely without undertaking a stabilized load. There were no proportional, elastic strain and young's modulus data presented.

7.3.4 Pellet thermochemical properties

Cellulose, hemicellulose, and lignin have different thermal stabilities [44]. The alternation of material compositions can be reflected in thermal gravimetric (TG, DTG) and differential scanning calorimetric (DSC) analyses. After dilute acid pretreatment and enzymatic hydrolysis, major weight loss of hydrolyzed residues showed a notable change in the TG analysis due to the increased overall lignin content. The curve of hydrolyzed residues slightly shifted to a higher temperature than raw materials (Figure 7.3A). Cellulose and hemicellulose decompose at 275-350 °C and 150-350 °C, respectively. Lignin decomposes between 350-450 °C and, the decomposition completes at around 500 °C [44]. At the end of this TG analysis, raw materials had much more mass remained than hydrolyzed residues. It indicates that there was higher non-structural composition within raw materials.

The DTG results (Figure 7.3B) show raw materials posed a much higher weight loss rate in the temperature ranging from 150-350 °C. On the contrary, the removal of amorphous cellulose II and hemicellulose attributed to a slower decomposition of hydrolyzed residues. After temperature reaching 350 °C, the decomposition rate of raw materials slowed down. This reflected that at this moment, the amorphous cellulose and hemicellulose were completely decomposed. However, the trend of slowing down around 350 °C was not observed for hydrolyzed residues due to its much lower cellulose II and hemicellulose content. As temperature approached 400 °C and above, hydrolyzed residues decomposed more severely than raw materials. This trend continued with further temperature increase to 500 °C. It is related to the better thermal stability of lignin and its higher content in hydrolyzed residues [45]. With further heating, remained hydrolyzed residues kept decomposing until the temperature reached over 700

°C. However, there were much fewer raw materials decomposed after 500 °C because of the higher non-compositional content.

The DSC analysis provides more insight on the exothermal performance of raw materials and hydrolyzed residues as shown in Figure 7.3C. When the temperature was lower than 250 °C, the two materials showed very similar heat flow patterns and trends. The first peak observed at 275 °C indicated the complete decomposition of hemicellulose. Afterward, the heat flow rate of raw material dropped dramatically when the temperature reached over 300 °C. Due to the higher concentration of crystalline cellulose in hydrolyzed residues, a second peak around 350 °C was observed with the complete decomposition of cellulose. However, the reduction of raw material heat flow rate slowed down at this temperature range. The lower total cellulose content in raw material might attribute to the less intensive exothermal activity. After that, the heat flow rate of hydrolyzed residues kept rising to the range of 400-600 °C. This observation agreed with TG and DTG results that more than 10% total mass of hydrolyzed residues was still under decomposition after reaching 550 °C. According to Asadieraghi et al., the generation of char, condensable gases, and inorganic carbonates can be related to this further decomposition [46]. The formations of CO, CO₂, and H₂ were caused by thermal cracking and dehydrogenation of high molecular weight compounds (aromatic and aliphatics). The breakage of the C-C bond then resulted in a higher degree of exothermal activity.

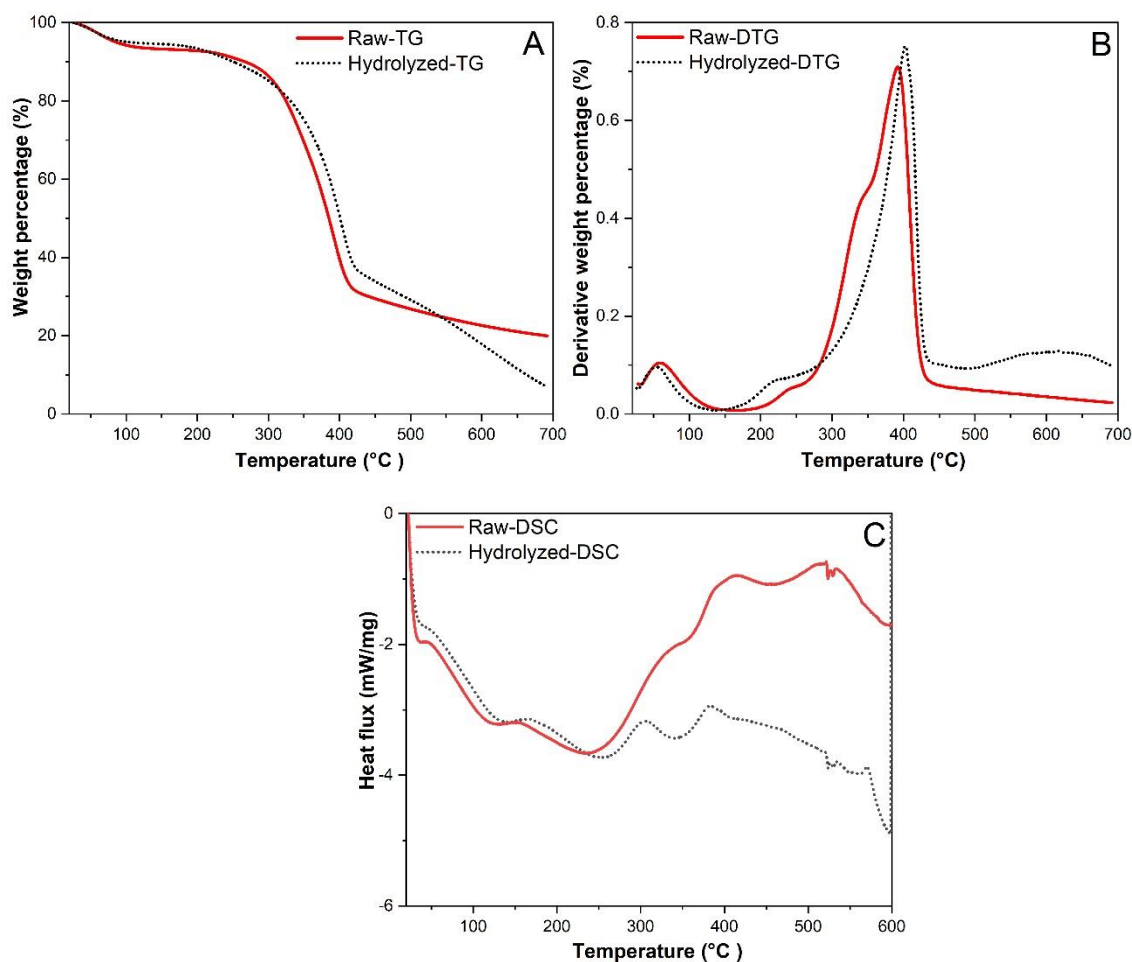


Figure 7.3. Thermal analyses results of raw and hydrolyzed biomass: (A) TG, (B) DTG and (C) DSC

7.3.5 FTIR and NMR results

FTIR spectra (Figure 7.4) were used to reveal organic and inorganic compounds in the samples. The focus was on lignin-related chemical bonds. As reported, the C=C stretching from lignin located between 1400-1600 cm^{-1} [47, 48]. The negative peak at 1508 cm^{-1} was related to the aromatic ring of lignin. The positive peak at 1550 cm^{-1} indicated a mixed signal from aromatic skeleton vibration and C=O stretching of lignin [49]. The negative peak at 1456 cm^{-1} is attributed to C-H bending and vibrations of aromatic groups that are also related to lignin [50]. These signals became stronger or produced after pretreatment and enzymatic hydrolysis. The

variations on FTIR spectra reflected the increased lignin content in hydrolyzed residues. It was also reported the signals around 1000 to 1250 cm⁻¹ are related to hydroxyl groups in polysaccharides [51]. The negative peak at 1060 cm⁻¹ can be originated from cellulose. Similarly, the stronger signals at 1160 cm⁻¹ and appearance at 1110 cm⁻¹ indicated the presence of higher amount of cellulose. The increased cellulose and lignin content consequently provided better bonding between particles since the binding effects of three components followed the order: lignin>cellulose>hemicellulose [52].

It was reported that corn stover contains all three types of monolignol units with β -o-4' as major inter-unit linkages[53, 54]. On NMR spectra, lignin structures in hydrolyzed residues were revealed with special focus. The main cross-signals in the aromatic region (δ H 6.0-8.0 ppm, δ C 100-150 ppm) and the side chain region (δ H 2.5-6 ppm, δ C 50-90 ppm) of lignin contents are shown in Figure 7.5 A & B. The results indicated that lignin content in aromatic region is composed of syringyl (S), guaiacyl (G), p-coumarate (pCA). Based on the spectra, G-type and S-type were the major lignin units in the aromatic region. G-type has a free C-5 position in the rings that is easy to link with phenolic hydroxyl that can activate the free ring positions and make them susceptible to react with other lignin units [55, 56]. While S-type units can transform into H-units by the demethoxylation process under high temperature. With freed C-3 and C-5 positions, H-unit can provide additional formation of self-bonding [57]. The heat generated during ultrasonic-assisted pelleting could further improve this binding effect. In the side chain region, four types of lignin β -aryl ether units (A), phenylcoumaran units (B), resinol units (C), and dibenzodioxocin units (D) were observed. Satoshi Kubo et al. reported that the dehydration of the C γ -hydroxyl group would enhance the thermal mobility of lignin molecules through plasticization [58]. A significant amount of peak signals appeared at C γ position in hydrolyzed

residues indicating the increase of lignin resinol units. With the increase of this type of lignin, hydrolyzed residues achieved a better binding effect under the rapid viscoelastic heating process in ultrasonic-assisted pelleting.

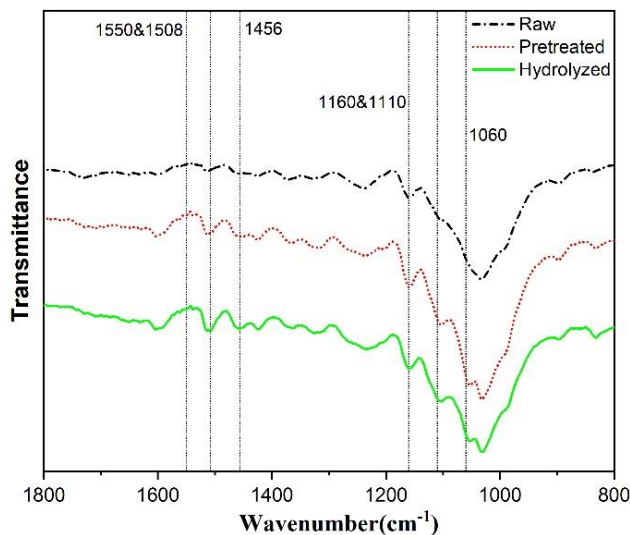


Figure 7.4. FTIR spectra of raw, pretreated and hydrolyzed biomass

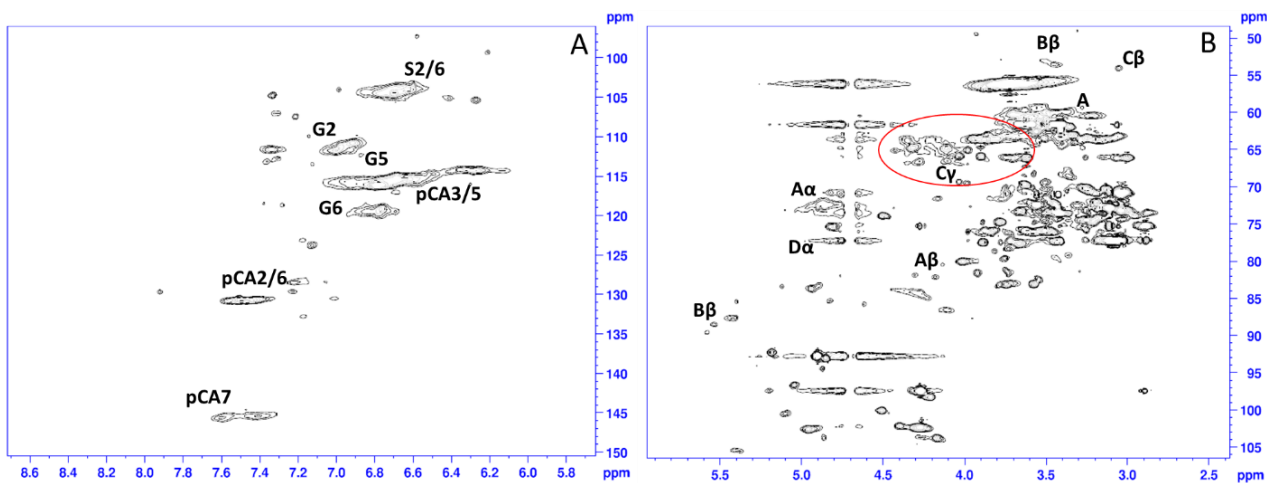


Figure 7.5. NMR spectra of hydrolyzed biomass

7.3.6 Pellet hygroscopic properties

Contact angle results (Figure 7.6A) showed that water droplets penetrated the pellet surface quickly for pellets made from material mixtures with adding 10% hydrolyzed residue. After adding hydrolyzed residues to 20%, water droplets stayed on the pellet surface for a

slightly longer time but were eventually absorbed. Further improvement of surface hydrophobicity was observed with a 50% hydrolyzed residue additive. The contact angle stayed at around 30° and the droplets were partially absorbed in the end of each test. At last, 100% hydrolyzed residues made pellets' contact angle stay around 60° constantly for even hours after droplets were put on pellet surface. Generally, the improvement of hydrophobic characteristic for pellet surface increased with raising hydrolyzed residue content. This trend can be further explained with surface morphology results in Figure 7.6 B-E. Microscopy images showed that particles were not completely consolidated and bonded together on pellet surfaces of raw material (B) and 10% additive (C) groups. The contour of material particles was still very clear, and there were significant amount of gaps in-between particles. This loosened structure resulted in the quick drop of contact angle and absorptions. With increased hydrolyzed residue content, pellets of 50% and 100% groups showed more compact structures. As a result, pellet surfaces became flatter. The shape of particles was no longer clear, and interlocking was formed. Due to the plasticization of lignin, a better bonding effect led to a hydrophobic pellet surface. It prevented water penetrations and absorptions. Further evaluations of pellet water resistance were performed with water immersion.

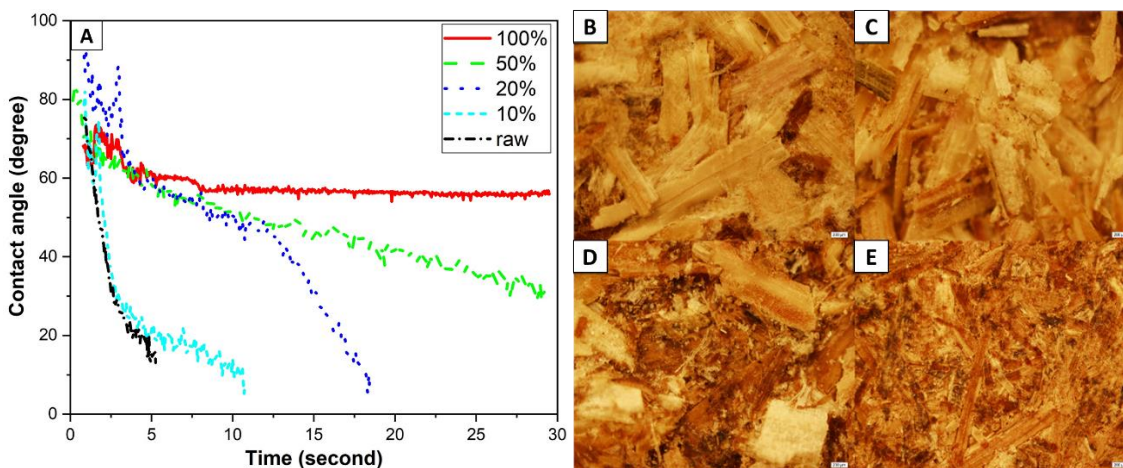


Figure 7.6. Contact angle (A) and Surface morphology (B-E)

Pellets made under each condition were also immersed in water to simulate an extreme wet condition. As shown in Figure 7.7, pellets made from raw material, 10% and 20% hydrolyzed residue mixtures were generally separated into particles after 5 minutes. While pellets made by 50% and 100% hydrolyzed residue maintained their integrity. No particles fell apart. After 20 minutes immersion, pellets were moved into nylon mesh to drain water. Raw and 10% mixture pellet groups completely fell apart, and 20% mixture group could barely hold the cylindrical shape. 50% mixture and 100% groups still held good cylindrical shapes with no particles separated. However, pellets in the 50% mixture group were clearly swelled and became softened. Pellets made by 100% hydrolyzed residues stayed compact, and there was no obvious swell. Particles were still completely bonded and the surface looked nearly identical compared to the original pellets. It can conclude that the additive of hydrolysis residues provided better pellet quality on the water resistance. A Clear impact can be observed with hydrolyzed residue increasing from 20% to 50%. Pellets that were fully made from hydrolysis residues provided the best pellet integrity after water immersion.

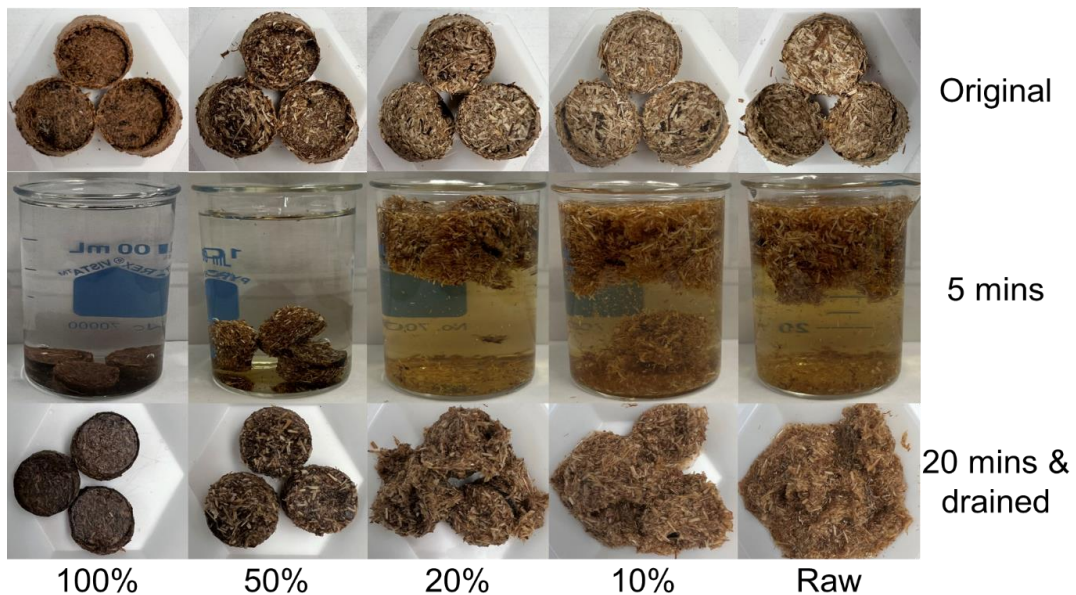


Figure 7.7 Water immersion images of pellets made from different percentage of hydrolyzed residues mixtures

7.4 Conclusions

This study evaluated the characteristics of pellets made from corn stover and its hydrolyzed residue mixtures. It showed that the addition of hydrolyzed residue enhanced the physical, thermochemical, and hygroscopic properties of pellets. These findings provide a potential path to utilizing hydrolyzed residues as solid fuels and platform chemical commodities for other applications. Detailed pellet property improvements are summarized as the following:

1. The addition of hydrolyzed residues is effective on improving physical characteristics. Pellet durability increased from 80.74% to 90.1% with just 10% hydrolyzed residue added to the material mixture. Further addition of hydrolyzed residues to 100% can increase the durability up to 92.83%. However, there was no apparent strengthening effect on pellet mechanical properties until 50% or more hydrolyzed residues were added.

2. The addition of hydrolyzed residue also attributes to the increase of pellet density (816 kg/m³ to 972 kg/m³) when the additive amount increased from 10% to 100%. Due to higher HHV of lignin content, making pellets from lignin-rich hydrolyzed residues also provided a higher energy density (17.62 GJ/m³) than using raw materials (13.69 GJ/m³)

3. The addition of hydrolyzed residue provides pellets with better thermochemical characteristics. Due to high thermal stability of lignin, pellet made from lignin-rich hydrolyzed residues are more thermal stable when temperature is above 350 °C and had continued exothermal activity after 400 °C.

4. The addition of hydrolysis residues contributes to the improvement of hygroscopic characteristics. The higher surface hydrophobicity, higher water resistance can be achieved because of the more compact pellet structure when 50% or more hydrolyzed residues were used in pelleting.

References

- [1] Robak, K., M.J.F.t. Balcerek, and biotechnology, Review of second generation bioethanol production from residual biomass. 2018. 56(2): p. 174.
- [2] Alvira, P., et al., Pretreatment technologies for an efficient bioethanol production process based on enzymatic hydrolysis: a review. 2010. 101(13): p. 4851-4861.
- [3] Agbor, V.B., et al., Biomass pretreatment: fundamentals toward application. 2011. 29(6): p. 675-685.
- [4] Carvalheiro, F., et al., Hemicellulose biorefineries: a review on biomass pretreatments. 2008: p. 849-864.
- [5] Lennartsson, P.R., P. Erlandsson, and M.J.J.B.t. Taherzadeh, Integration of the first and second generation bioethanol processes and the importance of by-products. 2014. 165: p. 3-8.
- [6] Eriksson, G. and B.J.A.E. Kjellström, Assessment of combined heat and power (CHP) integrated with wood-based ethanol production. 2010. 87(12): p. 3632-3641.
- [7] Ferreira, J.A., et al., A review of integration strategies of lignocelluloses and other wastes in 1st generation bioethanol processes. 2018. 75: p. 173-186.
- [8] Rajendran, K., et al., Updates on the pretreatment of lignocellulosic feedstocks for bioenergy production—a review. 2018. 8(2): p. 471-483.
- [9] Tomas-Pejo, E., J. Oliva, and M. Ballesteros, Realistic approach for full-scale bioethanol production from lignocellulose: a review. 2008.
- [10] Ayodele, B.V., M.A. Alsaffar, and S.I.J.J.o.C.P. Mustapa, An overview of integration opportunities for sustainable bioethanol production from first-and second-generation sugar-based feedstocks. 2020. 245: p. 118857.

- [11] Furlan, F.F., et al., Assessing the production of first and second generation bioethanol from sugarcane through the integration of global optimization and process detailed modeling. 2012. 43: p. 1-9.
- [12] Rajendran, K., S. Rajoli, and M.J.J.E. Taherzadeh, Techno-economic analysis of integrating first and second-generation ethanol production using filamentous fungi: an industrial case study. 2016. 9(5): p. 359.
- [13] Palacios-Bereche, R., A. Ensinas, and S.A.J.C.E.T. Nebra, Energy consumption in ethanol production by enzymatic hydrolysis—the integration with the conventional process using pinch analysis. 2011. 24: p. 1189-1194.
- [14] Macrelli, S., J. Mogensen, and G.J.B.f.b. Zacchi, Techno-economic evaluation of 2nd generation bioethanol production from sugar cane bagasse and leaves integrated with the sugar-based ethanol process. 2012. 5(1): p. 1-18.
- [15] Mikulski, D. and G.J.B.R. Kłosowski, Integration of first-and second-generation bioethanol production from beet molasses and distillery stillage after dilute sulfuric acid pretreatment. 2021: p. 1-12.
- [16] Dias, M.O., et al., Cogeneration in integrated first and second generation ethanol from sugarcane. 2013. 91(8): p. 1411-1417.
- [17] Dias, M.O., et al., Evaluation of process configurations for second generation integrated with first generation bioethanol production from sugarcane. 2013. 109: p. 84-89.
- [18] Oliveira, C., A. Cruz, and C.J.A.T.E. Costa, Improving second generation bioethanol production in sugarcane biorefineries through energy integration. 2016. 109: p. 819-827.

- [19] Song, H., et al., Techno-economic analysis of an integrated biorefinery system for poly-generation of power, heat, pellet and bioethanol. 2014. 38(5): p. 551-563.
- [20] Kaliyan, N., et al., Reducing life cycle greenhouse gas emissions of corn ethanol by integrating biomass to produce heat and power at ethanol plants. 2011. 35(3): p. 1103-1113.
- [21] Starfelt, F., et al., Performance evaluation of adding ethanol production into an existing combined heat and power plant. 2010. 101(2): p. 613-618.
- [22] Pfeffer, M., et al., Analysis and decrease of the energy demand of bioethanol-production by process integration. 2007. 27(16): p. 2657-2664.
- [23] Starfelt, F., et al., The impact of lignocellulosic ethanol yields in polygeneration with district heating—a case study. 2012. 92: p. 791-799.
- [24] Kaliyan, N., et al. Life Cycle Assessment of Corn Stover Torrefaction Plant Integrated with a Corn Ethanol Plant and a Coal Fired Power Plant. in 2013 Kansas City, Missouri, July 21-July 24, 2013. 2013. American Society of Agricultural and Biological Engineers.
- [25] Joelsson, E., et al., Techno-economic evaluation of integrated first-and second-generation ethanol production from grain and straw. 2016. 9(1): p. 1-16.
- [26] Osaki, M.R., P.J.E.C. Selegim Jr, and Management, Bioethanol and power from integrated second generation biomass: A Monte Carlo simulation. 2017. 141: p. 274-284.
- [27] Sermyagina, E., et al., Integration of torrefaction and CHP plant: Operational and economic analysis. 2016. 183: p. 88-99.

- [28] Eriksson, G., et al., Combustion of wood hydrolysis residue in a 150 kW powder burner. 2004. 83(11-12): p. 1635-1641.
- [29] Wahlund, B., et al., A total energy system of fuel upgrading by drying biomass feedstock for cogeneration: a case study of Skellefteå bioenergy combine. 2002. 23(4): p. 271-281.
- [30] Piccolo, C., F.J.B. Bezzo, and bioenergy, A techno-economic comparison between two technologies for bioethanol production from lignocellulose. 2009. 33(3): p. 478-491.
- [31] Starfelt, F., et al., Integration of torrefaction in CHP plants—A case study. 2015. 90: p. 427-435.
- [32] Kaliyan, N. and R.V.J.B.t. Morey, Natural binders and solid bridge type binding mechanisms in briquettes and pellets made from corn stover and switchgrass. 2010. 101(3): p. 1082-1090.
- [33] Öhman, M., et al., Residential combustion performance of pelletized hydrolysis residue from lignocellulosic ethanol production. 2006. 20(3): p. 1298-1304.
- [34] Huang, Y., et al., Study on structure and pyrolysis behavior of lignin derived from corncob acid hydrolysis residue. 2012. 93: p. 153-159.
- [35] Chang, F.-c., et al., Life cycle assessment of bioethanol production from three feedstocks and two fermentation waste reutilization schemes. 2017. 143: p. 973-979.
- [36] Hara, M., et al., Recent progress in the development of solid catalysts for biomass conversion into high value-added chemicals. 2015. 16(3): p. 034903.
- [37] Sluiter, A., et al., Determination of total solids in biomass and total dissolved solids in liquid process samples. 2008. 9.

- [38] Yang, Y., et al., A fundamental research on synchronized torrefaction and pelleting of biomass. 2019. 142: p. 668-676.
- [39] Sluiter, A., et al., Determination of structural carbohydrates and lignin in biomass. 2008. 1617: p. 1-16.
- [40] Maksimuk, Y., et al., Prediction of higher heating value (HHV) based on the structural composition for biomass. 2021. 299: p. 120860.
- [41] Demirbas, K. and A.J.E.S. Sahin-Demirbas, Part A, Compacting of biomass for energy densification. 2009. 31(12): p. 1063-1068.
- [42] Peng, J., et al., Effects of thermal treatment on energy density and hardness of torrefied wood pellets. 2015. 129: p. 168-173.
- [43] Williams, O., et al., Applicability of mechanical tests for biomass pellet characterisation for bioenergy applications. 2018. 11(8): p. 1329.
- [44] Sanchez-Silva, L., et al., Thermogravimetric–mass spectrometric analysis of lignocellulosic and marine biomass pyrolysis. 2012. 109: p. 163-172.
- [45] Yang, H., et al., Characteristics of hemicellulose, cellulose and lignin pyrolysis. 2007. 86(12-13): p. 1781-1788.
- [46] Asadieraghi, M., W.M.A.W.J.E.C. Daud, and Management, Characterization of lignocellulosic biomass thermal degradation and physiochemical structure: Effects of demineralization by diverse acid solutions. 2014. 82: p. 71-82.
- [47] Barsberg, S.J.T.j.o.p.c.B., Prediction of Vibrational Spectra of Polysaccharides□ Simulated IR Spectrum of Cellulose Based on Density Functional Theory (DFT). 2010. 114(36): p. 11703-11708.

- [48] Pandey, K.J.J.o.A.P.S., A study of chemical structure of soft and hardwood and wood polymers by FTIR spectroscopy. 1999. 71(12): p. 1969-1975.
- [49] Gierlinger, N., et al., In situ FT-IR microscopic study on enzymatic treatment of poplar wood cross-sections. 2008. 9(8): p. 2194-2201.
- [50] El Mansouri, N.E., Q. Yuan, and F.J.B. Huang, Characterization of alkaline lignins for use in phenol-formaldehyde and epoxy resins. 2011. 6(3): p. 2647-2662.
- [51] Timung, R., et al., Optimization of dilute acid and hot water pretreatment of different lignocellulosic biomass: a comparative study. 2015. 81: p. 9-18.
- [52] Xu, Y., et al., Effect of lignin, cellulose and hemicellulose on calcium looping behavior of CaO-based sorbents derived from extrusion-spherization method. 2018. 334: p. 2520-2529.
- [53] Fox, S.C. and A.G.J.B. McDonald, Chemical and thermal characterization of three industrial lignins and their corresponding lignin esters. 2010. 5(2): p. 990-1009.
- [54] Min, D.-y., et al., The structure of lignin of corn stover and its changes induced by mild sodium hydroxide treatment. 2014. 9(2): p. 2405-2414.
- [55] Feldman, D., et al., Blends of vinylic copolymer with plasticized lignin: thermal and mechanical properties. 2001. 81(4): p. 861-874.
- [56] Thring, R., P. Ni, and S.J.I.J.o.P.M. Aharoni, Molecular weight effects of the soft segment on the ultimate properties of lignin-derived polyurethanes. 2004. 53(6): p. 507-524.
- [57] Wen, J.-L., et al., Unveiling the structural heterogeneity of bamboo lignin by in situ HSQC NMR technique. 2012. 5(4): p. 886-903.

- [58] Kubo, S. and J.F.J.M. Kadla, Poly (ethylene oxide)/organosolv lignin blends: Relationship between thermal properties, chemical structure, and blend behavior. 2004. 37(18): p. 6904-6911.

Chapter 8 - Conclusion and Contributions

8.1 Conclusions

In this dissertation, effects of particle size of cellulosic biomass materials for bioethanol productions are investigated. The effects to size reduction energy consumption, pelleting energy consumption, pellet density and pellet durability in pre-processing are studied. In bio-conversion processes, effect of particle size on the modifications of biomass physical and chemical features such as enzyme-accessible surface area, crystallinity, surface morphology and total sugar recovery are investigated. Furthermore, feasible conditions to produce torrefied pellets with STP systems are studied. The fuel upgrading effects of STP are evaluated from physical, thermochemical and hygroscopic perspectives. Additionally, how these properties strengthened by adding biomass hydrolyzed residues for pellet productions are also studied for integration and valorization purposes.

Main conclusions drawn from this dissertation are:

1. In size reduction of cellulosic biomass using knife mill, energy consumption increased significantly as size became smaller. Afterward, particle size did not significantly affect energy consumption during pelleting. For the resulted pellets, smaller particles tended to have better durability but have no significant impact on pellet density.
2. In bioconversion process, solely rely on size reduction was insufficient to achieve economically feasible sugar yield. Reducing particle size to submillimeter particles increased enzyme accessible surface area and showed slight advantage (<10%) over millimeter particles in enzymatic hydrolysis efficiency. However, crystallinity index was rather a weak indicator of substrate's susceptibility to

enzymes. Drying showed negative impact to biomass enzymatic digestibility as it reduced enzyme-accessible surface area of dried biomass by collapsing its inherent pore structures.

3. Reducing particle size resulted in lower solid and cellulose recoveries. Submillimeter particles' advantage in enzymatic hydrolysis efficiency was outweighed by their low solid and sugar recoveries in pretreatment. As a result, when using total sugar yields as sugar definition there was no significant difference between particles size. Considering this trade off, there is no necessary to perform finer (submillimeter) size reduction.
4. Synchronized torrefaction and pelleting process was effective at enhancing pellet physical, thermochemical and hygroscopic properties. Torrefied biomass pellets showed comparable density and durability to commercial pellets. Corn stover and big bluestem pellets increased 6.03% and 9.81% of higher heating value. Furthermore, torrefied pellets performed better in water intake and absorbed approximately 15%-25% less moisture than non-torrefied pellets.
5. Using hydrolyzed biomass residue as additive in pelleting is effective on improving physical characteristics. Pellet durability increased from 80.74% to 90.1% with just 10% hydrolyzed residue added to the material mixture. Further addition of hydrolyzed residues to 100% can increase the durability up to 92.83%. pellet density also increased (816 kg/m³ to 972 kg/m³) when the additive amount increased from 10% to 100%. However, there was no apparent strengthening effect on pellet mechanical properties until 50% or more hydrolyzed residues were added.

6. Due to higher HHV and thermal stability of lignin content, making pellets from lignin-rich hydrolyzed residues provided a higher energy density (17.62 GJ/m³) than using raw materials (13.69 GJ/m³) and continued exothermal activity at higher temperatures.
7. Due to viscoelastic heating effect of lignin content, making pellets from lignin-rich hydrolyzed residues resulted in better inter-particle bonding. It provided higher surface hydrophobicity, higher water resistance to the pellets.

8.2 Contributions

Major contributions of this dissertation are:

1. This dissertation, for the first time, presents a comprehensive study on effects of particle size in both pre-processing and bio-conversion process. The impact of particle size to the modifications of biomass physical and chemical features are detailly revealed and ultimately explained the relationship with sugar yield. Results provides a resource-efficient guidance for particle size selection in larger scale applications.
2. This research is the first one to conduct two fuel upgrading actions (densification and torrefaction) simultaneously. Input parameters include material type, particle size, pressure, power level and pelleting time are systematically investigated.
3. This research is the first to evaluate torrefied pellets from physical, thermochemical and hygroscopic perspectives and make comparison with non-torrefied pellet produced by same pelleting system. More insight about pellet bonding mechanisms, hydrophobicity alternations are revealed for this unconventional process.

4. This research is the first to investigate the impacts of adding hydrolyzed residues on pellet major properties and bonding mechanisms when pellets are used as platform chemical commodities for applications other than solid fuel. The results will broaden the potential applications of hydrolyzed residues. It also fills gaps in the literature on the behaviors of lignin materials under heating and compression conditions.

Appendix A- Publications during Ph.D. study

Publications

- [1] Yang, Y., Zhang, M. and Wang, D., 2018. A Comprehensive Investigation on the Effects of Biomass Particle Size in Cellulosic Biofuel Production. *Journal of Energy Resources Technology*, 140(4).
- [2] Yang, Y., Sun, M., Zhang, M., Zhang, K., Wang, D. and Lei, C., 2019. A fundamental research on synchronized torrefaction and pelleting of biomass. *Renewable Energy*, 142, pp.668-676.
- [3] Yang, Y., Zhao, J., Zhang, M. and Wang, D., 2022. Effects of particle size on biomass pretreatment and hydrolysis performances in bioethanol conversion. *Biomass Conversion and Biorefinery*. DOI: 10.1007/s13399-021-02169-3
- [4] Song, X., Yang, Y., Zhang, M., Zhang, K. and Wang, D., 2018. Ultrasonic pelleting of torrefied lignocellulosic biomass for bioenergy production. *Renewable Energy*, 129, pp.56-62.
- [5] Sun, M., Yang, Y. and Zhang, M., 2019. A Temperature Model for Synchronized Ultrasonic Torrefaction and Pelleting of Biomass for Bioenergy Production. *Journal of Energy Resources Technology*, 141(10).
- [6] Zhao, J., Yang, Y., Zhang, M. and Wang, D., 2021. Effects of post-washing on pretreated biomass and hydrolysis of the mixture of acetic acid and sodium hydroxide pretreated biomass and their mixed filtrate. *Bioresource Technology*, 339, p.125605.
- [7] Zhao, J., Yang, Y., Zhang, M. and Wang, D., 2021. Minimizing water consumption for sugar and lignin recovery via the integration of acid and alkali pretreated biomass and their mixed filtrate without post-washing. *Bioresource Technology*, p.125389.

- [8] Zhao, J., Yang, Y., Lee, J., Zhang, M., Roozeboom, K. and Wang, D., 2022. Experimental and Technoeconomic Assessment of Monosaccharide and Furan Production under High Biomass Loading without Solid–Liquid Separation. *ACS Sustainable Chemistry & Engineering*.
- [9] Yang, Y., Eisenbarth, N., Song, X., Zhang, M. and Wang, D., 2017, June. Ultrasonic Pelleting and Synchronized Torrefaction of Cellulosic Biomass for Bioenergy Production. In *International Manufacturing Science and Engineering Conference* (Vol. 50732, p. V002T03A014). American Society of Mechanical Engineers.
- [10] Yang, Y., Deines, T., Zhang, M., Zhang, K. and Wang, D., 2018, June. Supercritical CO₂ pretreatment of cellulosic biomass for biofuel production: Effects of biomass particle size. In *International Manufacturing Science and Engineering Conference* (Vol. 51364, p. V002T04A018). American Society of Mechanical Engineers.
- [11] Yang, Y., Sun, M., Deines, T., Zhang, M., Li, J. and Wang, D., 2019, June. Effects of Particle Size on Biomass Pretreatment for Biofuel Production. In *International Manufacturing Science and Engineering Conference* (Vol. 58752, p. V002T03A011). American Society of Mechanical Engineers.
- [12] A study on utilizing biomass hydrolyzed residues as a pellet additive for solid fuels and feedstock commodities (under review)